



**Cape Peninsula  
University of Technology**

**Metabolic network modelling of nitrification and denitrification under  
cyanogenic conditions**

By

**Ncumisa Mpongwana  
Student number: 209013451**

**Thesis submitted in fulfilment of the requirements for the degree  
Doctor of Engineering in Chemical Engineering**

**Faculty of Engineering and Built Environment  
Cape Peninsula University of Technology**

**Supervisor: Prof. S.K.O. Ntwampe  
Co-Supervisor: Dr. E.I. Omodanisi  
Co-Supervisor: Dr. B.S. Chidi**

**Cape Town**

**December 2019**


**CPUT copyright information**

The thesis may not be published either in part (in scholarly, scientific or technical journals), or as a whole (as a monograph), unless permission has been obtained from the University

# DECLARATION

I, **Ncumisa Mpongwana**, declare that the contents of this thesis represent my own unaided work and that the thesis has not previously been submitted for academic examination towards any qualification. Furthermore, it represents my own opinions and not necessarily those of the Cape Peninsula University of Technology and the national research foundation of South Africa.

All intellectual concepts, theories, methodologies, and material derivations and model developments used in this thesis and published in various scientific journals (except those that the candidate is not the first author in) were derived solely by the candidate and first author of the published manuscripts. Where appropriate intellectual property of others was acknowledged by using appropriate references. The contribution of co-authors for the conference and the published manuscript was in training capacity, research assistance and supervisory capacity.

Signed: 

Date: 20 Jan 2019

# ABSTRACT

Simultaneous nitrification and aerobic denitrification (SNaD) is a preferred method for single stage total nitrogen (TN) removal, which was recently proposed to improve wastewater treatment plant design. However, SNaD processes are prone to inhibition by toxicant loading with free cyanide ( $\text{CN}^-$ ) possessing the highest inhibitory effect on such processes, rendering these processes ineffective. Despite the best efforts of regulators to limit toxicant disposal into municipal wastewater sewage systems (MWSSs), free cyanide ( $\text{CN}^-$ ) still enters MWSSs through various pathways; hence, it has been suggested that  $\text{CN}^-$  resistant or tolerant microorganisms be utilized for processes such as SNaD. To mitigate toxicant loading, organisms in SNaD have been observed to adopt a multiphase growth strategy to sequentially degrade  $\text{CN}^-$  during primary growth and subsequently degrade TN during the secondary growth phase. However,  $\text{CN}^-$  degrading microorganisms are not widely used for SNaD in MWSSs due to the inadequate application of suitable microorganisms (*Chromobacterium violaceum*, *Pseudomonas aeruginosa*, *Thiobacillus denitrificans*, *Rhodospirillum palustris*, *Klebsiella pneumoniae*, and *Alcaligenes faecalis*) commonly used in single-stage SNaD.

The use of  $\text{CN}^-$  degrading or resistant microorganisms for SNaD is a cost-effective method compared to the use of other methods of  $\text{CN}^-$  removal prior to TN removal, as they involve multi-stage systems (as currently observed in MWSSs). The use of  $\text{CN}^-$  degrading microorganisms, particularly when used as a consortium, presents a promising and sustainable resolution to mitigate inhibitory effects of  $\text{CN}^-$  in SNaD. However, SNaD is known to be completely inhibited by  $\text{CN}^-$  thus it is imperative to also study some thermodynamic parameters of SNaD under high  $\text{CN}^-$  conditions to see the feasibility of the process. The Gibbs free energy is significant to understand the feasibility of SNaD, it is also vital to study Gibbs free energy to determine whether or not the biological reaction is plausible. The relationship between the rate of nitrification and Gibbs free energy was also investigated.

The attained results showed that up to 37.55 mg  $\text{CN}^-/\text{L}$  did not have an effect on SNaD. The consortia degraded  $\text{CN}^-$  and achieved SNaD, with degradation efficiency of 92.9 and 97.7% while the degradation rate of 0.0234 and 0.139 mg/L/hr for ammonium-nitrogen ( $\text{NH}_4\text{-N}$ ) and  $\text{CN}^-$  respectively. Moreover, all the free Gibbs energy was describing the individual processes were found to be negative, with the lowest Gibbs free energy being -756.4 and -1830.9 Kcal/mol for nitritation and nitratation in the first 48 h of the biological, reaction respectively. Additionally, a linear relationship between the rate of  $\text{NH}_4\text{-N}$  and nitrite-nitrogen ( $\text{NO}_2\text{-N}$ ) degradation with their respective Gibbs free energy was observed. Linear model was also used to predict the relationship between  $\text{NH}_4\text{-N}$ ,  $\text{NO}_2\text{-N}$  degradation and Gibbs free energy. These results obtained showed a good correlation between the models and the experimental data with correlation efficiency being 0.94 and 0.93 for nitritation, and nitratation, respectively.

From the results found it can be deduced that SNaD is plausible under high cyanide conditions when cyanide degrading or tolerant microorganisms are employed. This can be a sustainable solution to SNaD inhibition by  $\text{CN}^-$  compounds during wastewater treatment.

Furthermore, a single strain was purified from the consortium and identified as *Acinetobacter courvalinii*. This bacterial strain was found to be able to perform sequential  $\text{CN}^-$  degradation, and SNaD; an ability associated with multiphase growth strategy of the microorganism when provided with multiple nitrogenous sources, i.e.  $\text{CN}^-$  and TN. The effect of  $\text{CN}^-$  on nitrification and aerobic denitrification including enzyme expression, activity and protein functionality of *Acinetobacter courvalinii* was investigated. It was found that  $\text{CN}^-$  concentration of up to 5.8 mg  $\text{CN}^-/\text{L}$  did not affect the growth of *Acinetobacter courvalinii*. In cultures whereby the *A. courvalinii* isolate was used, degradation rates of  $\text{CN}^-$  and  $\text{NH}_4\text{-N}$  were found to be 2.2 mg  $\text{CN}^-/\text{L}/\text{h}$  and 0.40 mg  $\text{NH}_4\text{-N}/\text{L}/\text{h}$ , respectively. Moreover, the effect of  $\text{CN}^-$  on  $\text{NH}_4\text{-N}$ , nitrate-nitrogen ( $\text{NO}_3\text{-N}$ ) and  $\text{NO}_2\text{-N}$  oxidizing enzymes was investigated, with findings indicating  $\text{CN}^-$  did not affect the expression and activity of ammonia monooxygenase (AMO), but affected the activity of nitrate reductase (NaR) and nitrite reductase (NiR). Nevertheless, a slow decrease in  $\text{NO}_2\text{-N}$  was observed after the addition of  $\text{CN}^-$  thus confirming the activity of NaR and the activation of the denitrification pathway by the  $\text{CN}^-$ . Moreover, five models' (Monod, Moser, Rate law, Haldane, and Andrew's model) ability to predict SNaD under  $\text{CN}^-$  conditions, indicated that only Rate law, Haldane and Andrew's models, were suited to predict both SNaD and  $\text{CN}^-$  degradation. Due to low degradation rates of  $\text{NH}_4\text{-N}$  and  $\text{CN}^-$ , optimization of SNaD was essential. Therefore, response surface methodology was used to optimize the SNaD under  $\text{CN}^-$  conditions.

The physiological parameters that were considered for optimization were temperature and pH; with the result showing that the optimum for pH and temperature was 6.5 and 36.5°C respectively, with  $\text{NH}_4\text{-N}$  and  $\text{CN}^-$  degradation efficiency of 50 and 80.2%, respectively. Furthermore, the degradation kinetics of  $\text{NH}_4\text{-N}$  and  $\text{CN}^-$  were also studied under the optimum conditions in batch culture reactors, and the results showed that up to 70.6% and 97.3% of  $\text{NH}_4\text{-N}$  and  $\text{CN}^-$  were simultaneously degraded with degradation rates of 0.66 and 0.41 mg/L/h, respectively. The predictive ability of RSM was further compared with cybernetic models, and cybernetic models were found to better predict SNaD under  $\text{CN}^-$  conditions. These results exhibited a promising solution in the management of inhibition effected of  $\text{CN}^-$  towards SNaD at an industrial scale.

**Keywords:** Aerobic denitrification; ammonia-oxidizing; biological nitrogen removal; cybernetic model; diauxic; free cyanide; Gibbs free energy; metabolic network; metabolism; modeling; nitrification; nitrification; nitrite-oxidizing bacteria; RSM models; simultaneous nitrification and aerobic denitrification; total nitrogen; wastewater treatment;

## DEDICATION

*I dedicate this thesis to all the family and friends that supported me throughout this journey, especial my mother (uMamthembu, Qhudeni, uMpafane, Umvelase uNgoza uMkhubukeli umakhonza egoduka), my late father (Unkwali, UBhukula, uMkwanase) and my baby Thalam who give me strength when I didn't think it was possible for me to finish my studies.*

# ACKNOWLEDGEMENTS

I would like to thank the following people and organizations:

- God for the courage and strength,
- My family for their support throughout this journey,
- Lukhanyo Yolwa for supporting me and babysitting my baby during my studies,
- My supervisors Prof. SKO Ntwampe, Dr. EI Omodanisi, and Dr. BS Chidi their assistance and guidance and technical advice throughout my studies,
- Cynthia Dlangamandla, Melody Mukandi, and Dr. Christine technical advice,
- Yolanda Mpentshu, Nkosikho Dlangamandla, Lukhanyo Mekuto and Zandile Jingxie for their technical support and advice,
- My Friends Nangamso Cawe, Mathabo Ludaka, Zandile Mdingi, Cynthia Dlangamandla and Thuletu Mbita for always being there for me throughout my hardships,
- The University Research Fund (RK16) and the National Research Foundation for financial support of this research, and
- All the postgraduate students at Bioresource Engineering Research Group (*BioERG*), Faculty of Applied Sciences, CPU.

# RESEARCH OUTPUTS

The following research outputs represent the contributions of the candidate to scientific knowledge and development during the doctoral candidacy (2017-2020):

## **DHET accredited manuscripts published/accepted for publication forming part of this thesis**

**N. Mpongwana**, S.K.O. Ntwampe, E.I. Omodanisi, B.S. Chidi, and L.C. Razanamahandry. 2019. Sustainable Approach to Eradicate the Inhibitory Effect of Free-Cyanide on Simultaneous Nitrification and Aerobic Denitrification during Wastewater Treatment. *Sustainability* 2019, 11(21), 6180; <https://doi.org/10.3390/su11216180> (Impact Factor: 2.592)

**Ncumisa Mpongwana**, Seteno K. O. Ntwampe, Boredi S. Chidi, Elizabeth I. Omodanisi. 2019. Kinetic Modelling of Free Energy for Simultaneous Nitrification and Aerobic Denitrification under High Cyanide Environments. 16<sup>th</sup> SOUTH AFRICAN International Conference on Agricultural, Chemical, Biological and Environmental Science (ACBES-19) Nov. 18-19 2019 Johannesburg (South Africa). Pp 305-306, ISBN–978-81-943403-0-0, <https://doi.org/10.17758/EARES8.EAP1119149>

**Ncumisa Mpongwana**, Seteno Karabo Obed Ntwampe, Elizabeth Ife Omodanisi, Boredi Silas Chidi, Lovasoa Christine Razanamahandry, Cynthia Dlangamandla, Melody Ruvimbo Mukandi. Bio-kinetics of simultaneous nitrification and aerobic denitrification (SNaD) by a cyanide degrading bacteria under cyanide-laden Conditions. Submitted to *Applied Sciences Manuscript ID: applsci-702267 (Accepted)* (Impact factor: 2.217)

## **Submitted manuscripts**

**N. Mpongwana**, S. K. O. Ntwampe, E. I. Omodanisi, B.S. Chidi, C. Dlangamandla, M.R. Mukandi. Significance of metabolic network modelling of total nitrogen removal in simultaneous nitrification and aerobic denitrification. Submitted to *Bioengineering (under review)*

**Ncumisa Mpongwana**, Seteno Karabo Obed Ntwampe, Lovasoa Christine Razanamahandry, Boredi Silas Chidi, Elizabeth Ife Omodanisi. Predictive capability of response surface methodology and cybernetic models for cyanogenic simultaneous nitrification and aerobic denitrification (SNaD) facilitated by cyanide-resistant bacteria. Submitted to *Microorganisms (under review)*

# LAYOUT OF THESIS

The general aim of this research study was to elucidate the metabolic network and modeling of simultaneous nitrification and aerobic denitrification (SNaD) under cyanogenic conditions using  $\text{CN}^-$  resistant/ tolerant microorganisms for SNaD as a single-stage process under  $\text{CN}^-$ . The experimental part of this study was conducted at the Cape Peninsula University of Technology, Bioresource Engineering Research Group (*BioERG*), South Africa. The references at the end of this thesis are listed in accordance with the CPUT Harvard method of referencing.

The thesis is divided into the following chapters:

- **Chapter 1:** Introduction; this chapter provides background information about total nitrogen biological removal and the challenges that affect total nitrogen removal, particularly inhibition of nitrification and aerobic denitrification by cyanide compounds. Additionally, it provides a problem statement, hypothesis, objectives, significance of study and delineation.
- **Chapter 2:** This chapter focuses on the literature consulted for which the detailed background of the developments and the challenges that are experienced during SNaD are explained, moreover, the sustainable methods to resolve these challenges are also reviewed.
- **Chapter 3:** This chapter focuses on literature consulted to highlight the significance of metabolic network modeling in wastewater treatment plants; furthermore, the cybernetic modeling approach is also reviewed.
- **Chapter 4:** This chapter lists the materials and methods used to achieve the aims of the study.
- **Chapter 5:** This chapter focuses on the kinetic modelling of free energy for SNaD under a high cyanide environment.
- **Chapter 6:** This chapter focuses on the biokinetics of SNaD by cyanide degrading bacteria under cyanide laden conditions.
- **Chapter 7:** The results on the predictive capability of RSM and cybernetic models for cyanogenic SNaD facilitated by cyanide resistant bacteria, are listed in this chapter.
- **Chapter 8:** This chapter presents the overall summary and conclusions and also provides answers to the research question listed in Chapter 1. Recommendations for future research, are also listed in this chapter.



- **Chapter 9:** This chapter consists of literature citations used in this study, in accordance with the CPUT Harvard style of referencing.

# TABLE OF CONTENTS

DECLARATION .....	ii
ABSTRACT.....	iii
DEDICATION.....	v
ACKNOWLEDGEMENTS .....	vi
RESEARCH OUTPUTS.....	vii
LAYOUT OF THESIS .....	viii
LIST OF FIGURES .....	14
LIST OF TABLES.....	16
GLOSSARY .....	18
CHAPTER 1 .....	23
INTRODUCTION .....	23
1.1. Introduction.....	23
1.2. Problem statement.....	23
1.3. Hypothesis.....	24
1.4. Research questions.....	24
1.5. Aims and objectives.....	24
1.6. Delineation of the study .....	25
1.7. Significance of the research.....	25
CHAPTER 2: .....	28
LITERATURE REVIEW 1 .....	28
2.1. Introduction.....	28
2.2. Nitrification and Subsequent Denitrification: An Obsolete Technology.....	29
2.3. Recent Advances in Nitrification and Denitrification Processes: Future Perspectives.....	34
2.4. Overall Remarks on Simultaneous Nitrification and Aerobic Denitrification (SNaD): Advances and Limitations.....	37
2.5. Challenges in Simultaneous Nitrification and Aerobic Denitrification (SNaD) processes.....	37
2.6. Prevention of Biomass Washout During the Start-Up of SNaD .....	38
2.7. Inhibition Mechanism of Simultaneous Nitrification and Aerobic Denitrification by Pollutants ...	39
2.8. FCN Wastewater in Municipal Wastewater Sewage Systems (MWSSs) and Its Impact on Nitrification and Denitrification: A Culture of Illegal Wastewater Dumping .....	40
2.9. Current Solutions to the Challenges in Simultaneous Nitrification and Aerobic Denitrification (SNaD).....	41
2.9.1. Physical Process Used as Remedial Strategy to Decrease the Inhibitory Effect of FCN on SNaD.....	41
2.9.2. Biological Systems Responsible for Lowering FCN Concentration Prior to SNaD.....	42
2.9.3. Overall Remarks on Remedial Strategies in Place to Mitigate FC in SNaD .....	43

2.10. A Proposed Sustainable Solution: Environmental Benignity at the Core of SNaD Development	43
2.10.1. Application of FCN Resistant Microorganisms in Simultaneous Nitrification and Aerobic Denitrification (SNaD) Under Cyanogenic Conditions	43
2.11. Conclusion	45
CHAPTER 3:	48
LITERATURE REVIEW 2	48
3.1. Introduction	48
3.2. Biological wastewater treatment: Total Nitrogen (TN) removal	49
3.3. Microbial population and contaminant metabolism in wastewater	51
3.3.1. Microbial metabolic interactions in wastewater treatment	51
3.3.2. Microbial metabolism during the removal of TN in wastewater treatment plant	52
3.4. The role of Thermodynamics and Stoichiometric analysis in metabolic networking	53
3.5. Metabolic pathways identified in the biological treatment of wastewater	53
3.6. Metabolic network modeling in wastewater treatment	55
3.6.1. Significance of metabolic network modeling in the wastewater treatment	55
3.6.2. Suitable metabolic network modeling approaches for biological wastewater treatment	56
3.6.3. Flux balance approach (FBA) for modeling wastewater treatment plant	61
3.6.4. Cybernetic modeling	62
3.7. Conclusions	64
CHAPTER 4:	66
MATERIALS AND METHODS	66
4.1. General background	66
4.1. PHASE 1: Thermodynamic evaluation of SNaD under cyanide-laden conditions	66
4.1.1. Isolation and Inoculum Development	66
4.1.2. Reactor Experimental Runs	66
4.1.3. Bioenergetic/Thermodynamic Models	67
4.2. PHASE 2: Assessing the predictive capability of existing models	68
4.2.1. Isolation and identification of the bacterial isolate of interest	68
4.2.2 Batch culture experiments	68
4.2.3. Enzyme extraction	69
4.2.4. Analytical procedure(s)	69
4.2.5. Kinetics model developed	69
4.2.6. Regression of experimental data and estimation of model kinetic parameters	70
4.2.7. Data handling and kinetic parameters	71
4.3. PHASE 3: Optimisation and evaluation of predictive ability of RSM and Cybernetic models	71
4.4. Microbial isolation and identification	71
4.5. Response surface methodology	71
4.5.1. Central composite design experiments	71

4.6. Statistics analyses.....	73
4.7. Cybernetic model.....	73
4.7.1. Batch culture experiment .....	73
4.7.2. Enzyme activity assessments .....	74
4.7.3. Analytical procedure .....	74
4.7.4. Model development.....	74
CHAPTER 5: .....	78
<b>KINETIC MODELLING OF FREE ENERGY FOR SIMULTANEOUS NITRIFICATION AND AEROBIC DENITRIFICATION UNDER HIGH CYANIDE ENVIRONMENTS .....</b>	<b>78</b>
5.1. Introduction.....	78
5.2. Objectives .....	78
5.3. Materials and methods .....	79
5.4. Result and Discussion .....	79
5.5. Conclusion .....	83
CHAPTER 6: .....	85
<b>BIO-KINETICS OF SIMULTANEOUS NITRIFICATION AND AEROBIC DENITRIFICATION (SNAD) BY A CYANIDE DEGRADING BACTERIA UNDER CYANIDE-LADEN CONDITIONS ..</b>	<b>85</b>
6.1. Introduction.....	85
6.2. Objectives .....	86
6.3. Materials and methods .....	86
6.4. Results and Discussion .....	87
6.4.1. Identification of bacterial Isolate .....	87
6.4.2. Degradation kinetics of Cyanide and NH <sub>4</sub> -N .....	87
6.4.3. Effect of Cyanide on AMO, NaR, and NiR .....	95
6.5. Conclusions.....	97
CHAPTER 7: .....	99
<b>PREDICTIVE CAPABILITY OF RESPONSE SURFACE METHODOLOGY AND CYBERNETIC MODELS FOR CYANOGENIC SIMULTANEOUS NITRIFICATION AND AEROBIC DENITRIFICATION (SNAD) FACILITATED BY CYANIDE-RESISTANT BACTERIA .....</b>	<b>99</b>
7.1. Introduction.....	99
7.2. Objectives .....	101
7.3. Materials and methods .....	101
7.4. Results and discussion .....	102
7.4.1. Predictive ability of Response Surface Methodology .....	102
7.4.1.1. Analysis of variance (ANOVA) for TN removal.....	102
7.4.1.2. Batch reactor experiment and model simulations .....	104
7.5. Prediction ability of RSM in comparison to cybernetic models .....	105
7.6. TN/ CN <sup>-</sup> biocatalysis.....	107

7.7. Conclusion .....	108
CHAPTER 8: .....	111
SUMMARY AND CONCLUSION.....	111
8.1 Summary and Conclusions.....	111
8.2 Recommendations for future work .....	112
CHAPTER 9: .....	115
CHAPTER 10: .....	132
APPENDIX A.....	132

# LIST OF FIGURES

- Figure 2.1.** Diagram representing nitrification and subsequent denitrification. (30)
- Figure 2.2.** Diagram representing (A) different simultaneous nitrification and aerobic denitrification mechanisms as well as simultaneous nitrification and aerobic denitrification via nitrite route. (B) Representation of floc in activated sludge with aerobic and anoxic zone. (35)
- Figure 2.3.** Principles of sequence batch reactor (SBR) and how interchangeable they can be with membrane biofilm reactors (MBfR) systems. (36)
- Figure 3.1.** Metabolic network and pathways for TN removal by AOB and NOB. (49)
- Figure 3.2.** The role of the ATP–ADP cycle in cell metabolism during wastewater treatment (Sokic-Lazic et al., 2008). (55)
- Figure 3.3.** A simple fictional metabolic network (Ao, 2005). (56)
- Figure 4.1.** Simplified metabolic network diagram of SNaD under cyanide-laden conditions (74)
- Figure 5.1.** Graphs representing simultaneous nitrification, denitrification, and cyanide degradation. A: nitrification and Cyanide degradation. B: NO<sub>2</sub>-N and NO<sub>3</sub>-N accumulation and degradation. (80)
- Figure 5.2.** Parity plots of predicted rate nitrification values versus experimental values. simulations of the linear model data into a rate of NH<sub>4</sub>-N degradation versus Gibbs free energy data and  $\Delta G$  as a function of [product]/[reactant]. (82)
- Figure 5.3.** Parity plots of predicted rate nitrification values versus experimental values. simulations of the linear model data into a rate of NO<sub>4</sub>-N degradation versus Gibbs free energy data and  $\Delta G$  as a function of [product]/[reactant]. (83)
- Figure 6.1.** Biodegradation kinetics of NH<sub>4</sub>-N and CN<sup>-</sup> by *Acinetobacter courvalinii*. A: Growth of *Acinetobacter courvalinii*, sequential degradation of CN<sup>-</sup> and NH<sub>4</sub>-N. B: NO<sub>3</sub>-N and NO<sub>2</sub>-N accumulation and degradation. (89)
- Figure 6.2.** Parity plots of predicted values versus experimental values. Assimilations of the model data into NH<sub>4</sub>-N degradation experimental data (Rate law, Haldane, and Andrew). (91)
- Figure 6.3.** Parity plots of predicted values versus experimental values. Assimilations of the model data into CN<sup>-</sup> degradation experimental data (Rate law, Haldane, and Andrews). (93)

**Figure 6.4.** The activity of  $\text{NH}_4\text{-N}$ ,  $\text{NO}_3\text{-N}$  and  $\text{NO}_2\text{-N}$  oxidizing enzymes and  $\text{CN}^-$  degrading enzyme. A: Effect of  $\text{CN}^-$  on the induction of  $\text{NH}_4\text{-N}$ ,  $\text{NO}_3\text{-N}$  and  $\text{NO}_2\text{-N}$  oxidizing enzymes by *A. courvalinii*. B: Effect of  $\text{CN}^-$  on free cell  $\text{NH}_4\text{-N}$ ,  $\text{NO}_3\text{-N}$  and  $\text{NO}_2\text{-N}$  oxidizing enzymes (96)

**Figure 7.1.** Surface response plot showing the interaction between pH, Temperature and TN removal. (103)

**Figure 7.2.** Degradation kinetics of TN and cyanide in a batch culture reactor. A: TN and  $\text{CN}^-$  degradation and cell concentration over time. B: model fitting into biomass plot. (104)

**Figure 7.3.** A comparison of the prediction ability of RSM and cybernetic models. A: prediction of TN removal efficiency by RSM model; B: parity plot comparing predicted total nitrogen removal efficiency and actual total nitrogen removal efficiency by RSM; C: Rate of TN removal predicted by cybernetic model; D: parity plot for comparing predicted rate of TN removal with actual rate of TN removal by cybernetic model. (105)

**Figure 7.4.** (a)  $\text{NH}_4\text{-N}$  and  $\text{CN}^-$  removal/ degradation. (b)  $\text{NO}_2\text{-N}$ , and  $\text{NO}_3\text{-N}$  removal. simulation of cybernetic model into (c) level of key enzyme  $e_1$  over time. (d) level of key enzyme  $e_2$  over time. (e) level of key enzyme  $e_3$  over time. (f) level of key enzyme  $e_4$ . (108)

**Figure 10.1.** Simultaneous nitrification and aerobic denitrification performed by cyanide degrading mix consortia under high cyanide conditions. (a)  $\text{NH}_4\text{-N}$  and  $\text{CN}^-$  degradation profile. (b)  $\text{NO}_2\text{-N}$  and  $\text{NO}_3\text{-N}$  degradation and accumulation profile. (132)

**Figure 10.2.** metagenomics report for the consortium. (a): Kingdom classification. (b): Phylum classification. (c): Class classification. (d); Order classification. E: Family classification. (134)

**Figure 10.3.** Parity plots of predicted values versus experimental values. Assimilations of the model data into  $\text{NH}_4\text{-N}$  degradation experimental data (Monod and Moser). (a) parity plot for Monod equation. (b) simulation of predicted rate of reaction by Monod into experimental data. (c) parity plot for Moser equation. (d) simulation of predicted rate of reaction by Moser into experimental data. (136)

**Figure 10.4.** Parity plots of predicted values versus experimental values. Assimilations of the model data into  $\text{CN}^-$  degradation experimental data (Monod, Moser and Andrews). (a) parity plot for Monod equation. (b) simulation of predicted rate of reaction by Monod into experimental data. (c) parity plot for Moser equation. (d) simulation of predicted rate of reaction by Moser into experimental data. (137)

# LIST OF TABLES

<b>Table 2.1.</b> Genes responsible for nitrification and denitrification and their functions (Clough et al., 2017).	(31-34)
<b>Table 2.2.</b> Studies that have successfully used cyanide degrading microorganisms for nitrification and aerobic denitrification.	(44-45)
<b>Table 3.1.</b> Organisms used for TN removal different wastewater sources (McLellan et al., 2002).	(50)
<b>Table 3.2.</b> Diagram representing microbial metabolic interaction versus ecological interaction. Where blue circles are species A, red circles are species B, and squares are substrates.	(51-52)
<b>Table 3.3.</b> Organic constituents and nitrogen matters other than those identified in wastewater treatment plants (Wagner et al., 2002).	(57-61)
<b>Table 4.1.</b> The independent variables included in central composite design experiments and their high, medium, low concentrations.	(72)
<b>Table 4.2.</b> Central composite design variables.	(72-73)
<b>Table 5.1.</b> Model variables for nitrification and nitratation	(80)
<b>Table 6.1.</b> Estimated kinetic parameter values for the models for $\text{NH}_4\text{-N}$ degradation, a rate limiting step in nitrification.	(89-90)
<b>Table 6.2.</b> Estimated values of kinetic parameters for the models for $\text{CN}^-$ degradation	(92)
<b>Table 6.3.</b> Kinetic parameters obtained from different studies assessing nitrification and aerobic denitrification.	(94-95)
<b>Table 7.1.</b> Analysis of variance (ANOVA) of the quadratic parameters for SNaD process used for TN removal under $\text{CN}^-$ conditions.	(104)
<b>Table 7.2.</b> Model parameter estimations.	(106)
<b>Table 7.3.</b> Statistical analysis of RSM and cybernetic models for SNaD under $\text{CN}^-$ conditions.	(107)



**Table 10.1.** Estimated values of kinetic parameters for the models for  $\text{NH}_4\text{-N}$  degradation, a limiting step in nitrification. (134)

**Table 10.2.** Estimated values of kinetic parameters for the models for  $\text{CN}^-$  degradation, a limiting step in nitrification. (134-235)

# GLOSSARY

Definition (units)	Abbreviations/Symbols
Adenosine 5'-triphosphate	ATP
Ammonia monooxygenase	AMO
Ammonia oxidising bacteria	AOB
Ammonium nitrogen	NH <sub>4</sub> -N
Anaerobic regulation of arginine	ANR
Analysis of variance	ANOVA
Anoxic ammonium oxidising bacteria	AnAOB
Biological nitrogen removal	BNR
Biomass yield coefficient (CFU/g substrate)	Y <sub>x/s</sub>
Cell concentration (CFU/mL)	X
Central composite design	CCD
Chemical oxygen demand	COD
Coefficients of the interaction parameters	β <sub>ij</sub>
Coefficients of the linear parameters	β <sub>i</sub>
Coefficients of the quadratic parameter	β <sub>ii</sub>
Colony-Forming Unit	CFU
Concentration of the Pollutant (mg/L)	C <sub>a</sub>
Constant term	β <sub>0</sub>
Consumption rate of nitrogenous source (mg/g.h)	r <sub>i</sub>
Correlation coefficient	R <sup>2</sup>

Cyanide degrading bacteria	CDB
Cyanide hydratases	CHTs
Cyanide monooxygenase	CNO
Degradation rate constant of the enzyme (mg/g.h)	$b$
Degree Celsius	°C
Denaturing gradient gel electrophoresis	DGGE
Dilution term due to growth rate (mg/g.h)	$r_g$
di-Nitrogen	N <sub>2</sub>
Dissimilative nitrate respiration regulator	DNR
Dissolved oxygen	DO
Electrodialysis	ED
Extracellular polymeric substances	EPS
Flavin adenine dinucleotide	FADH <sub>2</sub>
Fluorescence in-situ hybridization	FISH
Flux balance approach	FBA
Free ammonium	FA
Free cyanide	F-CN
Free energy change (Kcal/mol)	$\Delta G$
Fumarate and nitrate reductase	FNR
Gibbs energy (Kj/mol)	$\Delta G$
Heme iron atom of the heme protein	His-Fe <sup>2+</sup> -His
Hydrogen cyanide	HCN
Hydroxylamine oxidoreductase	HAO

Inductive rate (mg/g.h)	$\alpha_{ei}$
Ion exchange	IE
Linear function	F
Maximum level of enzyme $e_i$ (mg/L)	$e_i^{max}$
Maximum rate (mg/g.h)	$r_i^{max}$
Membrane biofilm reactors	MBfRs
Model fitting constant	n
Municipal wastewater sewage systems	MWSSs
Nicotinamide adenine dinucleotide	NADH
Nicotinamide adenine dinucleotide phosphate	NADPH
Nitrate nitrogen	NO <sub>3</sub> -N
Nitrate reductase	Nar
Nitric and nitrous oxide reductases	NorB/NosZ
Nitric oxide	NO
Nitric oxide reductase	Nor
Nitrite nitrogen	NO <sub>2</sub> -N
Nitrite oxidoreductase	NXR
Nitrite reductase	Nir
Nitrous oxide	N <sub>2</sub> O
Nitrous oxide reductase	Nos
Number of variables	k
Polyhydroxyalkanoates	PHA
Polymerase chain reaction	PCR

Potassium cyanide	KCN
Rate of degradation (mg/h)	$r$
Represents the variables	$x_i$
Residual associated to the experiments.	$\varepsilon$
Response surface methodology	RSM
Saturation constant (mg/L)	$K_i$
Sequence batch reactor	SBR
Simultaneous nitrification denitrification	SNaD
Specific degradation rate of the substrate	$V_m$
Specific growth rate ( $\text{h}^{-1}$ )	$\mu$
Substrate constant (mg/ L)	$K_i$
Substrate inhibition constant (mg/ L)	$K_s$
Temperature ( $^{\circ}\text{C}$ )	T
Terminal restriction fragment length polymorphism	T-RFLP
Thiocyanate	SCN
Time (h)	t
Total nitrogen	TN
Universal gas constant	R
Wastewater treatment plant	WWTP

# **CHAPTER 1**

## **GENERAL INTRODUCTION**

# CHAPTER 1

## INTRODUCTION

### 1.1. Introduction

Human activities such as the use of nitrogen-rich fertilizers result in excessive nitrogen being disposed into municipality wastewater treatment plants (WWTP) (Medhi *et al.*, 2017). Nitrification and denitrification have been extensively used in WWTP to treat reactive nitrogen into less toxic compounds. These processes are performed by ammonia oxidising bacteria (AOB) which oxidise ammonia-nitrogen ( $\text{NH}_4\text{-N}$ ) to nitrite-nitrogen ( $\text{NO}_2\text{-N}$ ) and nitrate oxidising bacteria (NOB) which further oxidises  $\text{NO}_2\text{-N}$  into nitrite-nitrogen ( $\text{NO}_3\text{-N}$ ) (Alzate Marin *et al.*, 2016). However, nitrification and denitrification are sensitive to toxic pollutant loadings such as free cyanide, i.e., as little as 1-2 mg/L of cyanide ( $\text{CN}^-$ ) inhibit metabolic functions of AOB and NOB, inhibiting nitrification and denitrification resulting in the deterioration in the performance of total nitrogen treatment processes (Kim *et al.*, 2011a).

Regardless of the toxicity of  $\text{CN}^-$  to biological processes that are performed in WWTP, industrial wastewater containing high  $\text{CN}^-$  loading still enter municipality WWTP (Akinpelu *et al.*, 2016); hence, some studies have suggested that cyanide-resistant microorganism must be used for nitrification and denitrification in order to avoid inhibition effect of  $\text{CN}^-$  (Han *et al.*, 2013b; Richards & Shieh, 1989). In order to understand nitrification and denitrification, mathematical models are developed to predict these processes. These models are crucial for proper control of the processes (Seifi & Fazaalipoor, 2012).

Some scientists have tried to model nitrification and denitrification (Khamar *et al.*, 2015); however, due to changes in metabolic functions of the microorganism in the presence of  $\text{CN}^-$ , such models would become reductant. Overall, existing models cannot be used to predict nitrification and denitrification when under cyanide conditions. Hence, this study focused on developing a simplified metabolic network and models for simultaneous nitrification and denitrification in the presence of  $\text{CN}^-$  for single-stage systems.

### 1.2. Problem statement

Nitrification and denitrification are biological processes used in WWTP for the removal of total dissolved nitrogen. However, these processes are susceptible to inhibition due to the slow growth of organisms involved in these processes. Furthermore, cyanide possesses the highest inhibition effect on these processes (Wild *et al.*, 1994). Despite the known toxicity of cyanide in biological processes; it still enters the municipality WWTP through various pathways. Hence, some studies have suggested the use of cyanide-resistant microorganisms for nitrification and denitrification (Han *et al.*, 2013; Richards & Shieh, 1989).

These microorganisms are able to thrive under high cyanide conditions by converting cyanide into less toxic compounds. Additionally, the metabolic functions of these microorganisms' changes in the presence of  $\text{CN}^-$ ; hence, the nitrification and denitrification behavior of these cyanide-resistant microorganisms is different from that of non-cyanide tolerant microorganisms. Therefore, mathematical models developed to predict the behavior of nitrification and denitrification in non-cyanide conditions cannot be used to describe nitrification and denitrification in cyanogenic conditions.

This will include the metabolic networks facilitating nitrification and denitrification. Hence, there is a need to develop metabolic network models that can be used to describe metabolic functions of nitrification and denitrification of the microorganisms under cyanogenic conditions. This will assist in proper controlling of nitrification and aerobic denitrification under cyanogenic conditions. The application of cyanogenic bacteria will be more practically applicable in WWTP.

### **1.3. Hypothesis**

Metabolic functions of bacterial strain used for nitrification and sequential denitrification differ when different toxicants are present in the wastewater thus mathematical models developed with nitrogen as a sole toxicant cannot suitably predict both nitrification and denitrification in cyanogenic conditions.

### **1.4. Research questions**

- Will the cyanide resistant/ tolerant microorganisms achieve SNaD under  $\text{CN}^-$  condition?
- What is the maximum concentration of  $\text{CN}^-$  can the isolated bacteria perform SNaD?
- Can the normal mathematical models predict SNaD under  $\text{CN}^-$  conditions well?
- What will be the optimum conditions for the isolated bacteria to perform SNaD under  $\text{CN}^-$  conditions?
- Can response surface methodology (RSM) models be used to predict SNaD under  $\text{CN}^-$ ?
- Can Cybernetic models be used for prediction of metabolic network of SNaD under  $\text{CN}^-$ ?

### **1.5. Aims and objectives**

**Aim 1:** Study feasibility of using cyanide resistant mix consortium for SNaD under  $\text{CN}^-$ -laden conditions.

**Objective 1:** Isolation of mix consortium from a  $\text{CN}^-$  environment.

**Objective 2:** Perform SNaD kinetic studies catalysed by the isolated mix consortium.



**Objective 3:** Model Gibbs free energy of the rate-limiting step (nitrification) of SNaD under  $\text{CN}^-$  conditions.

**Aim 2:** Assessing the predictive capability of different mathematical models towards simultaneous nitrification and aerobic denitrification.

**Objective 1:** Isolation of cyanide resistant single bacterial strain from the isolated mix consortium.

**Objective 2:** Assessing the ability of the isolated bacteria to perform SNaD under cyanogenic conditions.

**Objective 3:** Evaluating the predictive ability of different mathematical model towards removal/ degradation of multiple nitrogenous source ( $\text{NH}_4\text{-N}$  and  $\text{CN}^-$ )

**Objective 4:** Study the effect of free  $\text{CN}^-$  on nitrifying and denitrifying enzymes.

**Aim 3:** Optimisation of SNaD under  $\text{CN}^-$  conditions and development of cybernetic models for SNaD prediction.

**Objective 1:** Study Physico-chemical (pH and Temperature) conditions that affect SNaD and  $\text{CN}^-$  degradation.

**Objective 2:** Develop a simplified SNaD metabolic network for the development of a simple cybernetic model.

**Objective 3:** Comparison of RSM and cybernetic model predictive capability towards SNaD under  $\text{CN}^-$  conditions.

## 1.6. Delineation of the study

This study did not look at:

- The detailed of the gene responsible for simultaneous nitrification and aerobic denitrification, and
- The toxicity of the isolated strain on the wastewater treatment plant resident bacterial strains.

## 1.7. Significance of the research

$\text{CN}^-$  enters wastewater treatment plants from different industrial sources and inhibits biological processes performed in traditional wastewater treatment plants; hence, the use of cyanogen resistant microorganisms is recommended especially for sensitive processes such as nitrification and denitrification. In order to control these processes under cyanogenic conditions, metabolic network models that will predict the behavior of these processes under cyanogenic conditions are required; hence, the aim of this study is to

develop such a modeling network model that will describe nitrification and denitrification under cyanogenic conditions.

# CHAPTER 2

## LITERATURE REVIEW 1

**Published as:** Mpongwana, N., Ntwampe, S.K.O., Omodanisi, E.I., Chidi, B.S. & Razanamahandry. L.C. 2019. Sustainable Approach to Eradicate the Inhibitory Effect of Free-Cyanide on Simultaneous Nitrification and Aerobic Denitrification during Wastewater Treatment. *Sustainability* 2019, 11(21), 6180; <https://doi.org/10.3390/su11216180>

# CHAPTER 2:

## LITERATURE REVIEW 1

### 2.1. Introduction

Excessive nitrogenous compounds in wastewater discharged into water bodies such as rivers can result in dissolved oxygen (DO) depletion and eutrophication in the receiving rivers (Ali & Okabe, 2015). Due to governmental regulations in place to regulate treated wastewater discharge standards, it is important that wastewater containing a high concentration of nitrogenous compounds must be treated prior to discharge (Duan et al., 2015). This type of wastewater can be treated by biological processes such as simultaneous nitrification and aerobic denitrification (SNaD) or Physico-chemical processes such as ammonium stripping, chemical precipitation of ammonia, electrochemical conversion, and many other treatment technologies (Norton-Brandão et al., 2013).

However, biological treatment of total nitrogen (TN) laden wastewater via traditional methods, i.e., nitrification and subsequent anoxic denitrification in a two-step set-up, is the desired method for treatment of TN in generic municipal wastewater sewage systems (MWSSs) because these methods are efficient at a larger scale. Overall, biological treatment uses the metabolic activity of living organisms in consortia for pollutant removal, with microorganisms such as bacteria primarily being used in an agglomerated symbiotic biological potpourri of reactions in sequential or parallel processes. Nonetheless, biological treatment methods are not always suitable to treat some industrial wastewater due to the toxicity of organic and other substances therein (Oller et al., 2011), which reduces these methods' efficiency.

An example is coking wastewater, which contains a high concentration of free cyanide (FCN), which decomposes to ammonium-nitrogen, nitrates, and nitrite, herein referred to as TN and phenolics. Such wastewater, if treated in an inefficient primary process, would culminate in the inhibition of biologicals of downstream processes such as nitrification and denitrification, resulting in the disposal of partially treated wastewater still containing a high concentration of TN. Moreover, when primary and secondary wastewater treatment processes experience increased toxicant loading such as FCN from industrial processes in combination with secondary pollutants, e.g., phenolics or heavy metals, the discharged FCN containing wastewater would further contribute to receiving surface water pollution, a challenge which is further exacerbated by runoff from agricultural operations whereby the use of cyanogen-based pesticides is still in practice, especially in developing countries. In certain instances, the remedial strategy implementable to minimize FCN inhibition toward primary and secondary processes such as nitrification and denitrification sometimes involves the use of adsorbents such as activated carbon as a sorbent (Kim et al., 2008) for FCN adsorption. Conversely, the application of physical processes such as activated carbon would incur

additional operational costs associated with the procurement of the adsorbent and its disposal, including regeneration if it is to be used in multi-cycle operations.

Additionally, the use of sorbents such as activated carbon is less effective in eliminating the inhibitory effect of FCN in nitrification and subsequent denitrification, particularly when periodic spillovers to these processes downstream occur and when inadvertent adsorption-desorption processes in the primary process occur due to process conditions variation, including wastewater quality changes. This can also be due to the low absorption capability of poor quality activated carbon used in some operations and because the affinity of FCN to activated carbon is low (Kim et al., 2007). Therefore, it is prudent to invest in and investigate a sustainable method to eliminate the inhibition of FCN towards nitrification and denitrification. Kim et al. (2013) suggested the use of FCN degrading bacteria to eliminate cyanide inhibition towards nitrification and subsequent denitrification. Furthermore, although both nitrification and anoxic denitrification occur as separate processes at an industrial scale (Han et al., 2014), several research studies have indicated the use of simultaneous nitrification and aerobic denitrification (SNaD), which effectively culminates in the integration of a traditional two-stage process into a single-stage process (Shoda & Ishikawa, 2015; Chen et al., 2012) with an added benefit of having a reduced footprint; albeit, there is minimal literature on the utilization of SNaD as a sustainable process in which FCN degrading bacterial consortia are used, a practice yet to be adopted at an industrial scale.

## **2.2. Nitrification and Subsequent Denitrification: An Obsolete Technology**

The secondary treatment in wastewater uses biological processes due to its cost-effectiveness and environmental benignity compared to physical treatment technologies, which are expensive and produce toxic by-products. Biological treatment plays a crucial role during nutrient removal and for the prevention of eutrophication in receiving water bodies (Banning et al., 2015). Nitrification and subsequent denitrification are among the important biological processes that are currently being successfully employed in MWSSs for the removal of TN (Oller et al., 2011). Generally, the process of TN removal is initiated with aerobic ammonium-nitrogen ( $\text{NH}_4\text{-N}$ ) oxidation in a two-step process with the first step being nitrification and the second being denitrification. During nitrification, ammonia-oxidizing bacteria (AOB) oxidize  $\text{NH}_4\text{-N}$  to  $\text{NH}_2\text{OH}$  through ammonia monooxygenase (AMO) biocatalysis; the  $\text{NH}_2\text{OH}$  is oxidized further into  $\text{NO}_2^-$  through hydroxylamine oxidoreductase (HAO) (Banning et al., 2015).

This process is known as nitrification through the nitrite route and is ideal as it reduces carbon source requirements by up to 40%, thus reducing costs associated with carbon source utilization. The second step involves the oxidation of  $\text{NO}_2^-$  into  $\text{NO}_3^-$  by nitrite-oxidizing bacteria (NOB) catalyzed by nitrite oxidoreductase (NOR) (Ge et al., 2015b; Levy-Booth et al., 2014). Although nitrification is successfully applied in MWSSs for TN removal, it is a highly sensitive process (Shoda & Ishikawa, 2014). The effluent from nitrification is further processed in an anaerobic reactor for anoxic denitrification, whereby microorganisms oxidize

nitrites into gaseous nitric oxide (NO) and nitrous oxide (N<sub>2</sub>O) bio-catalytically facilitated by nitric and nitrous oxide reductases (NorB/NosZ). Furthermore, these exhaust gasses are reduced into di-nitrogen (N<sub>2</sub>) gas, which acts as a terminal acceptor for electron transport phosphorylation under anaerobic conditions (Toyoda et al., 2015). Anoxic denitrification also catalyzes the formation of the N–N bond from process (denitrification) intermediates, i.e., NO and N<sub>2</sub>O (Clough et al., 2017). Nitrification and denitrification pathways, as well as the enzymes involved, can be depicted summarily in Figure 2.1.

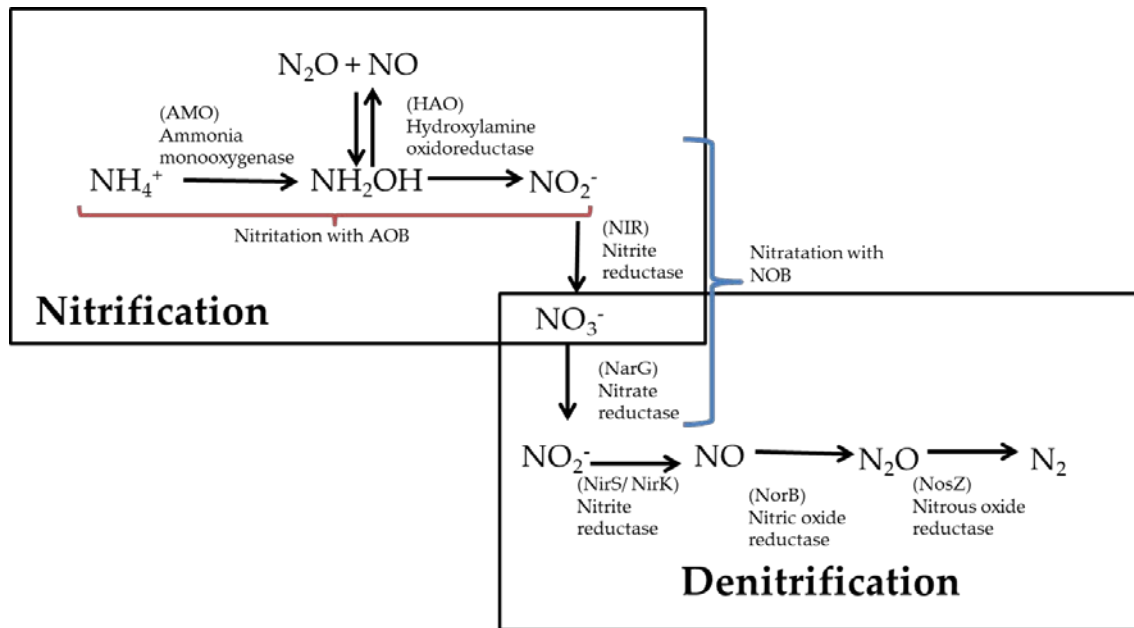


**Figure 2.1.** Diagram representing nitrification and subsequent denitrification.

Denitrification was also proven to occur under aerobic conditions (He et al., 2016); hence, this development offered a possibility for SNaD that is more cost-effective for TN removal than the traditional nitrification and the subsequent denitrification processes currently used in MWSSs (Shoda & Ishikawa, 2015; Chen et al., 2012). Some of the microorganisms that were proven to carry out denitrification under completely aerobic conditions include *Pseudomonas alcaligenes* AS-1, *Pseudomonas* species (sp.) 3–7, *Pseudomonas* sp. *Rhodoferax ferrireducens*, *Agrobacterium* sp. LAD9, *Rhodococcus* sp. CPZ 24, *Bacillus subtilis* A1, *Pseudomonas stutzeri* YZN-001, *Acinetobacter calcoaceticus* HNR, *Bacillus methylotrophicus* L7, *Diaphorobacter* sp., *Acinetobacter* sp. Y1, *Acinetobacter junii* YB, and *Marinobacter* sp (Shoda & Ishikawa, 2015; Chen et al., 2012; Zhang et al., 2012).

In addition, a number of other aerobic denitrifying bacteria have been isolated and identified, e.g., *Paracoccus* (*Micrococcus*) *denitrificans*, *Hyphomicrobium* strains, *Hyphomicrobium vulgare*, *Moraxella* species, and *Kingella denitrificans* (Liu et al., 2016). Although nitrification and denitrification were proven to be sustainable methods for treating TN, more research was done to improve these processes such that

they are more sustainable, more cost-effective, and easy to operate. Some of the important genes and the processes that are responsible for nitrification and denitrification are highlighted in Table 2.1.

**Table 2.1.** Genes responsible for nitrification and denitrification and their functions (Clough et al., 2017).

Category of Affected Process	Gene or Locus	Encoded Gene Product and Their Functions
Regulation	<i>anr</i>	Fumarate and nitrate reductase (FNR)-like global redox regulator for the expression of denitrification genes.
	<i>Dnr, fnrD</i>	FNR-like regulator that affects the expression of <i>nirS</i> and <i>norCB</i> .
	<i>Fixk<sub>2</sub></i>	FNR-like regulator that affects anaerobic growth on nitrate.
	<i>fnrP</i>	FNR-like regulator that affects the expression of <i>narGH</i> .
	<i>narL</i>	Nitrate responsive transcription factor of <i>Pseudomonas</i> of a <i>narXL</i> two-component system.
	<i>nirI</i>	A membrane protein with similarity to <i>NosR</i> affects <i>nirS</i> expression.
	<i>nirR</i>	<i>Pseudomonas</i> locus that affects the synthesis of <i>nirS</i> and <i>LysR</i> regulator.
	<i>nirY (orf 286)</i>	FNR-like regulator that affects expression <i>nirS</i> and <i>norCB</i> in <i>Paracoccus</i> and <i>Rhodobacter sp.</i>
	<i>nnrS</i>	Activate transcription of <i>nirK</i> and <i>nor</i> genes in <i>Rhodobacter sphaeroides</i> .
	<i>nosR</i>	Membrane-bound regulator required for transcription of <i>nosZ</i> .
	<i>rpoN</i>	Sigma factors affect denitrification in <i>Ralstonia eutropha</i>
Nitrate respiration	<i>narD</i>	Plasmid bone locus for <i>eutropha</i> respiratory nitrate reduction.
	<i>narG</i>	$\alpha$ -subunit of nitrate reductase respiration that binds to molybdopterin guanine dinucleotide (MGD).

	<i>narH</i>	B-subunit of nitrate reductase that binds to Fe-S cluster.
	<i>narI</i>	Cytochrome b subunit of respiratory nitrate reductase.
	<i>narJ</i>	Protein required for nitrate reductase assembles.
Periplasmic nitrate reduction	<i>napA</i>	The large subunit of periplasmic of nitrate reductase that binds to bis-molybdopterin guanine dinucleotide (MGD) and Fe-S cluster.
	<i>napB</i>	Small subunit of periplasmic of nitrate reductase, a diheme cytochrome c.
	<i>napD</i>	Cytoplasmic protein with presumed maturation function, homologous to <i>Escherichia Coli napD</i> (YojF).
	<i>napE</i>	Putative monotopic membrane protein; there are no known homologs.
Nitrite respiration	<i>nirB</i>	Cytochrome <i>c</i> <sub>552</sub> .
	<i>nirC</i>	Mono-heme cytochrome c with a putative function in <i>NirS</i> maturation.
	<i>nirK, nirU</i>	Cu-containing nitrite reductase.
	<i>nirN orf507</i>	It affects anaerobic growth and in-vivo nitrite reduction, similar to <i>NirS</i> .
	<i>nirQ</i>	Gene product that affects catalytic functions of <i>NirS</i> and <i>NorCB</i> .
	<i>nirS (denA)</i>	Cytochrome cd, nitrate reductase.
Heme D <sub>1</sub> Biosynthesis	<i>nirD</i>	Gene product affects heme D. Biosynthesis or processing.
	<i>nirE</i>	S-Adenosyl-L-Methionine uroporphyrinogen III methyltransferase.
	<i>nirF</i>	Needed for heme D biosynthesis and processing; similar to <i>NirS</i> .
	<i>nirG</i>	Gene product affects heme D. Biosynthesis or processing.



	<i>nirH</i>	Gene product affects heme D. Biosynthesis or processing.
	<i>nirJ, orf393</i>	Needed for heme D biosynthesis and processing; similar to PqqE, <i>NifB</i> , and <i>MoaA</i> .
	<i>nirL</i>	Gene product affects heme D. Biosynthesis or processing.
NO respiration	<i>norB</i>	Cytochrome b subunit of NO reductase.
	<i>norC</i>	Cytochrome c subunit of NO reductase.
	<i>norD, orf6</i>	Affect availability under denitrifying conditions.
	<i>norE, orf2, orf175</i>	Membrane protein: homologous with COX III.
	<i>norF</i>	Affect NO and nitrite reductase.
	<i>norQ</i>	Affect <i>NirS</i> and <i>NorCB</i> function; homolog of <i>NirQ</i> .
N <sub>2</sub> O respiration	<i>Fhp</i>	<i>R. eutropha</i> flavohemoglobin affects N <sub>2</sub> O and NO reduction.
	<i>nosA, oprC</i>	Channel-forming outer membrane protein; Cu-processing for <i>NosZ</i> .
	<i>nosD</i>	Periplasmic plastic involved in Cu insertion into <i>NosZ</i> .
	<i>nosF</i>	ATP or GDP binding protein involved in Cu insertion into <i>NosZ</i> .
	<i>nosL</i>	Part of <i>nos</i> gene cluster; putative outer membrane lipoprotein.
	<i>nosX</i>	Affect nitrous oxide reduction in <i>Sinorhizobium meliloti</i> .
	<i>nosY</i>	Inner membrane protein involved in Cu processing for <i>NosZ</i> .
	<i>nosZ</i>	Nitrous oxide reductase.
Electron transfer	<i>azu</i>	Azurin.
	<i>cycA</i>	Cytochrome C <sub>2</sub> (C <sub>550</sub> ).
	<i>napC</i>	Tetraheme cytochrome c; homologous to <i>NirT</i> .

	<i>nirM</i> ( <i>denB</i> )	Cytochrome C <sub>551</sub> .
	<i>nirT</i>	Putative membrane-anchored tetraheme c-type cytochrome.
	<i>paz</i>	Pseudoazurin.
Functionally unassigned	<i>Orf396</i>	A putative 12 span membrane protein of <i>Pseudomonas stutzeri</i> homologous to <i>NnrS</i> .
	<i>nirX</i>	A <i>Paracoccus</i> putative cytoplasmic protein; homologous to <i>NosX</i> .
	<i>orf7, orf63</i>	<i>Pseudomonas</i> gene downstream of <i>dnr</i> and <i>fnrD</i> .
	<i>orf247</i>	Putative member of the short-chain alcohol dehydrogenase family.

### 2.3. Recent Advances in Nitrification and Denitrification Processes: Future Perspectives

Denitrification was believed to occur under completely anoxic conditions (Shoda & Ishikawa, 2015; Chen et al., 2012), while nitrification emerged as an aerobic process (Zhang et al., 2012). Furthermore, the growth of nitrifiers depends on DO, which is lethal to traditional denitrifiers. Conversely, some microorganisms that are capable of heterotrophic nitrification and aerobic denitrification have been reported; hence, SNaD has recently drawn attention due to its potential to reduce cost related to the second anoxic tank whereby denitrification would have occurred (He et al., 2016; Ji et al., 2015; Khardenavis et al., 2007).

Additionally, aerobic denitrification can also regulate and maintain the pH in the reactor since nitrification causes acidification (Zhang et al., 2012). Aerobic denitrification occurs in two ways—the first is due to aerobic respiration aided by an enzyme known as periplasmic nitrite reductase (NAR)—see Figure 2.2 (A). This enzyme is essential for the conversion of nitrate to nitrite under aerobic conditions (He et al., 2016). However, due to the sensitivity of N<sub>2</sub>O reduction enzymes to DO, a significant amount of NO and N<sub>2</sub>O are emitted to the environment (Zheng et al., 2014). The second mechanism is through the transfer of DO into the activated sludge flocs for nitrification, which results in the diffusion competition whereby the DO consumption becomes greater in the outer zone of the floc, thus reducing DO penetration into the interior of the floc and leading to an anoxic zone in the center [see Figure 2.2 (B)] of flocs, which is suitable for denitrification (Pal et al., 2015).

The increase in operational costs resulting from the dosing of synthetic and industrial-grade chemicals in the biological MWSSs (Chen et al., 2009) was a major driver for SNaD development for a low-cost and environmentally benign process. This involves the use of agricultural waste to sustain microbial growth

during SNaD. The ability of SNaD microorganisms to grow onto agricultural waste is due to the availability of trace elements of micro and macro-nutrients on the waste itself, which can serve as readily available nutrient sources and a biomass immobilization matrix for microbial proliferation (Ntwampe & Santos, 2013; Santos et al., 2013).

Mekuto et al. (2013) also proved that agricultural waste can be used as a sole supplementation source of microbial growth during biodegradation of FCN-TN. However, the microorganism or consortia may also convert some unintentional sources within the agricultural waste into undesirable and desirable biomolecules such as citric, lactic, succinic acid, and alcohols (Sauer et al., 2008) during wastewater treatment. Furthermore, these biomolecules can also cause fluctuations in the wastewater pH, which will eventually lead to the inhibition of some essential microbial populations that are responsible for the biological processes in the MWSSs.

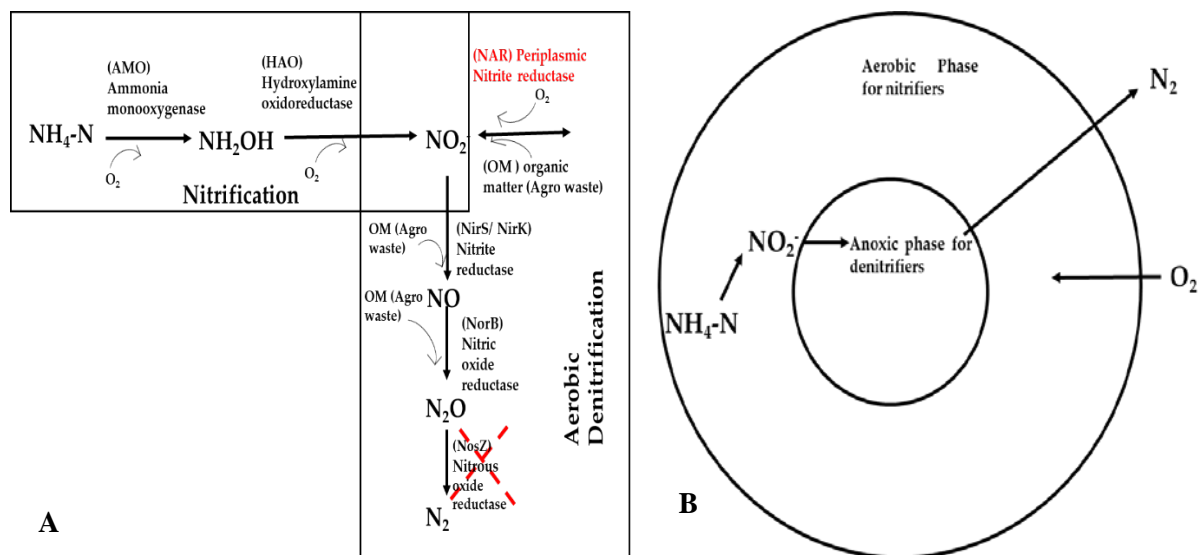


**Figure 2.2.** Diagram representing (A) different simultaneous nitrification and aerobic denitrification mechanisms as well as simultaneous nitrification and aerobic denitrification via nitrite route. (B) Representation of floc in activated sludge with aerobic and anoxic zone.

Additionally, activated sludge processes are known to be relatively high energy-consuming processes that lead to the escalation of plant operational costs, thus making biological processes less sustainable, especially in developing countries. This has led to strategies aiming at improving the operational conditions of these biological processes (Singh & Srivastava, 2011) by altering reactor configurations. Consequently, it has been reported that 2% of all electrical power in the USA is used by MWSSs, and a further 40–60% of all the energy is used for aeration and mechanical devices such as stirrers and diffusers (including nozzles), with only 5–25% of supplied air embedded oxygen being successfully transferred to the wastewater as DO and the rest becoming only pneumatically expunged oxygen in bubbles purged without transfer (Aybar et al., 2014).

As a result, the replacement of conventional activated sludge systems by cost-effective reactors was eminent for lowering operational costs and thus the adherent of the sequence batch reactor (SBR). Initially, the SBR was shown to be cost-effective for nitrification and sequential anoxic denitrification; hence, such reactors are easily adaptable to operate in a different mode and allow for both nitrification and aerobic denitrification to occur in the same tank, resulting in SNaD (Ma et al., 2017; Mahvi, 2008). Moreover, SBR is popular and is of interest since it was proven to save up to 60% of the expenses required by conventional activated sludge processes whilst being highly versatile and efficient. Additionally, it has a short retention time compared to other conventional activated sludge processes, which require 3–8 h of continuous aeration (Singh & Srivastava, 2011). In addition, other reactors, including the membrane biofilm reactors (MBfRs), are also known to be cost-effective and highly efficient (Aybar et al., 2014; He et al., 2017). A summary of process configurations is denoted in Figure 2.3.

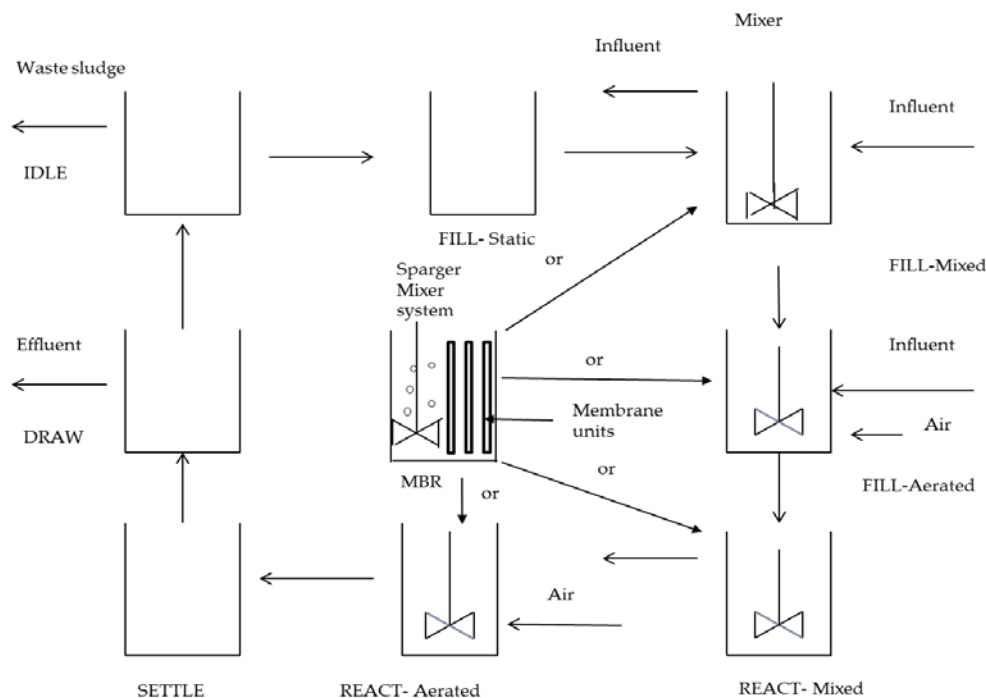


**Figure 2.3.** Principles of sequence batch reactor (SBR) and how interchangeable they can be with membrane biofilm reactors (MBfR) systems.

Modeling is another important aspect of sustaining a smooth operation of a process, e.g., wastewater treatment. Most MWSS plants are processes controlled using advanced process control models and systems. For SNaD in SBR type processes, modeling has been applied to predict and control environmental process conditions and wastewater quality for the SNaD to succeed. Different mathematical models have been used to predict oxidation of TN; however, these models fail to explore metabolic activities and networks of the microbial populations used during SNaD (Koch et al., 2000; Sin et al., 2008; Seifi & Fazaelipoor, 2012). A recently proposed mathematical exposition to explain SNaD is illustrated in Kanyenda et al. (2018).

These mathematical models also fail to accurately address the metabolic networking of microbial populations responsible for SNaD (Edwards et al., 2002). Thus, they cannot be used to describe biological processes used in MWSSs, since biological processes rely on the metabolic networking of microbial populations, particularly for consortia-catalyzed systems.

#### **2.4. Overall Remarks on Simultaneous Nitrification and Aerobic Denitrification (SNaD): Advances and Limitations**

All these improvements have contributed to a significant difference in the smooth operation of nitrification and denitrification for TN removal. Moreover, these improvements have also made a considerable reduction in the operational cost of these processes. Nevertheless, with all the efforts made to advance nitrification and denitrification, MWSSs still face challenges—they are easily inhibited by many contaminants present in the wastewater, resulting in a negative impact on the operation and rendering the overall process ineffective. Hence, efforts have been made to address such challenges.

#### **2.5. Challenges in Simultaneous Nitrification and Aerobic Denitrification (SNaD) processes**

The major challenges SNaD is currently facing are the slow growth rate and the sensitivity to temperature, pH, DO concentration, and toxicants, which negatively affect nitrifying and denitrifying organisms (Cui et al., 2014; Papirio et al., 2014). Additionally, high shear stress resulting from aeration can also result in the slow growth of nitrifying and denitrifying microorganisms (Lochmatter & Holliger, 2014), causing excessive biomass wash-out during wastewater treatment and resulting in reduced TN removal efficiency and SNaD failure (Szabó et al., 2016).

This could ensure SNaD susceptibility to inhibition by toxicants and heavy metals present in the wastewater. High concentrations of heavy metal are usually found in nitrogen-rich wastewaters from anaerobic digestates, e.g., anaerobically digested piggery and dairy slurries (Li et al., 2015a). Although heavy metals affect SNaD, they are required in small quantities to enhance microbial growth and stimulate the activity of microorganisms by stimulating enzymes and co-enzymes that play important roles in SNaD, e.g., copper and molybdenum, which are constituents of nitrite reductase and nitrite oxidoreductase, respectively, while other known enzymes involved in SNaD depend on other heavy metals such as nickel-dependent hydrogenase, ATP-dependent zinc metalloprotease FtsH 1, and zinc-containing dehydrogenase (Li et al., 2015b).

Although minute amounts of heavy metals such as Fe, CU, Co, Ni, and Zn are essential in wastewater treatment, their toxicity towards nitrifying and denitrifying microorganisms is mainly influenced by metal speciation, sludge health sloughing, and the type of reactor used (Aslan & Sozudogru, 2017). Moreover, denitrification inhibition by high concentrations of nitrate in wastewater also affects the metabolism of nitrifying and denitrifying organisms. Another challenge that hinders the practicality of SNaD is the

inhibition of denitrifiers by DO. Additionally, operational, maintenance, and process control strategies can produce better reactor performance in general wastewater systems but can also hamper SNaD, especially under rudimentary process control conditions that facilitate undesirable loadings and environmental conditions (Show et al., 2013).

Another challenge with SNaD is the elongated start-up and stabilization period, with the  $\text{NH}_4\text{-N}$  and  $\text{NO}_2^-$  concentrations within the system able to affect the growth of SNaD by stunting the microbial community proliferation during this period. Low  $\text{NH}_4\text{-N}$  and  $\text{NO}_2^-$  concentrations can also result in substrate limitation and can thus lead to a low growth rate of the SNaD microbial populations. Two start-up procedures for SNaD are known to exist, with the first involving directed evolution of the SNaD microorganisms by adaption to increasing  $\text{NH}_4\text{-N}$  and  $\text{NO}_2^-$  concentrations. The second procedure involves the physical inoculation with anoxic denitrifying consortium after the primary (nitrification) step of the SNaD has been initiated. Then, the nitrification and the partial aerobic denitrification in SNaD can thereafter ensue such that they are well established in one process unit (Zhang et al., 2014). The inhibition of SNaD by FCN is another common challenge, as FCN has been reported to possess the highest inhibitory effect toward SNaD; furthermore, some microorganisms suited for SNaD have been reported to use FCN as a nitrogenous source (Luque-Almagro et al., 2016).

## **2.6. Prevention of Biomass Washout During the Start-Up of SNaD**

Environmental engineers have been making efforts to reduce the start-up time of SNaD microorganisms in order to reduce biomass washout and maintain the TN removal efficiency (Lochmatter & Holliger, 2014). Different reactors with low retention times have been designed and studied, including the fluidized bed reactor, the membrane reactor, the gas lift reactor, the rotating biological reactor, and the up-flow anaerobic sludge blanket; however, a portion of biomass is still washed out with the effluent in all these systems, particularly for unstable periods, due to the cases overloading to increase wastewater treatment throughput, which induces biomass sloughing and flotation and which results in wash-out (Huang et al., 2016).

The sequencing batch reactor has been found to be the more suitable reactor for the growth of SNaD microorganisms and is efficient in biomass retention. The possibility of immobilization of SNaD microorganisms as biofilm on the surface carriers has also been explored as another alternative to reducing biomass washout. The materials that have been well studied as surface carriers include zeolite, polyethylene sponge strips, porous non-woven fabrics, novel acrylic resin materials, bamboo charcoal, and polyurethane spheres (Daverey et al., 2015).

Szabó et al. (2016) also showed that by gradually improving biomass, settling can also reduce SNaD washout. Parameters such as changing DO aeration strategy and contaminant load adaptation during the early stage of the start-up as well as the availability of soluble chemical oxygen demand (COD), which can

readily be consumed prior to the commencement of the aeration phase at a low temperature (20 °C) and a neutral pH, have been found to greatly affect the retention of biomass in SNaD. These parameters have been studied in order to optimize the functionality of the SNaD (Daverey et al., 2015; Gunatilake, 2015).

Furthermore, washout can be prevented by toxicant removal by the addition of psycho-chemical pre-treatments, which might involve chemical precipitation, adsorption, ion exchange, and electrochemical deposition.

Additionally, these psycho-chemical pre-treatments may result in additional process operational costs; hence, it is imperative to shift to a biotechnological approach to avoid slow startup and biomass retention by controlling the inhibition of SNaD organisms by toxic pollutants present in wastewater. FCN degrading bacteria have been reported to have a fast-growing rate; hence, they can provide a practical solution to the inhibition of FCN and eliminate challenges associated with the slow growth of SNaD microorganisms (Luque-Almagro et al., 2016).

## **2.7. Inhibition Mechanism of Simultaneous Nitrification and Aerobic Denitrification by Pollutants**

With all the efforts that have been made to improve SNaD, this process still faces challenges, such as inhibition by toxic pollutants. This is due to the slow growth of NOB, making SNaD prone to inhibition. It has been shown that SNaD is more sensitive to FCN and phenol loading; as little as 1–2 mg/L of hydrogen cyanide (HCN) could result in complete inhibition of metabolic functions of both AOB and NOB, even in consortia bio-catalyzed SNaD. The presence of high concentrations of FCN in the MWSSs can render the secondary treatment processes ineffective subsequent to the disposal of wastewater containing a high concentration of TN, resulting in the deterioration of the MWSS's effluent quality (Kim et al., 2011; Akinpelu et al., 2016). Different inhibition mechanisms of SNaD by different pollutants have been reported. Primary inhibition involves the deactivation of the actions or the activity of ammonia monooxygenase (AMO), which is an important enzyme in the primary step of nitrification, through inhibition of the respiration system of the microorganism by exogenous ligands that attach to the heme protein (His-Fe<sup>2+</sup>-His) (Wu et al., 2017). The heme protein is required for the mediation of the redox processes and respiration, which aid in the reduction of dissolved compounds by bacteria in MWSSs (Ruser & Schulz, 2015).

Secondary inhibition is through the binding of an inhibitor to the active site of the enzyme prohibiting the binding of the substrate (i.e., NH<sub>4</sub>-N), thus inhibiting its oxidation. Another inhibition phenomenon involves the removal of the AMO-Cu co-factor through chelation, culminating in the formation of an unreactive complex and rendering the whole SNaD process ineffective. The presence of Cu co-factors has been found to play a crucial role in the activity of AMO, which affects the oxidation of NH<sub>4</sub>-N. The last enzymatic inhibition involves substrate oxidation, which causes the substrate to be highly reactive, resulting in the premature excretion of the AMO as a secondary metabolite (Ruser & Schulz, 2015). FCN has been

proven to greatly inhibit SNaD in activated sludge systems, primarily due to inadequate AMO activity (Kim et al., 2008). FCN inhibits nitrification and denitrification by acting as an exogenous ligand, which binds into His-Fe<sup>2+</sup>-His in three sequential steps, which are: (1) the ionic exchange of the endogenous ligand; (2) the formation of a reactive penta-coordinated species; and (3) the binding of the external ligand (De Sanctis et al., 2006).

Additionally, Inglezakis et al. (2017) showed that the specific NH<sub>4</sub>-N uptake rate is less inhibited compared to a specific oxygenation rate. It was thus concluded that the autotrophic biomass was less sensitive to FCN than heterotrophic biomass. The inhibition of SNaD by FCN has been widely studied by many, including Kim et al. (2011). Moreover, efforts have been made to try to eradicate SNaD inhibition by using techniques such as the application of pretreatment systems with adsorption processes and the addition of a step whereby microorganisms are used to treat FCN to acceptable concentrations that have a lessened impact on TN removal subsequent to SNaD.

## **2.8. FCN Wastewater in Municipal Wastewater Sewage Systems (MWSSs) and Its Impact on Nitrification and Denitrification: A Culture of Illegal Wastewater Dumping**

FCN is a toxic carbon-nitrogen radical found in various inorganic and organic compounds, some of which are used on an industrial scale. A common form of FCN is hydrogen cyanide (HCN), which can be an odorless gas characterized by a faint, bitter, almond-like odor (Safa et al., 2017; Tiong et al., 2015). Cyanide can be found in different forms depending on the pH; at high pH, it is found as an ion of FCN and evaporates as HCN at neutral pH, pKa 9.2. Additionally, FCN has a high affinity for metals and thus can form complexes with metals found in nature even when released in agricultural soil (Itoba-Tombo, 2019). These metal FCN complexes can be categorized into two categories—weak acid dissociable (WAD) and strong acid dissociable (SAD) FCN (Han et al., 2014; Luque-Almagro et al., 2011). Microorganisms and animals also produce minute quantities of FCN as a protection mechanism, e.g., cassava, corn, and lima beans, forages (alfalfa, sorghum, and Sudan grasses), and horticulture plants (ornamental cherry and laurel). FCN is often released as a nitrogenous source when the plant is under stressed environmental conditions (Gupta et al., 2010).

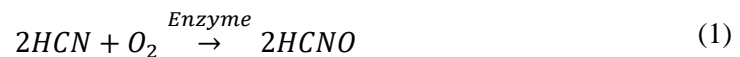
As such, FCN enters MWSSs via illegal disposal of wastewater, mostly from different industries (Luque-Almagro et al., 2016), and as runoff from the disposal of FCN containing agricultural wastes in landfills, the use of FCN containing pesticides, and through the use of FCN containing tar salts. FCN is known for being a metabolic inhibitor of many microorganisms, and as little as 0.3 mg/L can result in the loss of biological activity in microorganisms (Basheer et al., 1992). It alters the metabolic functions of the organism by forming a stable complex with transient metals that plays a significant role in the functioning of the proteins, including micro and macro-metallo contents within cells, which play an important role in nutritional sustenance of biomass intended for FCN bioremediation (Tiong et al., 2015). In the wastewater



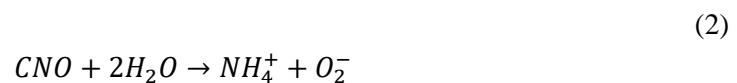
treatment process catalyzed by biomass, this can result in the inhibition of SNaD (Han et al., 2014; Han et al., 2013).

Some microorganisms produce minute quantities of cyanide for defensive purposes (Khamar et al., 2015), albeit they are able to carry out most metabolic functions in the presence of low FCN. Furthermore, some organisms are able to survive FCN expressing specialized enzymes for the degradation of FCN into NH<sub>4</sub>-N and CO<sub>2</sub> through nicotinamide adenine dinucleotide (NADH)-linked cyanide monoxygenase (CNO), including enzymes such as nitrilase and cyanide hydratases (CHTs) (Khamar et al., 2015; Rinágelová et al., 2014); these can be rendered ineffective by chelation reaction-side blockages and promotion of redundancy in the overall functionality of the bio-catalysis process.

FCN has been reported to be a highly poisonous compound known to man (Luque-Almagro et al., 2018), and it is hyper-toxic under aerobic conditions, which would mean higher toxicity for aerobic organisms used in SNaD. It inactivates the respiration of many microorganisms by binding to the cytochrome-c oxidase (Murugesan et al., 2018). However, some microorganisms have developed a metabolic FCN detoxification mechanism. These mechanisms have been studied in numerous microorganisms, which culminated in an interest in the research community in SNaD, even under toxicant loading and particularly under FCN loading. Studies have also shown that these microorganisms can either use FCN primarily as a nitrogenous or as a carbon source by converting it to NH<sub>4</sub>-N and CO<sub>2</sub> through NADH-linked cyanide oxygenase (Dwivedi et al., 2016). FCN degradation in aerobic conditions can be expressed as highlighted in Equation 1.



whereby the hydrogen cyanate is therefore hydrolyzed into NH<sub>4</sub>-N and CO<sub>2</sub> (Equation 2):



## 2.9. Current Solutions to the Challenges in Simultaneous Nitrification and Aerobic Denitrification (SNaD)

### 2.9.1. Physical Process Used as Remedial Strategy to Decrease the Inhibitory Effect of FCN on SNaD

Chemical methods have been employed to decrease the concentrations of FCN prior to SNaD. One of the few chemical methods used includes alkaline chlorination oxidation. This method is a preferred chemical method since it is highly effective; however, alkaline chlorination (and thus oxidation) results in undesirable byproducts and produces excess hypochlorite, which is a toxicant. Chemical precipitation by ferrous sulfate is another method that is preferred for FCN removal due to its cost-effectiveness and availability of the salt, but it produces large quantities of toxic sludge. Ion exchange can also be used to lower FCN concentration,

although it is difficult to operate and has high input costs (Cui et al., 2014). Activated carbon has also been widely used to effectively remove pollutants in MWSSs (Ramavandi, 2016). However, activated carbon has been reported to be less effective at removing metals and some inorganic pollutants—especially FCN—due to their low adsorbability in poor quality wastewater. It was reported that the adsorption capability of activated carbon depends on the potpourri of available chemical species, thus some research has suggested modification of different activated carbon functional groups to enhance selective adsorption capability (Singh et al., 2016). The use of such activated carbon can result in increased production cost, which would in turn increase operational costs of SNaD, thus making this option a less desirable remedial strategy for TN reduction when considering the inhibition of FCN. Thus, more appropriate and less costly methods are required, with some biological processes being proposed as suitable approaches (Özel et al., 2010).

### **2.9.2. Biological Systems Responsible for Lowering FCN Concentration Prior to SNaD**

As a remedial strategy, the elimination of FCN by microbial processes carried out during wastewater treatment is usually employed to detoxify FCN into  $\text{NH}_4\text{-N}$ . These microorganisms use different mechanisms for FCN degradation with five different FCN degradation mechanisms known, which are hydrolytic, oxidative, reductive, substitution/transfer, and synthesis pathways (Gupta et al., 2010). The hydrolytic, the oxidative, and the reductive pathways are because of enzymatic actions for which FCN is transformed into simple organic or inorganic byproducts such as  $\text{NH}_4\text{-N}$  and  $\text{CO}_2$ , and the other two mechanisms (substitution/transfer and synthesis mechanisms) are responsible for the assimilation of FCN (Gupta et al., 2010).

These pathways are used for the assimilation of FCN as a nitrogen and a carbon source. The hydrolytic pathway is catalyzed by five different enzymes, including cyanide hydratase, nitrile hydratase, and thiocyanate hydrolase. These enzymes have specific activators for and direct hydrolysis of FCN. Additionally, some hydrolyze the triple bond between the carbon and the nitrogen elements to form formaldehyde. Others, including nitrilase and cyanidase, are effective in the microbial metabolic activity and the conversion of FCN into  $\text{NH}_4\text{-N}$  and a carboxylic acid (Inglezakis et al., 2017; Dwivedi et al., 2016).

The oxidative pathway involves oxygenolytic conversion of the FCN into  $\text{CO}_2$  and  $\text{NH}_4\text{-N}$ , although this pathway requires an addition of a carbon source, e.g., agricultural waste extracts, and nicotinamide adenine dinucleotide phosphate (NADPH) to catalyze the degradation pathway (Inglezakis et al., 2017; Dwivedi et al., 2016). Moreover, the oxidative pathway is divided further into two distinctive pathways involving three enzymes, namely, cyanide monooxygenase, cyanase, and cyanide dioxygenase. The reductive pathway occurs anaerobically and is catalyzed by nitrogenase to convert FCN to methane and ammonium (Sharma et al., 2019), a process that is not facilitated in SNaD.

The substitution/transfer pathway catalyzes FCN assimilation for growth purposes with the aid of rhodenase and mercaptopyruvate sulfurtransferase by using FCN as a nitrogen source. The synthesis pathway is another FCN assimilation pathway that involves the production of an amino acid,  $\beta$ -cyanoalanine, and  $\gamma$ -cyano- $\alpha$ -aminobutyric acid, using other amino acid residues as precursors that react with the FCN compound (Sharma et al., 2019). Conversely, FCN degradation has been found to be significantly inhibited by some by-products of  $\text{NH}_4\text{-N}$  oxidation, such as those analogous to organic acids (Kao et al., 2003).

To date, there is still minimal literature on the exploitation of FCN resistant or tolerant organisms with an ability to mediate the inhibition effect of FCN compounds in MWSSs. Additionally, Mekuto et al. (2015) also reported SNaD at 100–300 mg FCN/L loading by the *Bacillus* species. According to the authors, whilst the use of cyanide degrading bacteria to lower toxicity levels of FCN is environmentally benign, the additional reactors in series prior to SNaD can be beneficial for FCN degradation, which can escalate operational costs in MWSSs.

Some FCN degrading microorganisms displayed the ability to degrade FCN subsequent to SNaD. This led to Kim et al. (2008) proposition of using FCN degrading microorganisms for SNaD, which is an interesting phenomenon that promotes the simultaneous removal of the FCN compound and TN and eventually results in the implementation of SNaD in lower operational cost associated settings, even in an FCN biodegradation reactor.

### **2.9.3. Overall Remarks on Remedial Strategies in Place to Mitigate FC in SNaD**

Although efforts have been made to address the inhibition of SNaD by FCN, the current strategies in place have their limitations; for example, the activated carbon is not effective in the absorption of FCN. Hence, this option is not an appropriate remedial strategy to lower FCN in wastewater on a large scale. The use of FCN degrading bacteria to lower FCN concentration to acceptable standards prior to SNaD has attracted more attention since it is an environmentally benign option. However, this option can result in the escalation of operational costs associated with the maintenance of the primary reactor designated for FCN degradation. Hence, it is important that this option be re-evaluated to minimize costs.

## **2.10. A Proposed Sustainable Solution: Environmental Benignity at the Core of SNaD Development**

### **2.10.1. Application of FCN Resistant Microorganisms in Simultaneous Nitrification and Aerobic Denitrification (SNaD) Under Cyanogenic Conditions**

Research has shown that there are FCN resistant microorganisms that can remain active even in concentrations above 18 mg FCN/L (Chen et al., 2008). Kim et al. (2013) successfully achieved SNaD under high FCN conditions using FCN degrading bacteria in a single reactor process (Han et al., 2014). Microorganisms use different mechanisms to resist the influence of FCN through the enzymatic mechanism for FCN degradation through the degradation of FCN into less toxic compounds (cyanotrophic organisms)

via different pathways, as previously mentioned, e.g., hydrolytic pathway, oxidative pathway, reductive pathway, substitution/transfer pathway, and synthesis pathway (Gupta et al., 2010; Basheer et al., 1992). *Pseudomonas pseudoalcaligenes* CECT5344 was sequenced, and it was revealed that four nitrilase genes were responsible for CN-assimilation and six other C-N hydrolase/nitrilase superfamily genes were found in cyanotrophic strains (Gupta et al., 2010). Nitrilases have been reported to play a role in the nitrogen metabolism of *Colwellia* sp. Arc7-635 (Lin et al., 2019).

Generally, heterotrophic bacteria that degrade FCN are typically able to assimilate NH<sub>4</sub>-N, i.e., a byproduct of FCN biodegradation, as a nitrogenous source. Thus, it has been reported that some of the FCN degrading bacteria are also nitrogen assimilators. The number of nitrifying bacteria has been found in FCN rich environments—an indication of the adaption of nitrifying and denitrifying microorganisms to FCN (Watts et al., 2016). Ryu et al. (2015) reported simultaneous nitrification and thiocyanate (SCN) degradation, demonstrating that FCN and SCN degrading bacteria can be used to mediate the FCN inhibition effect in SNaD systems. Other genes in *P. pseudoalcaligenes* CECT5344 indicated a presence of polyhydroxyalkanoates (PHA) synthesis, which has a potential to biodegrade numerous toxicants, including aromatic compounds such as phenol (Luque-Almagro et al., 2016).

Although some scientists have suggested the use of FCN degrading microorganisms to eliminate FCN inhibition on SNaD (Inglezakis et al., 2017; Salazar-Benites et al., 2016; Mekuto et al., 2018), more work still needs to be done in order to understand these processes when the wastewater experiences high concentrations of FCN compounds, including other secondary toxicants such as heavy metals (see Table 2.2). Furthermore, the description of SNaD using numerical models is underdeveloped.

Therefore, proper models that describe the behavior of these FCN degrading bacteria in SNaD, even when performing nitrification including denitrification under high FCN loading conditions, need to be developed and evaluated. Furthermore, the thermodynamics of SNaD under FCN conditions need to be assessed to theoretically elucidate the feasibility of these processes on an industrial scale. This will provide insight into SNaD facilitated by FCN degrading bacteria, which will enable the proper control of SNaD under high FCN conditions.

**Table 2.2.** Studies that have successfully used cyanide degrading microorganisms for nitrification and aerobic denitrification.

Microorganism	Description of Process Examined	Reference
<i>Bacillus</i> sp	Free cyanide (FCN) biodegradation subsequent nitrification and aerobic denitrification	(Mekuto et al., 2015)

CN <sup>-</sup> degrading consortium	Heterotrophic nitrification—aerobic denitrification potential of cyanide and thiocyanate degrading microbial communities under cyanogenic conditions	(Mekuto et al., 2018)
<i>Enterobacter</i> sp., <i>Yersinia</i> sp. And <i>Serratia</i> sp	Nitrification and aerobic denitrification under cyanogenic conditions	(mpongwana et al., 2016)
<i>Pseudomonas fluorescens</i>	Elimination of cyanide inhibition through cultivation of cyanide degrading bacteria	(Han et al., 2014)
<i>Thiobacillus</i> and <i>Micractinium</i>	Simultaneously remove SCN and total nitrogen	(Ryu et al., 2015)

## 2.11. Conclusion

SNaD system development faces many challenges; among these is the inhibition of SNaD consortia by FCN, a predominant challenge in most MWSSs. FCN is a byproduct of most industrial processes, such as electroplating and ore processing in the mining industry. FCN enters MWSSs through various pathways, which include runoffs from cyanide spills or disposal of FCN containing wastewater from numerous industries. Different psycho-chemical methods have been used to treat FCN prior to the SNaD process; however, these methods produce undesirable byproducts and they are expensive. Hence, it is important that a sustainable solution to the FCN inhibition of SNaD be developed. Biological removal of cyanide has been thoroughly studied, and it is the most commonly used method due to its cost-effectiveness and sustainability. This method has been used as pre-treatment of FCN prior to the influent entering the SNaD; nevertheless, this procedure increases the cost associated with the operation of the SNaD systems.

The ability of FCN degrading microorganisms to carry out simultaneous nitrification and SCN degradation has also been recommended for SNaD. This approach not only provides a solution to the inhibition of FCN but also provides a solution to the slow growth rate of common SNaD microorganisms. Therefore, the application of FCN degrading microorganisms could provide a sustainable solution to the inhibition of SNaD by other toxic pollutants and prevent biomass washout. The utilization of FCN resistant or degrading microorganisms for SNaD has been suggested by other scientists. However, for the use of FCN resistant or degrading microorganisms to minimize the inhibition effect of FCN towards processes of TN removal, mathematical and thermodynamic models are required to better understand SNaD as a sustainable approach to eradicating the inhibition effect of FCN in SNaD systems. There is still limited information about the

employment of these suitable microorganisms for SNaD; thus, this paper discusses the application of FCN resistant or degrading microorganisms for SNaD to reduce the effect of FCN inhibition, even under conditions whereby agricultural waste can be used as a supplementary nutrient source and as an immobilization surface for improved efficacy of microbial proliferation for the advancement of SNaD.

# CHAPTER 3

## LITERATURE REVIEW 2

**Submitted as:** N. Mpongwana, S. K. O. Ntwampe, E. I. Omodanisi, B.S. Chidi, C. Dlangamandla, M.R. Mukandi. Significance of metabolic network modeling of total nitrogen removal in simultaneous nitrification and aerobic denitrification. Submitted to *Bioengineering*

# CHAPTER 3:

## LITERATURE REVIEW 2

### 3.1. Introduction

Water pollution has become a worldwide challenge (Ceissen et al., 2015), with water becoming a scarce resource in many arid and semi-arid countries (Eliasson et al., 2015). It is important to implement a rigid wastewater treatment plan to promote the conservation of water (Lyu et al., 2016). and the reduction of environmental contaminants; thus, prevention of environmental degradation.

Biological processes are the core technology used for nutrient removal in particular total nitrogen removal (TN). Moreover, biological nitrogen removal (BNR) has drawn much interest due to its efficiency and cost-effectiveness (Peng & Zhu, 2006; Zhang et al., 2011). Stringent government regulations with regards to the disposal of water containing TN are currently in place and are strictly enforced globally (Chen et al., 2018). Hence, the need for appropriate understanding and proper control of TN removal processes which has become essential for BNR (Seifi & Fazaelpoor, 2012) since improper controlling of BNR can result in serious environmental and public health challenges (Hamed et al., 2004).

Substantial studies have been conducted to improve TN removal efficiency, thus lowering quantity TN being disposed into water bodies. These improvements include the use of microorganisms capable of simultaneously removing  $\text{NH}_4\text{-N}$  and  $\text{NO}_3\text{-N}$  under similar conditions, resulting in simultaneous nitrification and aerobic denitrification (SNaD) (Chen et al., 2012). Nevertheless, SNaD has been found to be heavily inhibited by heavy metals especially free cyanide (FCN); hence, the application of cyanogenic microorganisms that are able to use FCN and simultaneously degrade  $\text{NH}_4\text{-N}$  have been suggested (Kim et al., 2008).

Modeling plays an important role in accurate facilitation, controlling and designing of BNR (Gao et al., 2010). Various mathematical models have been developed for conventional nitrification and denitrification of wastewater (Sin et al., 2008). Although these mathematical models have been successfully employed, they have their limitations, i.e. most traditional models focus on nitrification and denitrification of which nitrification have been proven to be a two-step process, though in majority of wastewater treatment plants, nitrite accumulates insignificantly, making the model redundant (Gao et al., 2010; Sin et al., 2008).

In other cases, nitrite plays a crucial role in wastewater treatment; especially in SNaD through the nitrite route. These traditional models are less effective in such cases as they do not comprehensively pronounce nitrite accumulation and depletion. Additionally, since wastewater consists of different contaminants, these mathematical models do not account for microbial diauxic growth which is an important phenomenon in



wastewater treatment plants (WWTP). Moreover, these mathematical models do not describe metabolic networks of microbial populations of which BNR depends; hence, this review highlights the significance of metabolic network modeling of microorganisms used for SNaD for removal of multiple nitrogenous compounds.

### 3.2. Biological wastewater treatment: Total Nitrogen (TN) removal

Wastewater treatment has been used worldwide for pollutant removal and generally uses activated sludge processes which are known to be highly efficient (Ye et al., 2012). The activated sludge process uses bacterial suspension for the removal of toxins using biological mechanisms. These treatments have been efficiently used to lower TN, phosphorus and organic carbon (Gernaey et al., 2004). Furthermore, biological wastewater treatment plays an important role in preventing anthropogenic damage to the environment (Ofiteru et al., 2010).

TN removal occurs in a secondary treatment process, whereby the settled wastewater is introduced into a specially designed bioreactor under the semi-aerobic conditions. Most prokaryotic microorganisms dominate the wastewater treatment plants (Table 3.1) and use nitrogenous compounds as an energy source for their growth (Samer, 2015). The important role these microorganisms play in wastewater treatment has led to the elucidation of the interactions by advanced molecular techniques that determine the dynamics of the microbial communities in the wastewater treatment plant. These molecular methods can identify the role played by each microorganism in the TN removal process (Fig. 3.1) (Wagner et al., 2002). These methods include fluorescence in-situ hybridization (FISH), denaturing gradient gel electrophoresis (DGGE) and terminal restriction fragment length polymorphism (T-RFLP) ( Ofiteru et al., 2010).

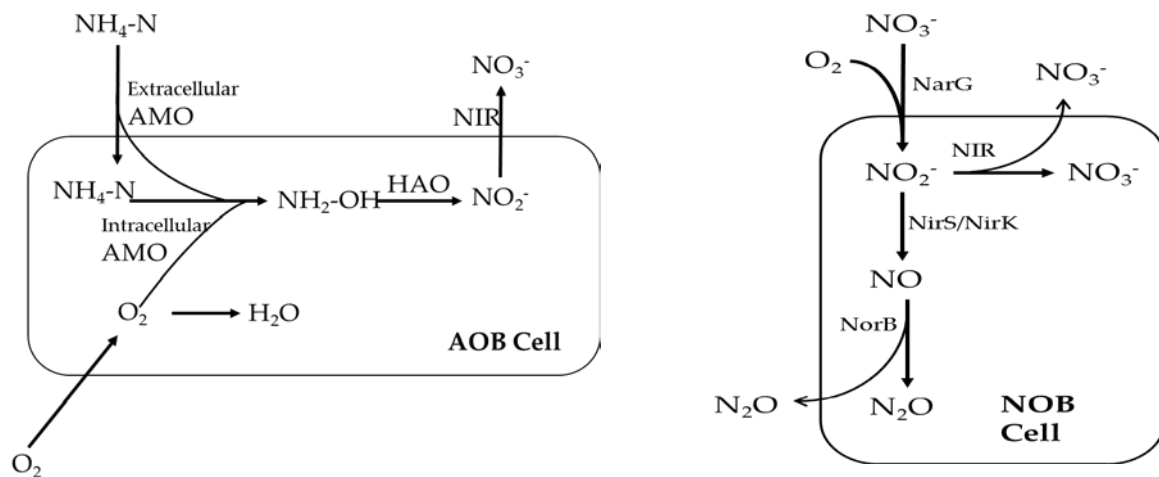


**Figure 3.1.** Metabolic network and pathways for TN removal by AOB and NOB.

**Table 3.1.** Organisms used for TN removal of different wastewater sources (McLellan et al., 2010).

Taxonomy Order/family	Genus (species)	Percentage of sequence tags		
		Human waste	Sewage wastewater	Surface water
<i>Lachnospiraceae</i>		40.78	5.49	0.03
<i>Bacteroidaceae</i>	<i>Bacteroides</i>	11.17	1.98	<0.01
<i>Ruminococcaceae</i>	<i>Faecalibacterium</i>	7.28	1.35	ND
<i>Bifidobacteriaceae</i>	<i>Bifidobacterium</i>	7.28	0.74	ND
<i>Ruminococcaceae</i>		4.87	0.91	0.02
<i>Ruminococcaceae</i>	<i>Subdoligranulum</i>	4.13	0.38	ND
<i>Lachnospiraceae</i>	<i>Roseburia</i>	4.09	0.37	ND
<i>Bacteroidaceae</i>	<i>Bacteroides ovatus</i>	2.25	0.17	ND
<i>Lachnospiraceae</i>	<i>Dorea</i>	2.17	0.30	ND
<i>Ruminococcaceae</i>	<i>Ruminococcus</i>	2.16	0.31	ND
<i>Coriobacteriaceae</i>	<i>Collinsella</i>	1.07	0.24	ND
<i>Alcaligenaceae</i>	<i>Sutterella</i>	1.00	0.05	0.01
<i>Porphyromonadaceae</i>	<i>Parabacteroides</i>	0.99	1.33	<0.01
<i>Clostridia</i>		0.95	0.17	<0.01
<i>Akkermansiaceae</i>	<i>Akkermansia</i>	0.93	0.08	ND
<i>Peptostreptococcaceae</i>		0.76	0.20	<0.01
<i>Lachnospiraceae</i>	<i>Lachnospira</i>	0.71	0.07	ND
<i>Bacteroidaceae</i>	<i>Bacteroides fragilis</i>	0.58	0.06	ND
<i>Bacteroidaceae</i>	<i>Bacteroides massiliensis</i>	0.57	0.12	ND
<i>Ruminococcaceae</i>	<i>Papillibacter</i>	0.48	0.06	<0.01
<b>Total</b>		95.24	14.35	0.07

The development of new high throughput technologies used for sequencing to identify microbial communities within a short period of time has made genomic sequencing, transcription, and proteomic data

readily available; e.g. elucidation of microbial populations involved in biological processes for SNaD. Important as this data is, there is a lack of data analysis tools that are capable of performing phenotypic characteristics of microorganisms and the exploration of SNaD. On the other hand, scientists are also using genic information to generate new understanding by automated genome annotation, metabolic network reconstruction, protein structure determination and, regulatory network reconstruction from microarray data (Edwards et al., 2002; Le et al., 2004; Zhou et al., 2015).

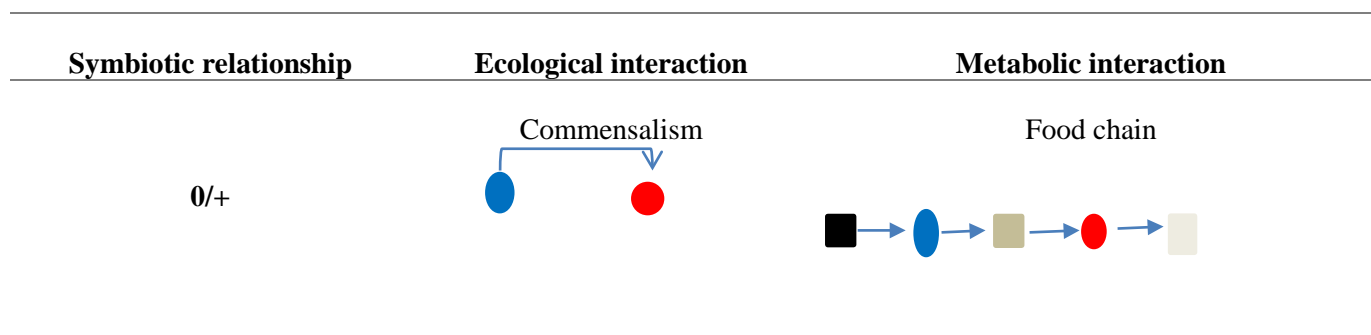
### 3.3. Microbial population and contaminant metabolism in wastewater

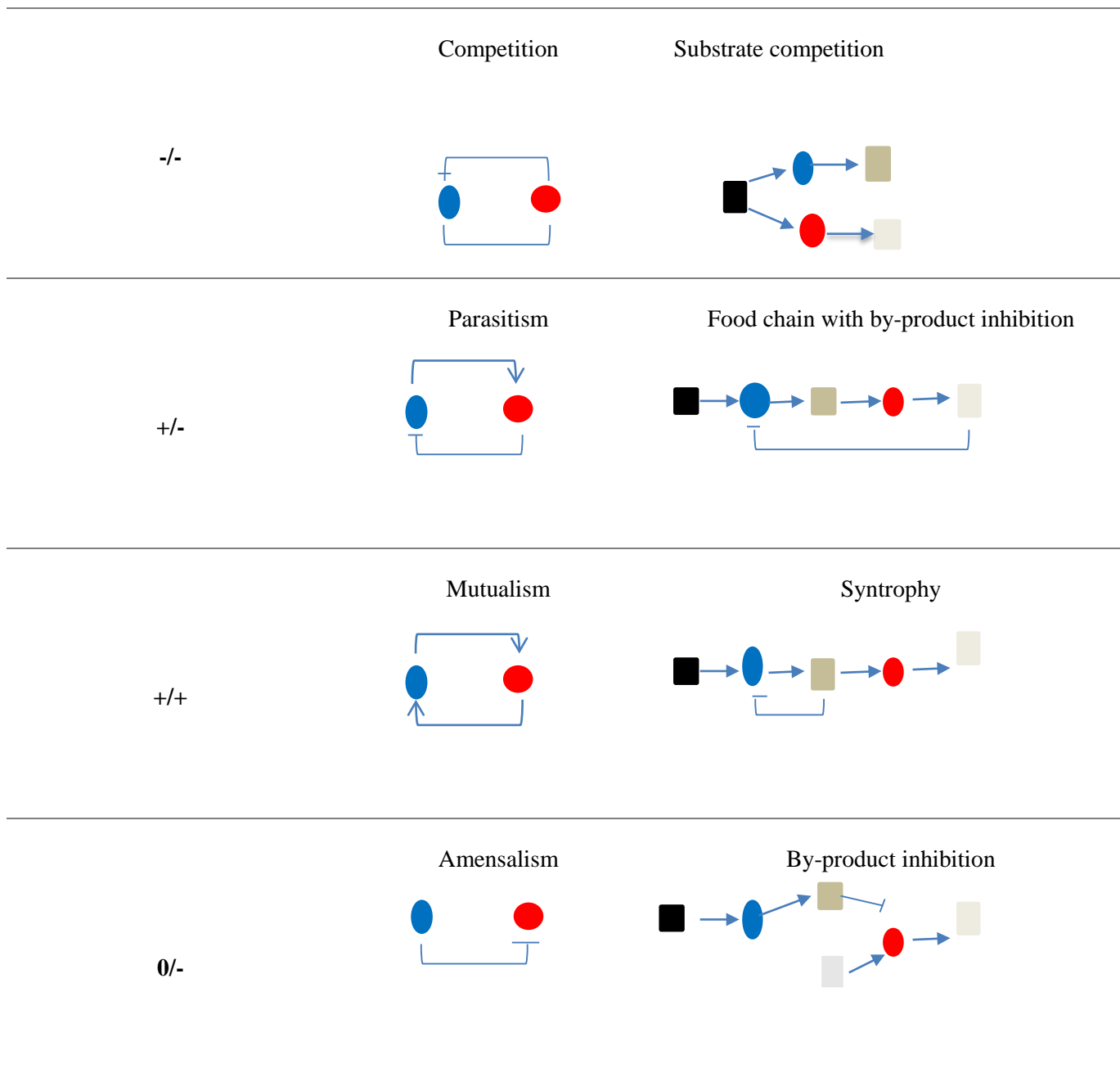
#### 3.3.1. Microbial metabolic interactions in wastewater treatment

Microorganisms are mostly found as sludge flocs or biofilm that are composed of a number of immersed species in wastewater treatment plants (Sheng et al., 2010). The function of these biofilms or flocs is determined by a number of factors including reaction rates of individual organisms. The matrix architecture, movement of substrate into biofilm or flocs, the composition of the extracellular polymeric substances (EPS) being produced and the interaction of microorganisms as a whole, also plays a role (Andersson et al., 2011).

EPS has been found to pose a significant impact on the protection of nitrifying and denitrifying biofilms from toxic contaminants. EPS significantly influence the physicochemical properties of microbial aggregates and many other properties of flocs including their structure, surface charge, flocculation, settling properties, dewatering properties, and adsorption ability (Sheng et al., 2010). The interactions of microbial species in wastewater is either metabolism-based or driven by ecological traits. The metabolic interaction involves the communication of different species through their metabolic products, i.e., the degradation of  $\text{NH}_4\text{-N}$  which then induces nitrifying and denitrifying enzymes leading to the initiation of SNaD (Wang et al., 2015). Moreover, the interaction between species can be either described as positive, negative or a neutral interaction (Table 3.2) (Perez-Garcia et al., 2016). To understand such an interaction metabolic network modeling is essential as the symbioses between different microbial species in the biocatalysis for TN removal during SNaD as this can be a rate-limiting step in wastewater treatment.

**Table 3.2.** Diagram representing microbial metabolic interaction versus ecological interaction. Where blue circles are species A, red circles are species B, and squares are substrates.





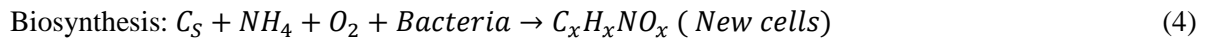
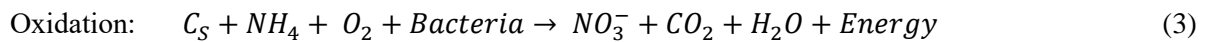
### 3.3.2. Microbial metabolism during the removal of TN in wastewater treatment plant

The secondary sludge process is composed of biological solids and inert sludge is responsible for the removal of TN and other nutrients in wastewater (Ye et al., 2012). The microorganisms remove TN through metabolic functions of immersed species within (Hu et al., 2012).

Most WWTP uses aerobic metabolism to remove TN through chemotrophic bacteria which nitrify  $\text{NH}_4\text{-N}$  into nitrate via the nitrite-nitrogen route (Low & Chase, 1999). Cellular metabolism comprises of the uptake and the transformation of TN using a complex network of reactions that are facilitated by specific enzymes. The production of components from TN removal known as metabolites and other metabolic by-products

which are then excreted into the abiotic phase are also part of cellular metabolism. During microbial facilitated TN removal, microbial metabolism releases a part of the substrate-bound carbon from the organic substrates present in wastewater during growth and assimilate a portion of it into individual cells (Low & Chase, 1999).

To achieve such carbon source assimilation two processes are known as catabolism and anabolism for which catabolism can be referred to as a biological processes involved into a breaking down of complex compounds into simple and small molecules, while anabolism is a process whereby the cell builds the molecules that it requires for growth. Understanding of these metabolic processes are important in optimisation and controlling of biological process and also provides the necessary information required for improved metabolic performance (Ramkrishna & Song 2012).



Where  $C_S$  is a carbon source.

### 3.4. The role of Thermodynamics and Stoichiometric analysis in metabolic networking

Thermodynamics has been used to predict the feasibility of the wastewater process under defined conditions, and it useful to study energy requirements and needs during the oxidation of pollutants for biological (Kushwaha et al., 2010). It can be used to study the viability of nitrification and denitrification (Wang et al., 2016). Moreover, since most reactions are redox reactions, the principle of an electron equivalent approach is necessary in accounting for electron flow and energy (Ebeling et al., 2006). During autotrophic nitrification, energy is generated from the oxidation of  $NH_4$ -N. The biomass yield coefficient and specific oxygen uptake can be estimated using the Eq.3 and 4 (Liu & Wang, 2012). Although notable work has been done to study thermodynamics and stoichiometric analysis of SNaD under defined conditions. Overall there is still minimal reporting of thermodynamic analysis of wastewater treatments.

### 3.5. Metabolic pathways identified in the biological treatment of wastewater

There are different pathways associated with organic matter reduction by chemo-organotrophs. The first one is the pyruvate formation during glycolysis, which is the most common pathway for microbial energy production in wastewater treatment plants. The energy produced during this process can be used as adenosine 5'-triphosphate (ATP), reduced nicotinamide adenine dinucleotide (NADH) and reduced flavin adenine dinucleotide ( $FADH_2$ ); however, this pathway results in minute energy production and the process does not require oxygen respiration hence it occurs under anaerobic conditions (Angenent et al., 2004; Blackall et al., 2002).

The second pathway is the Entner–Doudoroff pathway which is similar to glycolysis in producing pyruvate but less effective in ATP production. Among other few organisms, *Pseudomonas* sp uses this pathway for organic carbon reduction (Conway, 1992). During the process, the pyruvate is eventually used in the citric acid cycle to produce NADH and FADH<sub>2</sub> which are responsible for the high transfer potential of electron transport. These electrons move to molecular oxygen resulting in a large quantity of free energy to be transferred. The citric acid intermediates can also be withdrawn in order to form the materials required for microbial proliferation (Sokic-Lazic & Minteer, 2008).

During cellular respiration, the catabolised carbon is removed from the cell as CO<sub>2</sub> (Fig. 3.2). Chemosmotic process of oxidative phosphorylation is then used to conserve free energy transferred to NADH or FADH<sub>2</sub> through respiratory assemblies that contain a series of electron carriers that are positioned across the cell's cytoplasmic membrane. When the electron carriers are transferring electrons from NADH or FADH<sub>2</sub> to O<sub>2</sub>, the protons are being pumped out of the cell cytoplasm simultaneously (Low & Chase, 1999).

This generates a proton motive gradient across the membrane which then provides a driving force for the flow of the protons back into the cytoplasm, on the other hand, NAD<sup>+</sup> needs to be reduced through a fermentative process that utilises organic matter in order for anaerobic catabolism to proceed. Since these processes involve the formation of ATP, the overall ATP production becomes lower in anaerobic catabolism than in aerobic processes, thus anaerobic metabolism has lower biomass production than aerobic metabolism (Low & Chase, 1999).

The modeling of microbial metabolism in the wastewater treatment ensures the appropriate process control and optimisation can be conducted for these cultures. Hence, some models are currently used to describe biological processes in the wastewater treatment plants, but with limitations such as failing to express the biological reality (Ofiteru et al., 2010).

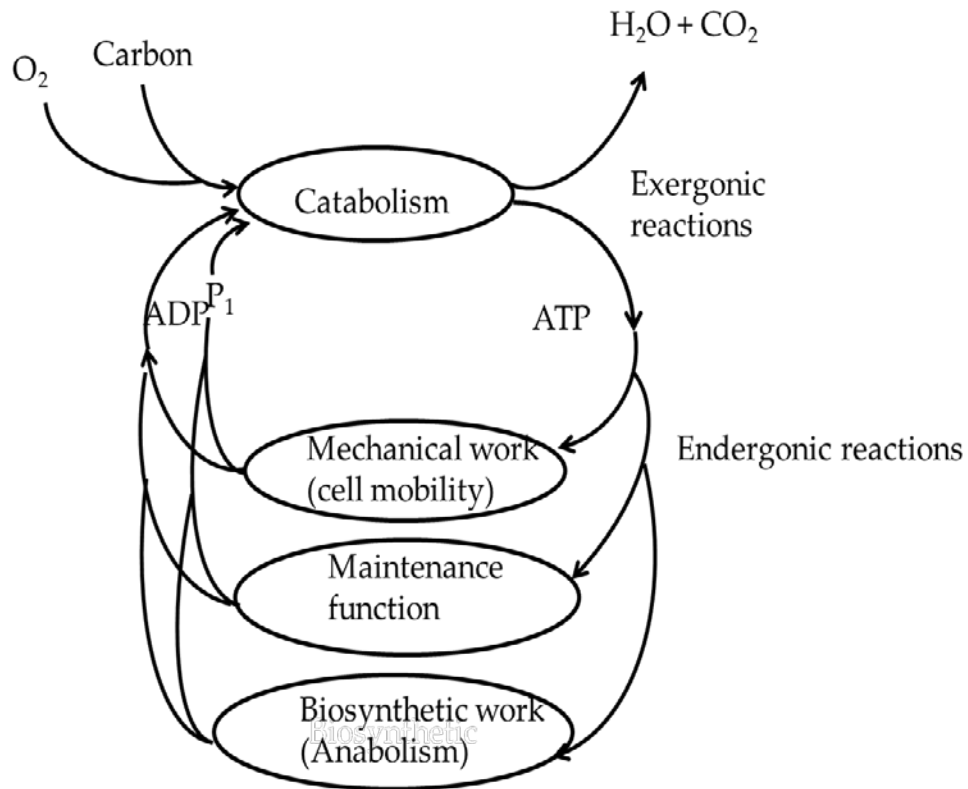


**Figure 3.2.** The role of the ATP–ADP cycle in cell metabolism during wastewater treatment (Sokic-Lazic et al., 2008).

### 3.6. Metabolic network modeling in wastewater treatment

#### 3.6.1. Significance of metabolic network modeling in the wastewater treatment

With all the current molecular advancements in studying the dynamics of the microbial population responsible for TN removal in the wastewater treatment plants, more genomic and protein expression data are increasingly becoming available to better understand phenotypic characteristics of each microorganism and their role in the TN removal (Ye et al., 2012).

Genome-scale metabolic network reconstructions (GENREs) can be employed successfully as a representation of microbes. However, with all the molecular data available we still do not understand the mechanisms that cause the microbial communities to interact and function as a whole (Biggs et al., 2015; Ao, 2005). Furthermore, the quality of wastewater changes periodically and molecular information currently available is not adequate to explain metabolic phenotypes that are expressed under certain environmental conditions (Edwards et al., 2002).

Considering the importance of the microbial communities in the wastewater treatment, there is a necessity to assess beyond the descriptive model approach by applying more functional, predictive models describing microbial community structure and function. Predictive models are important to improve many processes

such as the rational probiotic design of efficient chemical-producing consortia, or optimal bioremediation communities (Biggs et al., 2015).

Additionally, predictive models are essential for novel exploration to answer basic questions in microbial ecology functioning, thus giving us an insight into the development of microbial communities in wastewater treatment plants. Although, some models have been successfully used to describe well-studied processes such as traditional nitrification and subsequent denitrification further analysis is required (Ofiteru et al., 2010). Some models fail to describe the metabolic process that occurs in wastewater treatment plants. Thus, it is important to develop metabolic network models that will describe metabolic phenotypes within the WWTP (Le et al., 2004). A basic metabolic network diagram is denoted in Fig. 3.3.

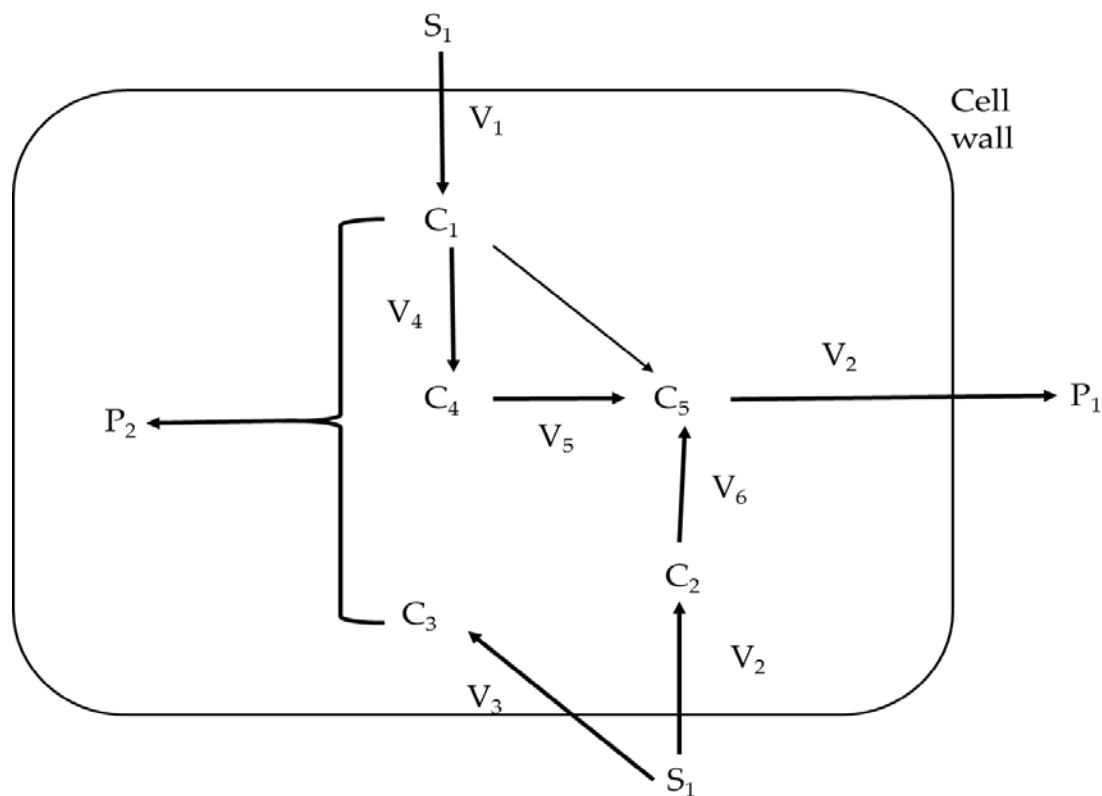


**Figure 3.3.** A simple fictional metabolic network (Ao, 2005).

### 3.6.2. Suitable metabolic network modeling approaches for biological wastewater treatment

Since the WWTP is composed of different sources of carbon, nitrogen, phosphate and sulfur e.t.c (Table 3.3), it is critical to consider diauxic growth when modeling biological wastewater treatment (Suga et al., 1975). Diauxic growth was first described by Monod as a sequential utilisation of carbon source by microorganisms in a batch system. This phenomenon is characterised by the appearance of two exponential growth phase which is separated by the lag phase.



Generally, in diauxic growth, the maximum specific growth rate of a microorganism is higher on the preferred substrate than on a less preferred substrate (Narang et al., 1997). Thus the modeling approaches that are suitable to model metabolic networking must incorporate diauxic growth. However, elsewhere (Ramkrishna & Song, 2012; Narang et al., 1997), a flux balance approach and cybernetic modeling have been proposed to be suitable for modeling system functionality while considering diauxic growth.

**Table 3.3.** Organic constituents and nitrogen matters other than those identified in wastewater treatment plants (Wagner et al., 2002).

Type	No.	Compound name	Conc. of the compound ( $\mu\text{g/L}$ )	TOC coefficient	TOC Conc. ( $\mu\text{g C/L}$ )	RT (min)
<b>Alkyl and aromaticity hydrocarbon</b>	1	Dodecane, 2-methyl-8-propyl-	1.99	0.85	1.69	21.82
	2	Cyclotetradecane, 1,7,11-trimethyl-4-(1-methylethyl)-	2.42	0.86	2.07	35.05
	3	Pentadecane	6.19	0.85	5.26	23.07
	4	Hexadecane, 2,6,10,14-tetramethyl-	2.91	0.85	2.47	23.20
	5	Cyclohexadecane	7.01	0.86	6.01	24.14
	6	Cyclohexadecane, 1,2-diethyl-	1.85	0.86	1.59	28.84
	7	Heptadecane	3.31	0.85	2.81	21.73
	8	Octadecane	0.57	0.94	0.53	29.97
	9	Nonadecane, 1-chloro-	1.25	0.75	0.94	28.94
	10	Eicosane	3.10	0.85	2.64	24.35
	11	Cyclopentasiloxane, decamethyl-	0.45	0.59	0.27	12.97
	12	Cinnoline, 3-phenyl-	1.75	0.87	1.52	26.83
	13	Naphthalene	0.16	0.94	0.15	13.45
	14	2-Methylnaphthalene	0.07	0.93	0.07	15.55
	15	Phenanthrene	0.06	0.94	0.06	22.95
	16	Fluoranthene	0.02	0.95	0.02	25.48
	17	Benzo(b)fluoranthene	0.18	0.95	0.17	33.72

	18	Benzo(k)fluoranthene	0.13	0.95	0.12	33.75
	19	Ideo(1,2,3-cd)pyrene	0.74	0.92	0.68	37.17
	20	Dibenzo(a,h)anthracene	0.52	0.95	0.49	37.25
	21	Benzo(ghi)perylene	1.12	0.96	1.07	37.77
	22	Toluene	0.75	0.92	0.69	3.75
	23	Benzo(a)pyrene	0.27	0.95	0.26	34.50
<b>Alkene</b>	24	7-Hexadecene, (Z)-	1.21	0.86	1.03	31.01
	25	1-Octadecene	8.60	0.87	7.49	26.59
	26	Cyclohexene, 1-methyl-3-(1-methylethenyl)-, (+/-)-	2.85	0.86	2.46	13.79
	27	8-Heptadecene	11.25	0.86	9.64	24.94
	28	2,6,10,14,18,22-Tetracosahexaene, 2,6,10,15,19,23-Hexamethyl-, (all-E)-	22.90	0.88	20.11	34.02
	29	9-Nonadecene	1.87	0.86	1.60	35.17
	30	17-Pentatriacontene	1.59	0.86	1.36	38.06
	31	Acenaphthylene	0.14	0.95	0.13	18.01
	32	1-Nonadecene	0.90	0.86	0.77	30.92
<b>Alcohols</b>	33	1-Hexanol, 2-ethyl-	6.30	0.74	4.65	10.38
	34	7-Octen-2-ol, 2,6-dimethyl-	1.63	0.77	1.26	11.29
	35	1,6-Octadien-3-ol, 3,7-dimethyl-	1.07	0.76	0.81	11.86
	36	Phenylethyl alcohol	1.98	0.79	1.56	12.21
	37	Isoborneol	1.37	0.78	1.07	13.19
	38	Cyclohexanol, 5-methyl-2-(1-methylethyl)-, (1alpha,2beta,5alpha)-(+/-)-	7.45	0.76	5.66	13.32
	39	3-Cyclohexene-1-methanol, .alpha.,.alpha.4-trimethyl- . .alpha.	9.67	0.77	7.49	13.66
	40	6-Octen-1-ol, 3,7-dimethyl-, (R)-	1.16	0.74	0.86	14.37

	41	5-Cholestene-3-ol, 24-methyl-	6.46	0.84	5.43	37.50
	42	Farnesol isomer a	1.11	0.81	0.90	33.75
	43	Beta-sitosterol	11.01	0.78	8.58	38.40
	44	Benzyl alcohol	0.92	0.68	0.63	10.60
	45	Cholestanol	35.37	0.82	29.08	36.22
	46	Cholesterol	59.32	0.84	49.79	35.56
<b>Organic acids</b>	47	Hexanoic acid, 2-methyl-	7.90	0.65	5.10	10.94
	48	Hexanoic acid, 2-ethyl-	1.42	0.67	0.94	12.44
	49	6-Octadecenoic acid, (Z)-	40.59	0.77	31.09	27.26
	50	Octadec-9-enoic acid	3.02	0.77	2.31	27.31
	51	Octadecanoic acid	45.26	0.76	34.43	27.54
	52	Heptadecanoic acid	2.05	0.76	1.55	26.34
	53	n-Hexadecanoic acid	103.27	0.75	77.45	25.27
	54	Dodecanoic acid	7.32	0.72	5.27	19.89
	55	Oleic acid	1.00	0.77	0.77	33.46
	56	Benzenepropanoic acid	0.61	0.72	0.44	16.41
	57	Tetradecanoic acid	11.45	0.74	8.44	22.64
<b>Ketone</b>	58	Cyclohexanone	0.92	0.73	0.68	7.07
	59	Bicyclo[2.2.1]heptan-2-one, 1,7,7-trimethyl-, (1R)-	2.21	0.79	1.75	12.75
	60	9,10-Anthracenedione	5.06	0.65	3.30	25.42
	61	Androstan-17-one, 3-hydroxy-, (3.alpha.,5.beta.)-	1.05	0.79	0.83	31.18
	62	Cholest-4-en-3-one	1.18	0.84	0.99	37.72
<b>Phenolic</b>	63	Phenol	8.43	0.77	6.46	9.45
	64	Chloroxylenol	8.93	0.61	5.48	17.16
	65	4-Methylphenol	1.44	0.78	1.12	11.52
	66	4-Chloro-3-methyl phenol	0.14	0.58	0.08	15.57

<b>Nitrogenous compounds</b>	67	5H-1-pyridine	2.84	0.76	2.15	15.59
	68	Quinoline, 2-methyl-	1.68	0.84	1.40	15.81
	69	Pyridine, 3-(1-methyl-2-pyrrolidinyl)-, (S)-	2.22	0.74	1.65	16.48
	70	Azobenzene	0.09	0.79	0.07	20.86
	71	Caffeine	13.66	0.49	6.76	23.85
	72	Pyridine-3-carboxamide, oxime, N-(2-trifluoromethylphenyl)-	1.55	0.59	0.91	40.97
<b>Ether</b>	73	3-tert-Butyl-4-hydroxyanisole	4.35	0.73	3.19	18.45
	74	Triethylene glycol monododecyl ether	2.13	0.59	1.27	28.67
	75	Bis(2-chloroisopropyl)ether	0.35	0.42	0.15	10.94
<b>Amine</b>	76	2H-Indazol-3-amine, 2-methyl-	3.39	0.68	2.30	18.84
	77	Benzenesulfonamide, N-ethyl-2-methyl-	4.23	0.50	2.11	21.25
	78	Aniline	0.10	0.35	0.04	9.27
	79	N-nitroso-di-n-propylamine	0.21	0.55	0.12	11.29
<b>Ester</b>	80	Cyclopentaneacetic acid, 3-oxo-2-pentyl-, methyl ester	4.16	0.69	2.87	21.17
	81	1,2-Benzenedicarboxylic acid, bis(2-methylpropyl) ester	17.30	0.69	11.95	24.03
	82	1,2-Benzenedicarboxylic acid, diisooctyl ester	9.60	0.74	7.09	31.47
	83	7-Trimethylsilyloxy-7-methyloctanoic acid, trimethylsilyl ester	4.45	0.70	3.09	37.14
	84	Dimethyl phthalate	0.09	0.62	0.06	18.22
	85	Diethyl phthalate	2.75	0.65	1.78	20.33
	86	di-n-Butyl phthalate	2.45	0.69	1.69	25.19
	87	di-n-Octyl phthalate	0.03	0.74	0.02	33.20
	88	bis(2-Ethylhexyl)phthalate	2.32	0.74	1.71	31.48

<b>Others</b>	89	Kitazin P	1.16	0.54	0.63	23.74
	90	Cyclic octa atomic sulfur	4.61	0.27	1.23	

### 3.6.3. Flux balance approach (FBA) for modeling wastewater treatment plant

Flux balance analysis is one of the widely accepted methods of modeling metabolism and is a popular approach to model biological systems such as activated sludge systems. This analysis can be done by quantifying the rate of reactions within the network formed by the chemical compounds and the sequence chemical reaction within the microbial metabolism (Perez-Garcia et al., 2014). It uses linear programming to predict fluxes thus providing knowledge on reaction stoichiometry, the composition of biomass and constraints i.e., limit on the uptake or excretion rate of nutrients and by-products respectively.

Flux balance provides detailed information about all the enzymes involved in a metabolic process (Kauffman et al., 2003) and can also be used for rational design of strain, prediction of theoretical yields and identification of bottlenecks or in understanding the metabolism for optimisation of processes (Boyle & Morgan, 2009). Moreover, flux balance analysis is used to describe the potential behavior of an organism under specific environmental conditions (Kauffman et al., 2003).

In previous years' flux balance analysis was successfully applied to model photosynthetic metabolism of *Cyanobacteria Synechocystis* sp and to model metabolic network of other *cyanobacteria* such as *Arthrospira platensis* (Boyle & Morgan, 2009; Wiechert, 2001). FBA is often used by metabolic engineers to quantitatively simulate microbial metabolism (Kauffman et al., 2003).

This modeling approach is a constraint-based model whereby the metabolic fluxes (reactions) are balanced around each node (metabolite) and it relies on the use of linear programming to predict, for example, the maximisation yield for biomass (Ramkrishna & Song, 2012). This modeling approach assumes that the metabolic networks will reach a steady-state and not be constrained by the stoichiometry. Generally, the mass balance is described by linear equations (Mahadevan et al., 2002)-see Eq 5.

$$A * v = 0 \quad (5)$$

Where A is m X n stoichiometric matrix of the reactions, n is the number fluxes and m is the number of metabolites. If a metabolic network consists of (m) metabolites and (n) fluxes, then the mass conservation equation for each metabolite can be (Eq 6):

$$\frac{dz}{dt} = AvX, \frac{dX}{dt} = \mu X, \mu = \sum w_i v_i \quad (6)$$

Where  $X$  is the biomass concentration,  $z$  is the vector of metabolite concentrations,  $\mu$  is the growth rate,  $A$  is the stoichiometric matrix of the metabolic network and  $w_i$  is the quantity of growth precursors needed per gram (DW) of biomass.

More constraints such as non-negative metabolite and the effect of flux level, limits on the rate of change of constituents fluxes, as such therefore nonlinear constraints can be applied on the transport fluxes in order to obtain a realistic prediction of the metabolite concentrations and the metabolic fluxes. Below is the general dynamic optimization problem (Eq 7).

$$\begin{aligned}
 & \text{MAX} \quad \hat{w}_{end} \Phi(Z, v, X)|_{t=tr} \\
 & Z(t), V(t), X(t) \\
 & + \hat{w}_{ins} \sum_{j=0}^M \int_{t_0}^{t_f} L(z, v, X(t)) \delta(t - t_j) dt \\
 & \text{S.t.} \quad \frac{dz}{dt} = AvX \\
 & \quad \quad \frac{dX}{dt} = \mu X \\
 & \quad \quad \mu = \sum w_i v_i \\
 & \quad \quad t_j = t_0 + j \frac{t_f - t_0}{M} \quad j = 0 \dots M \\
 & \quad \quad C(v, z) \leq 0 \quad |v| \leq v_{max} \quad \forall t \in [t_0, t_f] \\
 & \quad \quad z \geq 0 \quad X \geq 0 \quad \forall t \in [t_0, t_f] \\
 & \quad \quad z(t_0) = z_0 \quad X(t_0) = X_0
 \end{aligned} \tag{7}$$

#### 3.6.4. Cybernetic modeling

Genomic and biochemical information has been widely used to construct the cell metabolic network in the wastewater treatment plants; nevertheless, this information is inadequate to completely describe metabolic phenotypes expressed by an organism under various environmental conditions. Furthermore, metabolic phenotypes are described as flux distribution through the metabolic flux network (Edwards et al., 2002). The biological information in the WWTP is growing rapidly, yet there is still insufficient information that describes, in mathematical expressions, cellular metabolism of microorganisms.

Microbial growth consists of thousands of chemical reactions, some of the reactions become readily apparent when a microorganism grows on multiple simple substrates. The behavior of these

microorganisms in multiple substrates condition varies as some microbes may exhibit simultaneous utilization of substrate while others may use substrates sequentially for the benefit a whole process. It is critical to understand the internal regulatory processes responsible for these varied behavior patterns of microorganisms under certain conditions (Kompala et al., 1984).

In order to understand this phenomenon, cybernetic models have been employed to model microbial growth on multiple substrates. This model was first reported by (Ramkrishna et al., 1982). Cybernetic modeling considers the primary goal of microorganisms to maximise the growth rate (Patnaik, 2000). Additionally, it assumes that when microorganisms are subjected to limited resources for enzyme induction, they will allocate the limited resources for the induction of key enzymes (Mandli et al., 2015).

These modeling approaches can be used to model microbial and diauxic growth which is an important process in the wastewater treatment plant. Metabolism can be manipulated by controlling the synthesis of enzymes that are responsible for the reactions within the metabolic network, even when the reactions are performed under limited resource conditions. There are two vectors which are referred to as cybernetic variables.  $U$  and  $V$ , where  $u$  is a fractional allocation of resources required for enzyme synthesis, so that  $\sum_{i=1}^{n_i} u_i = 1$  and  $v$  represents the activity of different enzymes. Hence, we must have  $0 \leq u_i, v_i \leq 1$ ,  $i = 1, 2, \dots, n_i$  which is required to balance the reaction. For example, if the maximum synthesis rate  $r_{E_i}$  for enzyme  $E_i$  is regulated then  $u_i r_{E_i} \cdot v_i$  are needed for estimated regulated reaction rates; therefore, if  $r_i$  is the rate of  $i$ th reaction when enzyme  $E_i$  is fully active, the regulated  $i$ th reaction can be represented as  $v_i r_i$ . The reaction rates are determined by specifications  $\Psi, u, v$ . Therefore, the system dynamics can be described as in Eq 8:

$$\frac{d\Psi}{dt} = f(\Psi, u, v) \quad (8)$$

It is known that the ultimate goal of an organism is to maximise or minimise its functions that are required for microbial survival over any time interval  $(t, t + \tau)$  which can be described in terms of the state vector  $\Psi$ . This function can be denoted as  $\Delta J = J(t + \tau) - J(t)$ , thus the goal of the organism can be described as in Eq 9:

$$\begin{aligned} & \text{MAX } \Delta J \\ & Z(t), V(t), X(t) \end{aligned} \quad (9)$$

such that:

$$\sum_{i=1}^{n_i} u_i = 1 \quad 0 \leq u_i, v_i \leq 1 \quad (10)$$

$\mu_i$  and  $v_i$  are the variables of interest in cybernetic models and they are at time  $t$ ; however, the planning horizon is at  $(t, t + \tau)$ . When Equation 3 has been solved then  $\mu_i$  and  $v_i$  can be defined making Equation 6 a fully descriptive model.

### **3.7. Conclusions**

TN removal is an important process in wastewater treatment as it takes advantage of microbial metabolic pathways for efficient removal of TN to acceptable levels. Considering the significance of the microbial population in TN removal, it is important to put a special emphasis on BNR operation and its control in order to promote the smooth operation of this process. Models have been successfully applied in mathematical expression of TN removal processes; however, these models do not consider the metabolic involvement of processes such as SNaD, which makes it complex, during the manipulation of certain pathways responsible. The current review, therefore emphasises the importance of network modeling.



# **CHAPTER 4**

## **MATERIALS AND METHODS**

# CHAPTER 4:

## MATERIALS AND METHODS

### 4.1. General background

The experiments for this study were separated into 3 phases in order to achieve the aims and the objectives as listed in Chapter 1, section 1.5.

### 4.1. PHASE 1: Thermodynamic evaluation of SNaD under cyanide-laden conditions

This Phase aims to Assess the feasibility of nitrification and aerobic denitrification under high  $\text{CN}^-$  conditions through thermodynamics modeling.

#### 4.1.1. Isolation and Inoculum Development

The consortia were isolated from  $\text{CN}^-$  containing waste at the Bioresource Engineering research group (BioERG), Cape Peninsula University of Technology (CPUT) and it was sequenced at Inqaba Biotech SA for identification. They were cultured into a complex media at sterile conditions for 5 days; thereafter, it was transferred into 100 ml of basal media containing: 7.9 g  $\text{Na}_2\text{HPO}_4$ , 1.5 g  $\text{KH}_2\text{PO}_4$ , 0.5 g  $\text{MgSO}_4 \cdot 7\text{H}_2\text{O}$  and 1 mL trace elemental solution. The trace elemental solution was composed of: 1.1 g  $(\text{NH}_4)_6\text{Mo}_7\text{O}_{24} \cdot 4\text{H}_2\text{O}$ , 50 g EDTA, 2.2 g  $\text{ZnSO}_4 \cdot 7\text{H}_2\text{O}$ , 5.5 g  $\text{CaCl}_2$ , 5.0 g  $\text{FeSO}_4 \cdot 7\text{H}_2\text{O}$ , 5.06 g  $\text{MnCl}_2 \cdot 4\text{H}_2\text{O}$ , 1.61 g  $\text{CoCl}_2 \cdot 6\text{H}_2\text{O}$ , 1.57 g  $\text{CuSO}_4 \cdot 5\text{H}_2\text{O}$  (per liter). The consortia were incubated at  $36.5^\circ\text{C}$  for 48 h and was used as an inoculum for the reactor experiment.

#### 4.1.2. Reactor Experimental Runs

The basal media as indicated in section 4.1.1 was used for the reactor experiment. 1 L reactor was used for this experiment. It was inoculated with 10% of the 48 h culture and the microorganisms were grown for 5 days, the contaminants were added on day 6. The pH and temperature were maintained at 6.5 and  $36.5^\circ\text{C}$  throughout the experiment respectively. A concentration, i.e. 285 and 37.55 mg/L of  $\text{NH}_4\text{-N}$  and  $\text{CN}^-$  were then added to the reactors, respectively. After the addition of the toxicant, the reactors were tightly closed and covered with foil to avoid ammonium stripping and volatilization of  $\text{CN}^-$ . Samples were collected every 24 h to analyze residual  $\text{CN}^-$ ,  $\text{NH}_4\text{-N}$ ,  $\text{NO}_2\text{-N}$ , and  $\text{NO}_3\text{-N}$  using test kits obtained from Merck SA and Merck ANOVA Spectroquant. All the analysis was performed in duplicates. The bases of the cyanide test kit are based on the reaction of cyanide with Chloramines-T and pyridine-barbituric acid (Lambert et al., 1975). The ammonium test kit function based on the reaction of Berthelot reagent, ammonium, chlorine and phenolic compounds, to form indophenol dyes (Patton and Crouch, 1977). The nitrate test kit uses concentrated sulphuric acid in the presence of a benzoic acid derivative to produce a calorimetrically

quantifiable by-product, while the nitrite test kit is based on the reaction of nitrite ions with sulfanilic acid to form diazonium salt (Rider & Mellon, 1946). The microbial growth rate in the cultures was determined using a UV-VIS spectrophotometer at 660 nm.

#### 4.1.3. Bioenergetic/Thermodynamic Models

The free energy ( $\Delta G$ ) equation for nitrification can be expressed as:

$$NH_4 - N + 1.05O_2 \rightarrow NO_2^- + H^+ \Delta G = 65 + RT \ln \left\{ \frac{[NO_2^-](10^{-pH})^2}{[NH_4 - N][O_2]^{1.5}} \right\} \quad (11)$$

$$NO_2^- + 0.5O_2 \rightarrow NO_3^- \Delta G = 18.5 + RT \ln \left\{ \frac{[NO_3^- - N]}{[NO_2^- - N][O_2]^{0.5}} \right\} \quad (12)$$

Where  $\Delta G$  is a free energy change in Kcal/mol,  $NH_4-N$  is the molar concentration of ammonium ions,  $NO_2-N$  is the molar concentration of  $NO_2-N$  and  $O_2$  is a molar concentration of oxygen gas,  $R$  is the universal gas constant and  $T$  is temperature. However, when the experiment is operated at steady-state with constant Temperature, pH and abundance of  $O_2$  Eq. (11) and (12) becomes:

$$\Delta G = 65 + RT \ln \left( \frac{[NO_2^- - N]}{[NH_4 - N]} \right) \quad (13)$$

$$\Delta G = 18.5 + RT \ln \left( \frac{[NO_3^- - N]}{[NO_2^- - N]} \right) \quad (14)$$

The model used to estimate the rates with respect to their corresponding Free energies is as explained by Mirbagheri et al. (2010). The model assumes that when nitrifying bacteria remain constant then the rate of microbial growth could be described as a function of  $\Delta G$ , therefore:

$$\mu = F \Delta G \quad (15)$$

Where  $\mu$  is a growth rate,  $F$  is a linear function. However  $\mu = (1/X)(dx/dt)$  and  $Y = dx/dt, ds/dt$  the equation can be rearranged as follow:

$$\frac{ds}{dt} = \frac{X}{Y} F \Delta G \quad (16)$$

Where  $X$  is biomass concentration and  $Y$  is biomass yield. At steady-state and when the bacterial yield is constant the equation can be rearranged as:

$$\frac{ds}{dt} = F \Delta G \quad (17)$$

The value of  $\Delta G$  was determined as using with equations 13 and 14, thereafter, Eq. 17 was for linear regression using polymath 10.0.

## **4.2. PHASE 2: Assessing the predictive capability of existing models**

The aim of this phase was to compare the predictive capability of existing mathematical models towards simultaneous nitrification and aerobic denitrification under high  $\text{CN}^-$  conditions.

### **4.2.1. Isolation and identification of the bacterial isolate of interest**

The isolate used in this study was isolated from  $\text{CN}^-$  containing waste at the Bioresource Engineering Research Group (*BioERG*) laboratory, Cape Peninsula University of Technology, Cape Town, South Africa. This organism was sub-cultured to obtain pure colonies and subjected to toxicant ( $\text{CN}^-$ ) resistance testing to determine the highest  $\text{CN}^-$  concentration it can withstand subsequent to gram staining. The genomic DNA was extracted from the pure cultures using the Quick-DNA™, Fungal/Bacterial Miniprep kit, to target the 16S rRNA gene (Zymo Research, Irvine, CA, Catalogue No. D6005). This region was amplified using the OneTaq® Quick-Load® 2X Master Mix (Zymo Research, Irvine, CA, Catalogue No. M0486) and the primers which were used were the 16S-27F and 16S-1492R with sequence (5' to 3') AGAGTTTGATCMTGGCTCAG, and CGGTTACCTTGTTACGACTT, respectively.

The PCR products were run on an agarose gel and the gel fragments were extracted using the Zymoclean™ Gel DNA Recovery Kit (Zymo Research, Irvine, CA, Catalogue No. D4001). The extracted fragments were sequenced in the forward and reverse direction using the Nimagen BrilliantDye™ Terminator Cycle Sequencing kit v3.1 and further purified using the Zymo Research, ZR-96 DNA Sequencing Clean-up kit™. The purified fragments were analyzed using the ABI 3500XL Genetic Analyzer (Applied Biosystems, ThermoFisher Scientific, Massachusetts, USA). CLC Bio Main Workbench v7.6 was used to analyze the files generated by the ABI 3500XL Genetic Analyzer and results were obtained through a BLAST search (NCBI).

### **4.2.2 Batch culture experiments**

A basal medium similar to the one used in 4.1.1 was used for SNaD and  $\text{CN}^-$  degradation studies. Erlenmeyer flasks (250mL) were used with a working volume of 100 mL of basal media. The media was inoculated with a loop full of an overnight agar grown bacterial culture. The inoculated media was initially grown for 72 h without  $\text{NH}_4\text{-N}$  and  $\text{CN}^-$ , thereafter; 20 mg $\text{NH}_4\text{-N}$  /L and 20 mg  $\text{CN}^-$ /L were added to the inoculated basal medium whereby samples were collected on a 24 h interval for 168 h to analyze  $\text{CN}^-$ ,  $\text{NH}_4\text{-N}$ ,  $\text{NO}_2\text{-N}$ ,  $\text{NO}_3\text{-N}$  and microbial growth at OD660 nm. The biomass concentration at OD660 nm was calculated by Eq. 18 (from calibrated values in triplicate).

$$\text{OD}_{660} = 0.0089 \text{ (CFU)} - 0.3097$$

(18)

#### 4.2.3. Enzyme extraction

To analyze the activities of the enzymes, i.e. AMO, NaR and NiR, cold acetone was added to the collected samples, forming a pellet that was separated from the supernatant by centrifuging each sample at 5000 g for 15 min. The pellet was lysed using a sonicator and the supernatant was collected by centrifugation at 16000 rpm for 5 min. Thereafter, the precipitate was washed three times and resuspended in phosphate (360 mg/L) buffer solution (pH 7.4).  $\text{NH}_4\text{-N}$  and  $\text{CN}^-$  solutions were prepared and the enzyme extracts were added into the  $\text{NH}_4\text{-N}$  and  $\text{CN}^-$  solutions, while the changes in  $\text{CN}^-$  (09701),  $\text{NH}_4\text{-N}$  (00683),  $\text{NO}_2\text{-N}$  (110057) and  $\text{NO}_3\text{-N}$  (14773) were monitored and analyzed using the Merck test kits (Merck & Co., New Jersey, USA).

The activity of the  $\text{NH}_4\text{-N}$  oxidizing enzyme was monitored by measuring the changes in  $\text{NH}_4\text{-N}$  after the addition of the enzyme extracts into the  $\text{NH}_4\text{-N}$  solution. The formation of  $\text{NO}_3\text{-N}$  from  $\text{NO}_2\text{-N}$  and the disappearance of  $\text{NO}_3\text{-N}$  were also monitored in order to determine the activity of both  $\text{NO}_3\text{-N}$  and  $\text{NO}_2\text{-N}$  oxidizing enzymes, i.e. NaR and NiR. The  $\text{CN}^-$  degrading enzymes were monitored with the changes in the concentration of  $\text{CN}^-$ .

#### 4.2.4. Analytical procedure(s)

All the test kits used for the analyses of the samples in this study were obtained from Merck SA a subsidiary of Merck & Co., New Jersey, USA. Furthermore, the Merck Spectroquant Nova 60 instrument was used to quantify the residual  $\text{CN}^-$ ,  $\text{NH}_4\text{-N}$ ,  $\text{NO}_2\text{-N}$ , and  $\text{NO}_3^-$  concentrations. The tests were conducted as per the manufacturer's instructions.

#### 4.2.5. Kinetics model developed

During  $\text{CN}^-$  biodegradation, microorganisms convert  $\text{CN}^-$  to  $\text{NH}_4\text{-N}$  which was then used as a nitrogenous source. Mekuto et al. (2015) reported the ability of cyanide degrading bacteria to degrade  $\text{CN}^-$  and subsequently utilize  $\text{NH}_4\text{-N}$ , with a further indication that some microorganisms are able to use  $\text{NH}_4\text{-N}$  and  $\text{CN}^-$  as nitrogenous sources simultaneously. It has been shown by Mpongwana et al. (2016) that when a cyanide degrading microorganism is used for nitrification and denitrification under cyanide conditions, the microorganism undergoes, multiple growth phases, i.e. mostly diauxic growth; hence, growth models that describe diauxic growth must be considered when evaluating growth kinetic parameters of such microorganisms when removing TN. The multiphase growth rate was first described by Monod. (1942) as a sequential utilization of substrates accompanied by distinct exponential growth phases during a period in which the individual substrates were utilized.

In this study, Monod's and other models were also used to describe simultaneous  $\text{CN}^-$  degradation, and SNaD, with all the experiments being carried out in a closed system (1L batch culture). The rate of toxicant pollutant degradation can be described as in Eq. 19.

$$-\frac{dC_a}{dt} = r_a = K_i C_a^n \quad (19)$$

Where  $r_a$  is the rate of pollutant degradation,  $K_i$  is the saturation constant,  $C_a$  is the concentration of the pollutant,  $-dC_a/dt$  is the disappearance rate of the pollutant, and  $n$  is the model fitting constant.

When TN is the sole nitrogenous source, the system is considered to be a non-inhibited system. As such, Monod's' proposed kinetic model (Eq. 20) for non-inhibited systems, is deemed suitable to model such systems.

$$-\frac{dC_a}{dt} = \frac{V_m * C_a}{K_i + C_a} \quad (20)$$

Where  $V_m$ , is the maximum specific degradation rate of the pollutant.

Haldane (Annuar et al., 2008) also represented pollutant degradation kinetics using a model as shown in Eq. 21.

$$-\frac{dC_a}{dt} = \frac{V_m C_a}{C_a + \frac{C_a^2}{K_i}} \quad (21)$$

Due to the possibility of inhibition of SNaD by  $\text{CN}^-$ , a model (Andrew's model) representing the kinetics of a primary pollutants' degradation in which a secondary inhibitory pollutant is present, was deemed necessary to use, as presented in Eq. 22 (Annuar et al., 2008).

$$\frac{dC_a}{dt} = -V_m \left[ 1 - \left( \frac{K_i}{C_a} \right) \right] \left[ 1 + \left( \frac{C_a}{K_s} \right) \right] \quad (22)$$

Where  $K_s$  is a secondary pollutants' inhibition constant.

#### 4.2.6. Regression of experimental data and estimation of model kinetic parameters

Mathematical models describing  $\text{CN}^-$  and  $\text{NH}_4\text{-N}$  accumulation and degradation were fitted to the experimental data generated. Additionally, the models describing  $\text{NH}_4\text{-N}$  degradation with pollutant inhibition were also fitted into  $\text{NH}_4\text{-N}$  accumulation and accumulation experimental data. A nonlinear regression function on Polymath 6.0 software was used for simulations, thus the generation of simulation data (using estimated kinetic parameters) that was compared to experimental data.

#### 4.2.7. Data handling and kinetic parameters

The data were computed and analyzed using Microsoft Excel v2016. The mean was determined using Eq. 23; Moreover, Polymath 6.0 was used to estimate kinetic parameters in Eq. (s) 19, 21 and 22. The data obtained from polymath was plotted using Microsoft Excel v2016.

$$Mean = \frac{\sum X}{n} \quad (23)$$

Where  $\sum X$  is the sum of the data points, while  $n$  is the number of experimental experiments conducted.

### 4.3. PHASE 3: Optimisation and evaluation of predictive ability of RSM and Cybernetic models

The aim of this phase was to optimise SNaD and cyanide degradation, subsequent to evaluation of predictive ability of RSM versus the cybernetic model for SNaD and CN<sup>-</sup> degradation.

#### 4.4. Microbial isolation and identification

The bacteria used for this study was isolated from CN<sup>-</sup> containing waste at the Bioresource Engineering Research Group (*BioERG*) facility at the Cape Peninsula University of Technology (CPUT), South Africa. Isolates were cultured on nutrient agar to obtain pure colonies. Thereafter, they were grown on nutrient agar (NA) containing different concentrations of CN<sup>-</sup> 10 to 300 mg/L of CN<sup>-</sup> to determine the highest concentration of CN<sup>-</sup> that they can withstand, subsequent to gram staining. The cyanide tolerant bacteria's 16S RNA was sequenced and identified the bacteria as *Acinetobacter courvalinii*, accession number AB602910.1 or NR\_148843.1 (Stephen et al., 1997).

### 4.5. Response surface methodology

#### 4.5.1. Central composite design experiments

The central composite design was used for the optimization of SNaD under CN<sup>-</sup> conditions. This was done by determining the independent variables, i.e. temperature and pH, optima which have been reported to affect SNaD (Mekuto et al., 2015). In this study, a 13-run experimental plan which included the variation in independent variables (temperature and pH) was generated using central composite design (CCD) (see Table 4.1).

**Table 4.2.** The dependent variables included in the central composite design experiments and their high, medium, low concentrations.

<b>Factor</b>	<b>Name</b>	<b>Units</b>	<b>Type</b>	<b>Low Actual</b>	<b>High Actual</b>	<b>Low Coded</b>	<b>High Coded</b>
<b>A</b>	Temperature	deg C	Numeric	34.00	39.00	-1.000	1.000
<b>B</b>	pH		Numeric	4.00	9.00	-1.000	1.000

The experimental design used for this study is shown in Table 4.2, with the corresponding response being primarily TN removal and CN<sup>-</sup> degradation. Synthetic wastewater containing NH<sub>4</sub>-N /L (20 mg) and CN<sup>-</sup> /L (20 mg) were used for these experiments. The isolated strain was grown in a 250 mL multipoint Erlenmeyer flask with 40 mL basal media containing: 1.5 g KH<sub>2</sub>PO<sub>4</sub>, 7.9 g Na<sub>2</sub>HPO<sub>4</sub>, 0.5 g MgSO<sub>4</sub>.7H<sub>2</sub>O and 1 mL of trace elemental solution per liter. The trace element solution contained (per liter): 50 g EDTA, 2.2 g ZnSO<sub>4</sub>.7H<sub>2</sub>O, 5.5 g CaCl<sub>2</sub>, 5.06 g MnCl<sub>2</sub>.4H<sub>2</sub>O, 5.0 g FeSO<sub>4</sub>.7H<sub>2</sub>O, 1.1 g (NH<sub>4</sub>)<sub>6</sub>Mo<sub>7</sub>O<sub>2</sub>.4H<sub>2</sub>O, 1.57 g CuSO<sub>4</sub>.5H<sub>2</sub>O, 1.61 g CoCl<sub>2</sub>.6H<sub>2</sub>O. The isolate was allowed to grow for 24 h prior to the addition of toxicants; KCN as CN<sup>-</sup> and NH<sub>4</sub>SO<sub>4</sub> as NH<sub>4</sub>-N. The Erlenmeyer flasks that were used for this experiment had a sealable sampling port to avoid volatilization of CN<sup>-</sup>. After the addition of the toxicant, each experiment was monitored for 5 h and samples were taken after every 1 h to analyse for CN<sup>-</sup>, and TN as NH<sub>4</sub>-N, NO<sub>2</sub>-N, and NO<sub>3</sub>-N, using Merck test kits and a Merck Spectroquant. All the experiments were done in duplicates with control experiments that did not contain the microorganism in order to account for the volatilization of CN<sup>-</sup> and NH<sub>4</sub>-N stripping.

**Table 4.3.** Central composite design variables.

<b>Run</b>	<b>A: Temperature deg C</b>	<b>B: pH</b>
<b>1</b>	36.5	6.5
<b>2</b>	36.5	2.96
<b>3</b>	36.5	6.5
<b>4</b>	34	4
<b>5</b>	36.5	6.5
<b>6</b>	36.5	6.5
<b>7</b>	34	9
<b>8</b>	39	4



<b>9</b>	36.5	6.5
<b>10</b>	40.04	6.5
<b>11</b>	32.96	6.5
<b>12</b>	36.5	10.04
<b>13</b>	39	9

To determine the critical points (maximum, minimum, target or within range) a polynomial function that contains quadratic terms were used (Eq. 24) (Mekuto et al., 2015).

$$y = \beta_0 + \sum_{i=1}^k \beta_i X_i + \sum_{i=1}^k \beta_{ii} X_i^2 + \sum_{1 < i < j}^k \beta_{ij} X_i X_j + \varepsilon \quad (24)$$

Where k is the number of variables,  $\beta_0$  is the constant term,  $\beta_i$  is the coefficients of the linear parameters,  $\beta_{ij}$  is the coefficients of the interaction parameters,  $\beta_{ii}$  is the coefficients of the quadratic parameter,  $x_i$  represents the variables, and  $\varepsilon$  is the residual associated with the experiments.

#### 4.6. Statistics analyses

The statistical analyses were centered on the lack of fit test which describes the fitness of mean and reduced the quadratic model of TN removal and the sequential model sum of squares. The model as represented in Eq.1 indicated the relationship between the dependent variables and TN removal efficiency by the isolate in  $\text{CN}^-$  containing wastewater. Furthermore, the significance of each variable in the model was analysed using Analysis of Variance (ANOVA) with a Multiple Regression Analysis being used to analyse the experimental data obtained.

#### 4.7. Cybernetic model

##### 4.7.1. Batch culture experiment

A basal media similar to that used for the RSM experiments was used in batch cultures; although, the experiment was carried out in 1 L reactors. The media was inoculated with 100 mL of an overnight grown culture (24 h) incubated at 36.5 °C, with the media being maintained at a pH of 6.5 throughout the experiment. The culture was incubated for 168 h prior to the supplementation of  $\text{CN}^-/\text{L}$  (40mg) and  $\text{NH}_4\text{-N}/\text{L}$  (250mg); a combination that was shown to have little growth inhibition during toxicity assessments, with 2mL samples being taken periodically (24 h intervals) for analyses, i.e.  $\text{CN}^-$ ,  $\text{NH}_4\text{-N}$ ,  $\text{NO}_2\text{-N}$ , and  $\text{NO}_3\text{-N}$ . Enzymes, assumed to have been produced extracellularly, were extracted using cold acetone daily from the cultures, to quantify maximum enzyme activity ( $e_i^{max}$ ).

#### 4.7.2. Enzyme activity assessments

The suspended bacterial cells in samples were removed by centrifuging each sample at 5000 g for 5 min; thereafter, to the cell-free supernatant, cold acetone was added, forming a precipitate which was then separated from the supernatant by centrifugation at 16000 g for 15 min. The precipitate was washed ( $n = 3$ ) and resuspended in 360 mg/L phosphate buffer solution (pH 7.4) at  $-18^{\circ}\text{C}$ .  $\text{NH}_4\text{-N}$  and  $\text{CN}^-$  solutions with initial concentration of 10 mg/L were prepared and the enzyme extract was added into the solution, while the changes in  $\text{CN}^-$  (09701),  $\text{NH}_4\text{-N}$  (00683),  $\text{NO}_2\text{-N}$  (110057) and  $\text{NO}_3\text{-N}$  (14773) were monitored and analyzed using the Merck test kits and a Spectroquant (Merck, South Africa).

#### 4.7.3. Analytical procedure

All the test kits used for the analysis of the samples were obtained from Merck SA. Furthermore, a Merck Spectroquant Nova 60 instrument was used to analyse residual  $\text{CN}^-$ ,  $\text{NH}_4\text{-N}$ ,  $\text{NO}_2\text{-N}$ , and  $\text{NO}_3\text{-N}$ . The kits were used as per the manufacturer's instructions.

#### 4.7.4. Model development

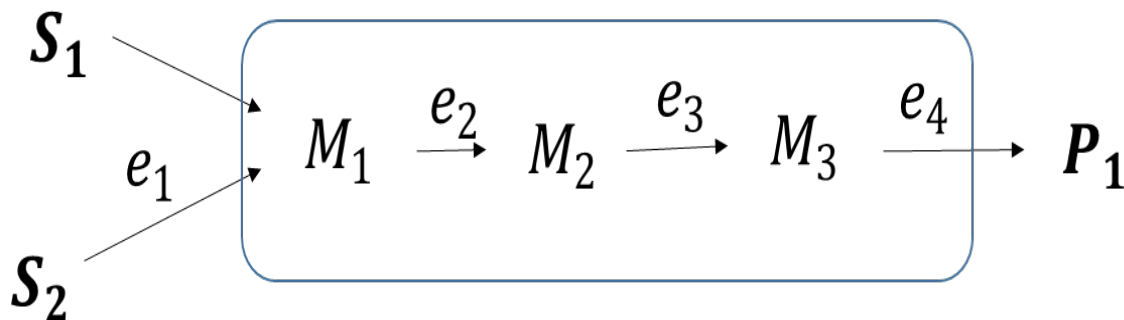


**Figure 4.1.** Simplified metabolic network diagram of SNaD under cyanide-laden conditions. Key:  $S_1$ :  $\text{NH}_4\text{-N}$ ,  $S_2$ :  $\text{CN}^-$ ,  $M_1$ :  $\text{NH}_4\text{-N}$ ,  $M_2$ :  $\text{NO}_2\text{-N}$ ,  $M_3$ :  $\text{NO}_3\text{-N}$  and  $P_1$ :  $\text{N}_2$

A simplified model for prediction of SNaD as well as  $\text{CN}^-$  degradation in a single reactor was developed as shown in Fig 1. Two nitrogenous compounds  $\text{NH}_4\text{-N}$  and  $\text{CN}^-$  were used as pollutants with  $S_1$  and  $S_2$  presenting  $\text{NH}_4\text{-N}$  which is assimilated none-enzymatically into the cell and  $\text{CN}^-$  respectively, while  $M_1$ ,  $M_2$ , and  $M_3$ , represented intermediates,  $\text{NH}_4\text{-N}$ ,  $\text{NO}_2\text{-N}$ , and  $\text{NO}_3\text{-N}$  respectively. The biomass used was deemed capable of using both  $\text{NH}_4\text{-N}$  and  $\text{CN}^-$  as primary pollutants to be degraded. The biomass converts  $\text{CN}^-$  into  $\text{NH}_4\text{-N}$  for which a part of  $\text{NH}_4\text{-N}$  is assimilated for proliferation and the other portion is further converted into intermediates  $\text{NO}_2\text{-N}$ , and  $\text{NO}_3\text{-N}$ . The presence of  $\text{NO}_3\text{-N}$  can induce denitrification enzymes production thus resulting in the initiation of the denitrification process which involves the conversion of  $\text{NO}_3\text{-N}$  denoted as  $M_3$  into nitrogenous gas ( $\text{N}_2$ ) denoted as  $P_1$ . Under optimized conditions, it has been shown that when the biomass is provided with  $\text{NH}_4\text{-N}$  and  $\text{CN}^-$  it undergoes multiphase growth

while simultaneously degrading the pollutants. Therefore, the predictive capability of cybernetic models was evaluated to estimate the simultaneous degradation of  $\text{NH}_4\text{-N}$  and  $\text{CN}^-$  using the cyanide degrading bacteria *Acinetobacter courvalinii*. The model was developed based on the metabolic reaction network as illustrated in Fig 4.1. All these processes are catalysed by specific enzymes, i.e. ammonia monooxygenase (AMO), nitrate reductase (NaR) and nitrite reductase (NiR). When modeling metabolic networks, two vectors are considered important for cybernetic variables. These vectors are  $u$  and  $v$ , for which  $u$  is a fractional allocation of resources needed for enzyme synthesis, such that  $\sum_{i=1}^{n_i} u_i = 1$  and with  $v$  representing the activity of the different enzymes. Conditions  $0 \leq u_i, v_i \leq 1$ , whereby  $i = 1, 2, 3, 4$ .  $u$  is needed for balancing the reaction. For example, when the maximum synthesis rate  $r_E$  for enzyme  $E_i$  is regulated then  $u_i r_{E_i}$ . Moreover,  $v_i$  is required to estimate the regulated reaction rates; thus,  $r_i$  will be the rate of the  $i^{\text{th}}$  reaction when enzyme  $E_i$  is fully active. The regulated  $i^{\text{th}}$  reaction can also be written as  $r = v_r r_i$ .

Monods' model was used to express the rate of TN removal ( $r_i$ ) for pollutant  $S_i$  and  $S_j$  catalysed by enzyme  $e_i$  to form intermediate  $M_2$  and  $M_3$  (Eq. 25).

$$r_i = r_i^{\max} \frac{s_1}{s_1 + K_i} \left( \frac{e_1}{e_1^{\max}} \right) \quad i = 1, 2, 3, 4 \quad (25)$$

The cell growth rate was model using rate law equation (1<sup>st</sup> order) indicated in Eq. 26.

$$\frac{dx}{dt} = r_g X \quad (26)$$

Where  $r_i^{\max}$  is the are maximum pollutant removal rate and  $K_i$  is the pollutant saturation constant,  $X$  is cell concentration and  $r_g$  is the cell growth rate.

Enzyme synthesis for the two pollutants,  $S_1$  and  $S_2$  was assumed to be maximized as the growth rate of biomass increased such that (Eq. 27);

$$u = \frac{r_i/M_i}{\sum_{j=1}^2 r_j/M_j} \quad v = \frac{r_i/M_i}{\max(r_i/M_i)} \quad i = 1, 2, 3, 4 \quad (27)$$

It was hypothesised that  $\text{NH}_4\text{-N}$  was broken down into  $\text{NO}_2\text{-N}$  via AMO (represented by  $e_2$ ) catalysis while  $\text{CN}^-$  was decomposed by cyanide degrading enzyme(s) represented as  $e_1$ . The intermediate  $\text{NO}_2\text{-N}$  was further broken down into  $\text{NO}_3\text{-N}$  facilitated by NiR represented in the diagram as  $e_3$ , with  $\text{NO}_3\text{-N}$  being further decomposed into  $\text{N}_2$  by NaR represented as  $e_4$ . The model, Eq. 28, would thus represent the rate of enzyme(s) synthesis responsible for the SNaD under cyanogenic conditions.

$$\frac{de_1}{dt} = \alpha_{e_1} + r_{e_1} u_1 - (D_g + b_1) e_1 \quad (28)$$

Where  $\alpha_{ei}$  represents an inductive rate,  $b_i$  is the activity of the enzyme responsible for decomposition of a pollutant,  $r_{ei}$  the decomposition rate of the nitrogenous pollutant,  $b_i$  is the degradation rate constant of the enzyme,  $D_g$  dilution term due to growth rate. The model parameters were estimated by polymath software v6.0 using experimental data.

## CHAPTER 5

# **Kinetic Modelling of Free Energy for Simultaneous Nitrification and Aerobic Denitrification under High Cyanide Environments**

*Published as:* Ncumisa Mpongwana, Seteno K. O. Ntwampe, Boredi S. Chidi, Elizabeth I. Omodanisi.2019. Kinetic Modelling of Free Energy for Simultaneous Nitrification and Aerobic Denitrification under High Cyanide Environments. 16<sup>th</sup> SOUTH AFRICAN International Conference on Agricultural, Chemical, Biological and Environmental Science (ACBES-19) Nov. 18-19 2019 Johannesburg (South Africa). Pp 305-306, ISBN-978-81-943403-0-0, <https://doi.org/10.17758/EARES8.EAP1119149>

# CHAPTER 5:

## KINETIC MODELLING OF FREE ENERGY FOR SIMULTANEOUS NITRIFICATION AND AEROBIC DENITRIFICATION UNDER HIGH CYANIDE ENVIRONMENTS

### 5.1. Introduction

Cyanide ( $\text{CN}^-$ ) is a toxic compound known to inhibit most biological process that is being performed in wastewater treatment plants (WWTP). Nitrification and denitrification are among the process that are heavily affected by  $\text{CN}^-$  compounds (Kapoor et al., 2016; Kim et al., 2008). Remedial procedures such as the use of activated carbon have been recognized to eradicate inhibition effect of toxic compounds on nitrification and denitrification; however, the use of activated carbon is not feasible in  $\text{CN}^-$  containing wastewater due to its low absorption capability; furthermore, the use of activated carbon may also result in additional costs (Kim et al., 2008). Han et al. (2013) proposed that cyanide degrading bacteria must be employed to eliminate the inhibition effect of  $\text{CN}^-$  toward nitrification and denitrification. Mpongwana et al. (2016) has proven the feasibility of using cyanide degrading bacteria as a remedial option for inhibition of nitrification and denitrification by  $\text{CN}^-$ .

However, the application of cyanide degrading microorganisms is not yet established in a large scale WWTP due to fear of irretrievable process failure, thus more information that will ease the process control is still required. This study investigates the thermodynamics to understand the simultaneous nitrification and aerobic denitrification (SNaD) by cyanide degrading consortium in the presence of high  $\text{CN}^-$  conditions. The Gibbs free energy of nitritation and nitrataion were investigated since nitritation is known to be a rate-limiting step. A linear relationship is known to exist between the rate of biochemical reaction and their respective free energies (Rottenberg & Gutman, 1977). The Gibbs free energy was selected for this study since it is known to be a driving force of a reaction. The reaction is judged based on the principles of whether the reaction is spontaneous ( $\Delta G < 0$ ), at equilibrium ( $\Delta G = 0$ ) and impossible if ( $\Delta G > 0$ ) (Zhang et al., 2010).

### 5.2. Objectives

The objectives of this section was to:

- Isolate and identify a cyanide resistant mix consortia.

- Asses the feasibility of using the cyanide resistant mix consortia for SNaD at  $\text{CN}^-$  environments.
- Model Gibbs free energy of SNaD under  $\text{CN}^-$  environments.

### 5.3. Materials and methods

The mix consortium was isolated at Bioresource Engineering research group (BioERG), Cape Peninsula University of Technology (CPUT). It was sequenced and identified at Inqaba biotech SA. The mix consortia were grown in a 250 mL Erlenmeyer flask containing 100 mL of basal media explained in section 4.1.1. Thereafter it was incubated at 36.5°C for five days, samples were collected every 24 h to analyse  $\text{NH}_4\text{-N}$ ,  $\text{NO}_2\text{-N}$ ,  $\text{NO}_3\text{-N}$ , and  $\text{CN}^-$ . (All the experiments were conducted in duplicates).

### 5.4. Result and Discussion

An experiment was conducted to study the effect of high  $\text{CN}^-$  concentrations on the ability of cyanide degrading mix consortia to achieve SNaD. The experiment was conducted in a batch reactor. The results obtained reveal that 37.55 mg/L of  $\text{CN}^-$  did not affect the SNaD. The consortia rapidly degraded  $\text{CN}^-$  from 37.55 to 12 mg/L in the first 48 h of the experiment. This could be a defensive mechanism for the consortia to detoxify the  $\text{CN}^-$  concentration into less toxic concentrations. The consortia achieved nitrification, denitrification and cyanide degradation simultaneously.

The degradation efficiency over 288 h was found to be 92.9%, 97.7% with the degradation rate of 0.0234 and 0.139 mg/L/hr for nitrification and  $\text{CN}^-$  degradation respectively. The removal efficiency found in this study is greater than that of a study conducted by Kapoor et al. (2016). Furthermore, Han et al. (2013) found similar results when using cyanide degrading bacteria for nitrification subsequent denitrification. However, the conversion of  $\text{NH}_4\text{-N}$  to  $\text{NO}_2\text{-N}$  did not make a stoichiometric logic as the concentration of  $\text{NH}_4\text{-N}$  used did not correspond with the  $\text{NO}_2\text{-N}$  produced. This phenomenon could be an indication of the residual  $\text{NO}_2\text{-N}$  being used for microbial proliferation or may be caused by high nitrite reductase which rapidly converts  $\text{NO}_2\text{-N}$  into  $\text{NO}_3\text{-N}$ . Jin et al. (2014) also found similar results in a study conducted using *Pseudomonas sp.* ADN-42 for Heterotrophic SNaD under saline conditions. The existence of denitrification was demonstrated by the decrease in the  $\text{NO}_3\text{-N}$  -see Fig. 5.1. Nevertheless, the production of the nitrogenous gasses was not examined during this study.

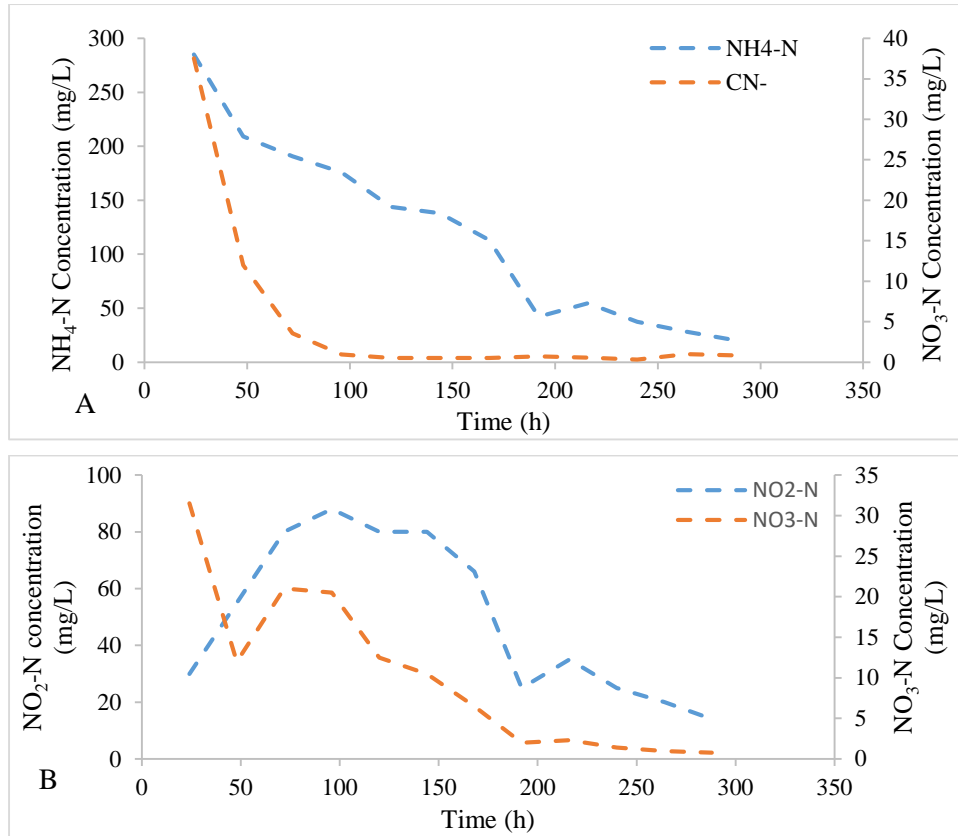


**Figure 5.1.** Graphs representing simultaneous nitrification, denitrification, and cyanide degradation. A:  $\text{NH}_4\text{-N}$  and  $\text{CN}^-$  degradation. B:  $\text{NO}_2\text{-N}$  and  $\text{NO}_3\text{-N}$  accumulation and degradation.

**Table 5.4.** Model variables for nitrification and nitration

Model	F	a	$R^2$	variance	$R^2$ adj
$\frac{d[\text{NH}_4\text{-N}]}{dt} = F\Delta G$	- 0.0001	-	0.93	0.0001	0.93
$\frac{d[\text{NO}_2\text{-N}]}{dt} = F\Delta G + a$	0.001	1.85	0.93	0.0140	0.93

Gibbs free energy ( $\Delta G$ ) was plot as a function of  $[\text{NO}_2\text{-N}]/[\text{NH}_4\text{-N}]$  and  $[\text{NO}_3\text{-N}]/[\text{NO}_2\text{-N}]$ , all the valued of Gibbs free energy were found to be negative for both nitrification and nitration. This is an indication of thermodynamic feasibility and the spontaneity of nitrification and nitration under the  $\text{CN}^-$  conditions (Kushwaha et al., 2010; Khataee et al., 2013). At the beginning of the experiment, the Gibbs free energy was low with the lowest free energy of -756.4 and -1830.9 Kcal/mol for nitrification and nitration respectively. This shows that the reaction was more rapid at the beginning of the experiment (Chowdhury

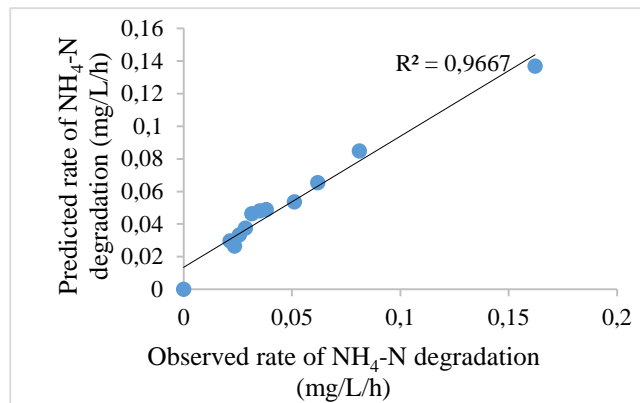


et al., 2011), as the concentration of the toxicant becomes exhausted the free Gibbs energy increases. It has been documented that when a rate of reaction has a strongly negative  $\Delta G$  values, it implies that they are kinetically controlled, meaning they are feasible in wide concentration ranges, this is more likely to occur in oxidation reaction with stronger electron acceptor like oxygen and nitrate (Rodríguez et al., 2008).

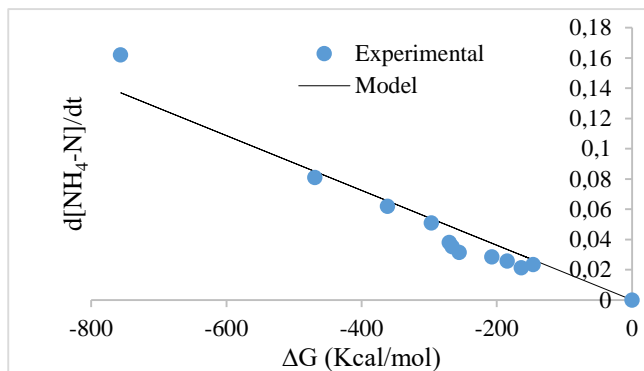
This could also be linked with microorganisms reaching the stationary phase, thus the decrease in energy. Literature claims that there's a linear relationship that exists between biochemical reaction with their corresponding  $\Delta G$  (Rottenberg & Gutman, 1977). The relationship between the rate of  $\text{NH}_4\text{-N}$  and  $\text{NO}_2\text{-N}$  degradation and their corresponding  $\Delta G$  was studied and it was apparent that there is a linear correlation between the rate of  $\text{NH}_4\text{-N}$  and  $\text{NO}_2\text{-N}$  degradation and their corresponding  $\Delta G$ . Lüttge et al. (2006), also reported a linear relationship between the rate of albite dissolution and their corresponding  $\Delta G$ . Furthermore, the Linear models were used to predict the relationship between the rate of  $\text{NH}_4\text{-N}$  and  $\text{NO}_2\text{-N}$  degradation with their corresponding  $\Delta G$ . the model fitted well into the experiment with correlation coefficient of 0.94 and 0.93 for nitritation and nitrataion respectively. Additionally, the observed rate of  $\text{NH}_4\text{-N}$  and  $\text{NO}_2\text{-N}$  degradation was plotted against the predicted rate of degradation for both  $\text{NH}_4\text{-N}$  and  $\text{NO}_2\text{-N}$ , the result showed that the observed rate and the predicted rate had a good linear correlation with the correlation coefficient of 0.97 and 0.93 for nitritation and nitrataion respectively- Fig 5.2 and 5.3.

**Model:** Change =  $F \cdot G$

Parity plot



Simulation of the model



$\Delta G$  as a function of  $[\text{product}]/[\text{reactant}]$

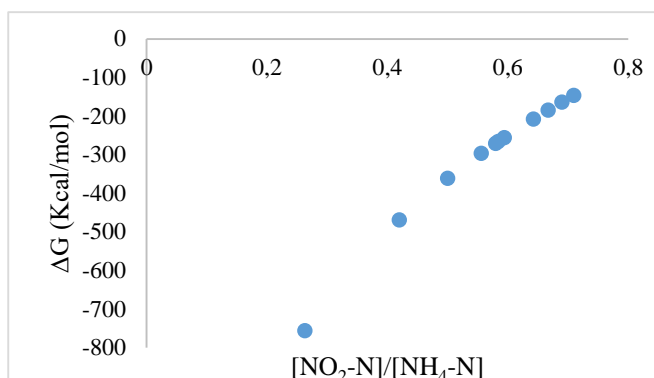
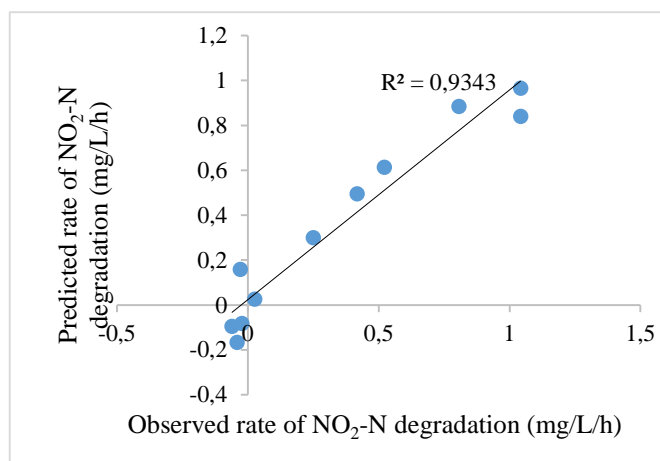


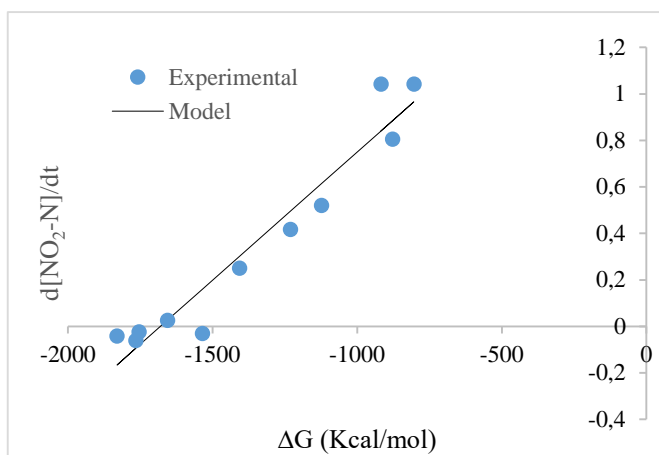
**Figure 5.2.** Parity plots of predicted rate nitrification values versus experimental values. simulations of the linear model data into a rate of  $\text{NH}_4\text{-N}$  degradation versus Gibbs free energy data and  $\Delta G$  as a function of  $[\text{product}]/[\text{reactant}]$ .

**Model:**  $\text{Change} = a + F \cdot G$

Parity plot



Simulation of the model



$\Delta G$  as a function of [product]/[reactant]

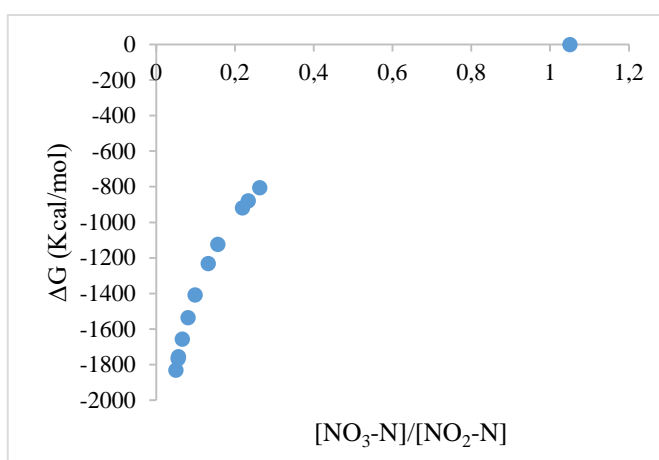


**Figure 5.3.** Parity plots of predicted rate nitration values versus experimental values. simulations of the linear model data into a rate of  $\text{NO}_2\text{-N}$  degradation versus Gibbs free energy data and  $\Delta G$  as a function of [product]/[reactant].

## 5.5. Conclusion

The isolated consortia presented an interesting characteristic, it performed nitrification, denitrification and degraded  $\text{CN}^-$  simultaneously. The Gibbs free energy was also studied to confirm the feasibility of the nitrification and aerobic denitrification under high  $\text{CN}^-$  conditions. Negative  $\Delta G$  were obtained for both nitratation and nitritation, this indicated that the reactions are feasible, spontaneous and rapid. Furthermore, the relationship between the rate of  $\text{NH}_4\text{-N}$  and  $\text{NO}_2\text{-N}$  degradation and  $\Delta G$  was investigated, the results showed that there is a linear correlation between rate of  $\text{NH}_4\text{-N}$  and  $\text{NO}_2\text{-N}$  degradation and their respective  $\Delta G$ . The equilibrium constant was also investigated (results not shown) since the nature of equilibrium constant can also articulate whether the reaction is spontaneous or not, an increase in equilibrium constant with the decrease in  $\Delta G$  was observed, this is also a proof that SNaD reaction occurs spontaneously and does not require additional energy.

## CHAPTER 6

# BIO-KINETICS OF SIMULTANEOUS NITRIFICATION AND AEROBIC DENITRIFICATION (SNAD) BY A CYANIDE DEGRADING BACTERIA UNDER CYANIDE- LADEN CONDITIONS

**Submitted as:** Ncumisa Mpongwana, Seteno Karabo Obed Ntwampe, Elizabeth Ife Omodanisi, Boredi Silas Chidi, Lovasoa Christine Razanamahandry, Cynthia Dlangamandla, Melody Ruvimbo Mukandi. Kinetic modelling of free energy for simultaneous nitrification and aerobic denitrification under high cyanide environments. *Applied Sciences Manuscript ID: applsci-702267 (Accepted)*

# CHAPTER 6:

## BIO-KINETICS OF SIMULTANEOUS NITRIFICATION AND AEROBIC DENITRIFICATION (SNaD) BY A CYANIDE DEGRADING BACTERIA UNDER CYANIDE- LADEN CONDITIONS

### 6.1. Introduction

Untreated total nitrogen (TN) containing wastewater in the environment can result in eutrophication, thus the treatment of such wastewater containing TN is crucial in wastewater treatment plants (WWTPs) (Duan et al., 2015). This type of wastewater may be treated by either physicochemical or biological methods. Most municipal and industrial wastewater treatment plants use biological methods such as simultaneous nitrification and aerobic denitrification (SNaD) for the treatment of contaminated water due to the cost-effectiveness of such processes (Ge et al., 2015a; He et al., 2016).

However, SNaD is sensitive to toxicant loading (Daims et al., 2015; Li et al., 2014; Kim et al., 2008), particularly free cyanide ( $\text{CN}^-$ ) (Daims et al., 2015). Physical and chemical methods have been used to reduce  $\text{CN}^-$  effects on SNaD; however, these methods are relatively expensive, complex and produce undesirable by-products such as hypochlorite, and toxicant loaded sludge (Kapoor et al., 2015). Hence, the biological removal of  $\text{CN}^-$  prior to SNaD has recently received the most attention. Biological  $\text{CN}^-$  removal has been proven to be an ideal option because of its cost-effectiveness and environmental benignity (Inglezakis et al., 2017). Although biological  $\text{CN}^-$  removal reduces the production of undesirable by-products, conducting  $\text{CN}^-$  degradation in a separate reactor with SNaD in sequential two-stage reactor systems, may result in the escalation of costs associated with the operation of the multiple independent reactors dedicated to the biodegradation of  $\text{CN}^-$  and TN. Han et al. (2014) proposed that  $\text{CN}^-$  degrading and resistant microorganisms can be used for SNaD in order to lower the inhibition effect of  $\text{CN}^-$  towards SNaD in a single reactor system.

Mekuto et al. (2015) reported that *Bacillus* species were capable of degrading up to 300 mg  $\text{CN}^-/\text{L}$  and subsequently utilize the by-products which were  $\text{NH}_4\text{-N}$ ,  $\text{NO}_3\text{-N}$ , and  $\text{NO}_2\text{-N}$ . Additionally, Mpongwana et al. (2016) isolated a  $\text{CN}^-$  tolerant strain capable of simultaneous  $\text{CN}^-$  degradation and SNaD. However, the applicability of  $\text{CN}^-$  degrading and resistant microorganisms is still restricted due to the lack of information necessary to adequately control SNaD under high  $\text{CN}^-$  loading conditions. Hence, this paper reports on the isolation of an organism that simultaneously degrades  $\text{CN}^-$  while performing SNaD, with the phenomena

of simultaneous  $\text{CN}^-$  degradation and  $\text{NH}_4\text{-N}$  removal being modeled by the determination of kinetic parameters using numerous decay models. The mechanism by which  $\text{CN}^-$  affects the nitrification and denitrification enzymes is still not documented, thus making it difficult to apply  $\text{CN}^-$  resistant microorganisms in SNaD systems, in which  $\text{CN}^-$  laden wastewater is being treated. To also address this research gap, the expression and activity of ammonia monooxygenase (AMO), nitrate reductase (NaR) and nitrite reductase (NiR) present in the  $\text{CN}^-$  resistant isolates' supernatant, deemed suitable for this research, was also conducted.

## 6.2. Objectives

- Isolation of a single strain of cyanide resistant bacteria from the isolated mix consortium.
- Asses the ability of the isolated single strain to perform SNaD under  $\text{CN}^-$  conditions.
- Evaluating the predictive capability of different mathematical models towards simultaneous nitrification and aerobic denitrification under  $\text{CN}^-$  environments.
- Evaluate the effect of  $\text{CN}^-$  on nitrifying and denitrifying enzymes.

## 6.3. Materials and methods

The single microorganism was isolated from the mix consortium. The Isolated strain was subjected to toxicity test, whereby it was grown in a nutrient agar containing varied concentrations of  $\text{NH}_4\text{-N}$  and  $\text{CN}^-$ . The 16sRNA of the isolated strain was sequenced at Inqaba biotech SA using 16S-27F and 16S-1492R primers with sequence (5' to 3') AGAGTTTGATCMTGGCTCAG, and CGGTTACCTTGTTACGACTT, respectively. Thereafter, the basal medium mentioned in section 4.1.1 was used for batch culture experiments, the microorganism was initially grown for 3 days subsequent to the addition of 20 mg  $\text{NH}_4\text{-N/L}$  and 20 mg  $\text{CN}^-/\text{L}$  into the basal media. samples were collected at a 24 h' interval for 7 days to examine  $\text{CN}^-$ ,  $\text{NH}_4\text{-N}$ ,  $\text{NO}_2\text{-N}$ ,  $\text{NO}_3\text{-N}$  and microbial growth at OD660 nm. The analysis was performed using Merck SA test kits and ANOVA Spectroquant as per manufactures instructions. The effect of  $\text{CN}^-$  on the nitrification and denitrification enzyme was examined. The enzymes were extracted by primary lysing of the cell using sonicator; thereafter, the enzymes were collected from the free cell extract using cold acetone. The free cell extract was also analysed by FTIR to assess whether the  $\text{CN}^-$  attaches to the proteins of the cell.

## 6.4. Results and Discussion

### 6.4.1. Identification of bacterial Isolate

The CN<sup>-</sup> resistant bacterial strain was characterized by sequencing 16sRNA using the universal primers 27F and 1492R to amplify the target region. The results were obtained by a BLAST search. The sequence on NCBI indicated that the isolated bacteria was *Acinetobacter courvalinii*, accession number AB602910.1/NR\_148843.1.

### 6.4.2. Degradation kinetics of Cyanide and NH<sub>4</sub>-N

An experiment was conducted to investigate the growth of *A. courvalinii* under CN<sup>-</sup> conditions, subsequent to CN<sup>-</sup> and TN biodegradation studies by the isolate. The growth of *A. courvalinii* was shown not to be affected by CN<sup>-</sup> concentration of up to 20 mg CN<sup>-</sup>/L; therefore, it was selected for the assessment of its ability to perform SNaD under cyanogenic conditions. The isolate was found to possess a special ability of sequential utilization of CN<sup>-</sup> and TN by exploiting its multi-phased growth attributes, by initially utilizing of CN<sup>-</sup> and subsequently, NH<sub>4</sub>-N, which was evident by the appearance of a secondary logarithmic phase as seen in Fig. 6.1A.

Fig. 6.1A demonstrates that *A. courvalinii* utilized CN<sup>-</sup> primarily, from a concentration of 20 mg CN<sup>-</sup>/L to 5.8 mg CN<sup>-</sup>/L followed by NH<sub>4</sub>-N. The rate of degradation for both CN<sup>-</sup> and NH<sub>4</sub>-N was 2.2 mg CN<sup>-</sup>/L/h and 0.40 mg NH<sub>4</sub>-N/L/h, respectively. Moreover, a cyanide degrading consortium was also assessed (Fig 10.1 Appendix A) as it was having similar attributes to the isolate used in this study; albeit, due to a large percentage of organisms within the consortium being identified as unknown (Fig 10.2 Appendix A), the results were not included nor discussed herein. Overall, an increase of CN<sup>-</sup> in the first 24 h was observed, with a subsequent CN<sup>-</sup> decrease from 58.1 mg CN<sup>-</sup>/L to 5.8 mg CN<sup>-</sup>/L, being observed. The initial increase in CN<sup>-</sup> was associated with the activation of the ANR cascade which results in the production of HCN and denitrification enzymes (NAR, NIR, NOR, and N<sub>2</sub>OR) Fig. 6.1A.

Arai et al. (1997) reported the regulation of ANR cascade for transcription of denitrification enzymes resulting in the production of HCN by *Pseudomonas aeruginosa*. Moreover, the Pseudomonadaceae have been reported to possess aerobic denitrification capability needed in the aiding and furtherance of SNaD (Yunjie et al., 2020). *A. courvalinii* exhibited similar characteristics to those of *Pseudomonas sp.* Mpongwana et al. (2016) also reported an increase in CN<sup>-</sup> concentration during the expression of denitrification enzymes. For this study, a decrease in NH<sub>4</sub>-N from 64.2 to 28.4 mgNH<sub>4</sub>-N/L was observed, indicating an initiation of nitrification from the threshold limit of 5.8 mg CN<sup>-</sup>/L Fig. 6.1A. This indicated that a concentration of 5.8 mg CN<sup>-</sup>/L did not completely inhibit nitrification; albeit, this concentration is above the threshold concentration of CN<sup>-</sup> known to completely inhibit nitrification reaction (Kim et al., 2008). Kim et al. (2007) reported the complete inhibition of nitrification by 1 mg CN<sup>-</sup>/L. The inhibition is largely associated with enzyme redundancy, non-production and deactivation.

The NAR which is activated during the regulation of ANR is a significant enzyme that aid in aerobic respiration; thus, converting  $\text{NO}_3\text{-N}$  back into  $\text{NO}_2\text{-N}$  during aerobic denitrification (Mpongwana et al., 2019). The increase of  $\text{CN}^-$  during the experiment, confirmed the ability of the *A. courvalinii* to induce ANR advocated for its ability to carry out SNaD. Minute accumulation of  $\text{NO}_2\text{-N}$  was observed compared to  $\text{NO}_3\text{-N}$  which was produced in significant quantities in the first 24 h of the experiments Fig. 6.1B. This was deemed normal as some studies have reported that  $\text{NO}_2\text{-N}$  accumulate in insignificant quantities during SNaD (Sin et al., 2008). The  $\text{NO}_2\text{-N}$  increase between 48-72 h, was associated with the conversion of  $\text{NO}_3\text{-N}$  to  $\text{NO}_2\text{-N}$  catalysed by NAR during aerobic respiration culminating in the distinct feature of SNaD, a phenomenon also supported by the observed decrease in  $\text{NO}_3\text{-N}$  between 24 and 72 h which corresponded with the increase of  $\text{NO}_2\text{-N}$ , confirming the ability of *A. courvalinii* to carry-out aerobic respiration thus performing SNaD.

A multi-phased growth as observed in Fig. 6.1A confirmed multiple distinct dual lag phases with a stationary phase being observed between 72-96 h. This stationary phase was associated with biomass switching utilization from one nitrogenous source to another, i.e. from using  $\text{CN}^-$  to  $\text{NH}_4\text{-N}$ . The first lag phase from 0-72 h was linked with the isolates' growth as a result of  $\text{CN}^-$  presence, using it as a source of nitrogen, while the second lag phase from 96-120 h was linked with the growth of *A. courvalinii* as a result of  $\text{NH}_4\text{-N}$  consumption and/or removal, with growth rate being 1.35 and 3.12  $\text{h}^{-1}$  for first and second growth phases, respectively. This indicated that *A. courvalinii* grows well when supported by less toxic nitrogenous source ( $\text{NH}_4\text{-N}$ ) than when growing in an inhibitory toxicant ( $\text{CN}^-$ ) even if it's a nitrogenous source that can be utilized by the organism. However, the rate of  $\text{NH}_4\text{-N}$  removal was low thus, optimization studies are needed, in order to increase the nitrification efficiency, which is the initial step in SNaD. Subsequent to the monitoring of TN and  $\text{CN}^-$  removal, five models were used to assess their predictive ability of SNaD under  $\text{CN}^-$  conditions, with kinetic parameters in each model being determined.



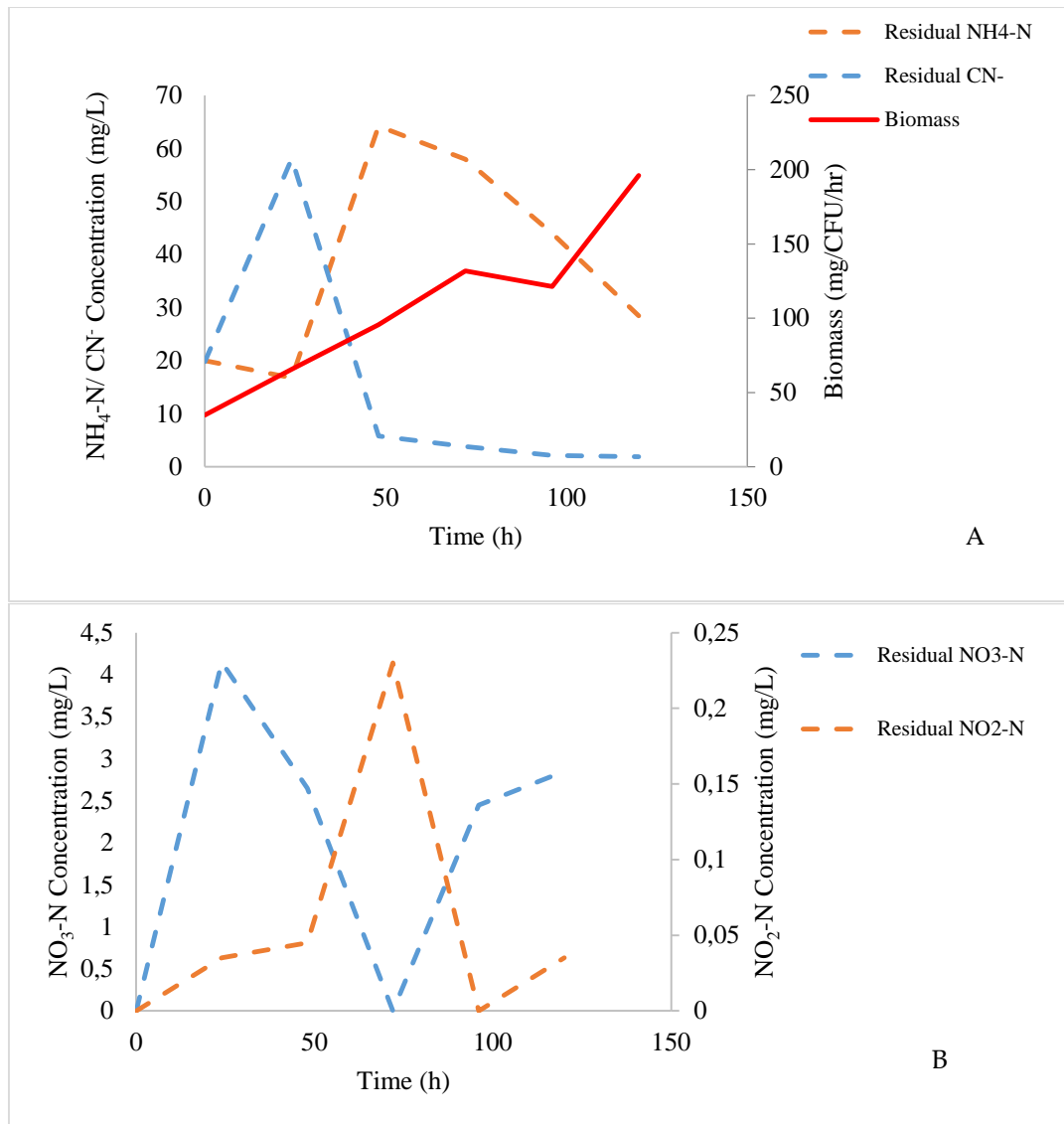


**Figure 6.1.** Biodegradation kinetics of  $\text{NH}_4\text{-N}$  and  $\text{CN}^-$  by *Acinetobacter courvalinii*. A: Growth of *Acinetobacter courvalinii*, sequential degradation of  $\text{CN}^-$  and  $\text{NH}_4\text{-N}$ . B:  $\text{NO}_3\text{-N}$  and  $\text{NO}_2\text{-N}$  accumulation and degradation.

**Table 6.1.** Estimated kinetic parameter values for the models for  $\text{NH}_4\text{-N}$  degradation, a rate-limiting step in nitrification

Fitting constants and the values of kinetic parameter						
( $\pm 95\%$ confidence interval)						
Model	$V_m (h^{-1})$	$K_i (mgL^{-1})$	$K_s (mgL^{-1})$	$n (-)$	$R^2$	variance
Rate law	-	6.29E-05	-	2.27	0.91	0.02

$$-\frac{dCa}{dt} = r = K_i C_a^n$$

<b>Haldane</b>	0.45	23.94	-	-	0.9 2	0.02
$-\frac{dC_a}{dt} = \frac{V_m C_a}{C_a + \frac{C_a^2}{K_i}}$						
<b>Model with substrate inhibition</b>						
<b>Andrews</b>	0.36	27.54	13.22	-	0.94	0.02
$-\frac{dC_a}{dt} = V_m \left[ 1 - \frac{K_i}{C_a} \right] \left[ 1 + \frac{C_a}{K_s} \right]$						

\*Equations 2 to 6 were obtained from Annuar et al (2008)

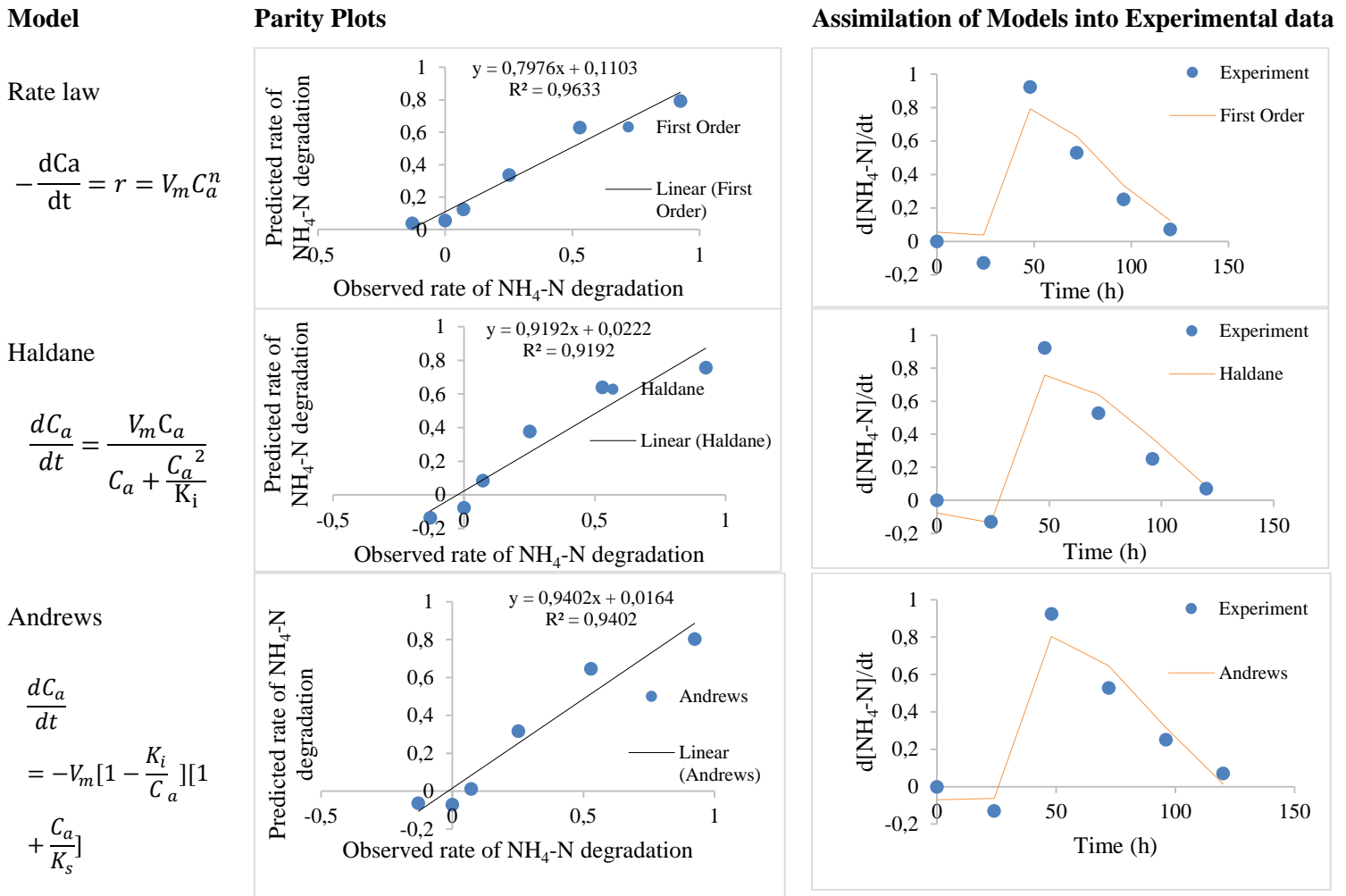


**Figure 6.2.** Parity plots of predicted values versus experimental values. Assimilations of the model data into  $\text{NH}_4\text{-N}$  degradation experimental data (Rate law, Haldane, and Andrew).

The predictive capability of the three models on  $\text{NH}_4\text{-N}$  degradation was analyzed. This was done by simulating the predicted model data in comparison to experimental data and also by plotting parity plots to assess the relationship between predicted data with the observed experimental values. The selected models included the Rate law, Haldane and Andrew's models. The experimental data were fitted into the models to estimate kinetic constant in each model, using Polymath 6.0 software. The Rate law and Haldane models adequately described the experimental data of the nitrification step with a determination coefficient ( $R^2$ ) of 0.91 and 0.92, respectively.

Furthermore, the adjusted determination coefficient ( $\text{Adj } R^2$ ) was 0.89 and 0.89 respectively, with such a high  $\text{Adj } R^2$  signifying a high significance, thus suitability of the estimated model kinetic constants. Furthermore, the variance was 0.015 and 0.016 for the generic rate law and the Haldane model, respectively. This variance is very low and is evidence that the predicted (modeled) values generated using estimated

kinetic parameters did not differ much from experimental data. Similarly, Andrews model-generated data with substrate inhibition was also compared to experimental data. The model gave a better fit with a correlation coefficient of 0.94 and a linear correlation efficiency of 0.98 and an Adj R<sup>2</sup> 0.90.

The average standard deviations were compared for the selection of the better predicting model for NH<sub>4</sub>-N degradation as a limiting step, with a standard deviation of Haldane, Rate law and Andrews model being 0.041, 0.043, and 0.036, respectively. However, for the selection of the model that is adequate in predicting multiple nitrogenous pollutants (CN<sup>-</sup>, NH<sub>4</sub>-N, NO<sub>2</sub>-N and NO<sub>3</sub>-N) removal, the prediction ability of the model towards CN<sup>-</sup> degradation needed to be considered. The parity plot indicated a satisfactory correlation between the experimental rate of NH<sub>4</sub>-N degradation and the predicted rates with R<sup>2</sup> being 0.96, 0.92, and 0.94 for Rate law, Haldane and Andrew's model respectively.

Moreover, the variance for Andrews's model also proved the significance of the model with variance being 0.015. This variance was minute which indicated that there was a negligible difference between the model and experimental data (see Fig. 6.2 and Table 6.1). Monod and Moser models were also assessed for their predictive ability of NH<sub>4</sub>-N and CN<sup>-</sup> degradation rates; however, they did not fit well into the experimental data (Fig. 10.3 and 10.4, Appendix A).

**Table 6.2.** Estimated values of kinetic parameters for the models for CN<sup>-</sup> degradation

Model	Values of kinetic Parameter (±95% confidence interval)					R <sup>2</sup>	variance
	V <sub>m</sub> (h <sup>-1</sup> )	K <sub>i</sub> (mgL <sup>-1</sup> )	K <sub>s</sub> (mgL <sup>-1</sup> )	n (-)			
Rate law $-\frac{dC_a}{dt} = r = K_i C_a^n$	-	3.33E-05	-	2.65		0.92	0.05
Haldane $\frac{dC_a}{dt} = \frac{V_m C_a}{C_a + \frac{C_a^2}{K_i}}$	0.36	11.36	-	-		0.95	365.43

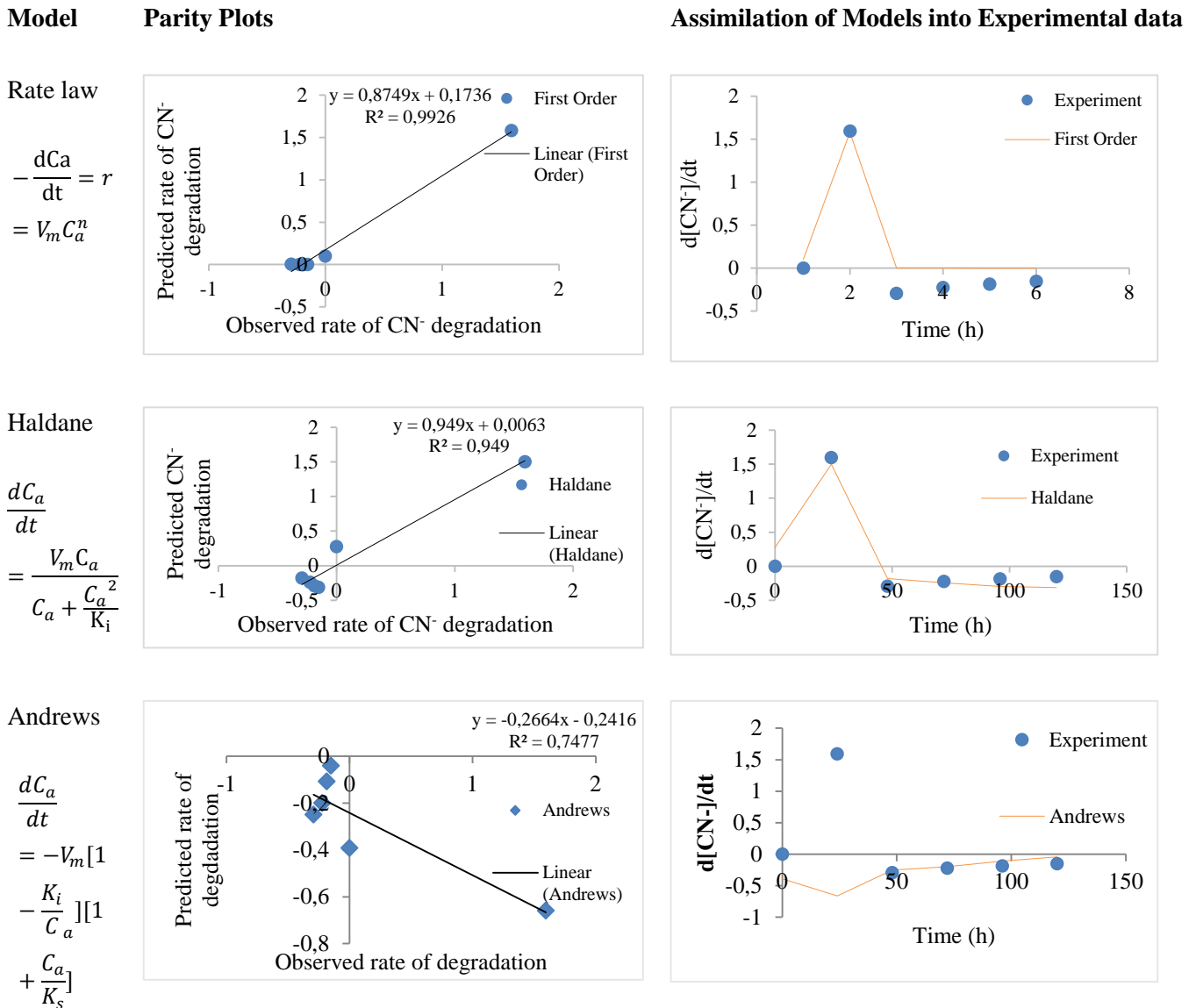


**Figure 6.3.** Parity plots of predicted values versus experimental values. Assimilations of the model data into CN<sup>-</sup> degradation experimental data (Rate law, Haldane, and Andrews).

Overall, the models used and reported in this research also fitted the CN<sup>-</sup> degradation data well. The models that gave a better fit were the rate law ( $R^2 = 0.92$ ,  $\text{Adj } R^2 = 0.90$ , variance = 0.052 and standard deviation = 0.076) and Haldane model ( $R^2 = 0.95$ ,  $\text{adj } R^2 = 0.94$ , variance = 0.034 and standard deviation = 0.061) - see Table 3. Andrew models' had a poor prediction of CN<sup>-</sup> degradation with ( $R^2 = -0.99$ ,  $\text{adj } R^2 = -2.31$ , variance = 1.75, and standard deviation = 0.38). This indicated that CN<sup>-</sup> degradation was not inhibited by the presence of NH<sub>4</sub>-N, as some organisms would rather alternatively use the less inhibitory pollutant; although, inhibitory compound biodegradation might be a favorable alternative. Andrew's model was developed to predict substrate utilization in systems with substrate inhibition, thus the models' inability to model CN<sup>-</sup> removal.

Ge et al. (2015) studied the kinetics of SNaD under high phenol concentrations using bacterial strains capable of phenol degradation, heterotrophic nitrification, and aerobic denitrification. Additionally, Vasiliadou et al. (2006) also studied the kinetics of denitrification with nitrate inhibition. Additionally, Li et al. (2019) also determined that the Haldane model predicted  $\text{CN}^-$  well with  $R^2$  being 0.99. These studies indicated the feasibility of SNaD even under inhibitory pollutant loading. Moreover, the kinetic parameters obtained were comparable to those obtained for this study (Table 6.3).

Overall, the variance and standard deviation of the model showed that all three models predicted  $\text{NH}_4\text{-N}$  degradation better as opposed to  $\text{CN}^-$  degradation. This was shown with the higher variances and standard deviation of  $\text{CN}^-$  degradation than those of  $\text{NH}_4\text{-N}$  degradation. Although, all three models adequately represented  $\text{NH}_4\text{-N}$  removal with high  $R^2$  and adj  $R^2$ , the rate law and Andrews models had higher average standard deviation and variance for predicted rate of  $\text{CN}^-$  degradation in comparison to actual experimental data; thus rendering unusable as candidate prediction models for removal systems with multiple nitrogenous pollutants.

Moreover, Haldanes' model was selected as a better predictor of  $\text{NH}_4\text{-N}$  removal under  $\text{CN}^-$  conditions. This decision was based on its standard deviation and the variance being the lowest for both  $\text{NH}_4\text{-N}$  and  $\text{CN}^-$  degradation, indicating that the predicted rate of  $\text{NH}_4\text{-N}$  and  $\text{CN}^-$  by Haldane had a minute deviation from the experimental data thus qualifying it as a better model to be used for multiple nitrogenous pollutants systems, especially, SNaD.

The result obtained in this study were consistent with those that were previously reported by Pradhan et al. (2019) describing dual substrate kinetics of ammonia oxidation by Haldane model, with  $R^2 > 0.98$  and adj  $R^2 > 0.98$  and low standard errors (RMSE)  $< 0.61$ . Additionally, Wang et al. (2019) reported a high correlation between Haldane prediction and experimental data with adjusted  $R^2$  (0.995),  $K_s$  ( $2.997 \pm 0.041$  mg/L) and  $K_i$  ( $64.736 \pm 0.023$  mg/L).

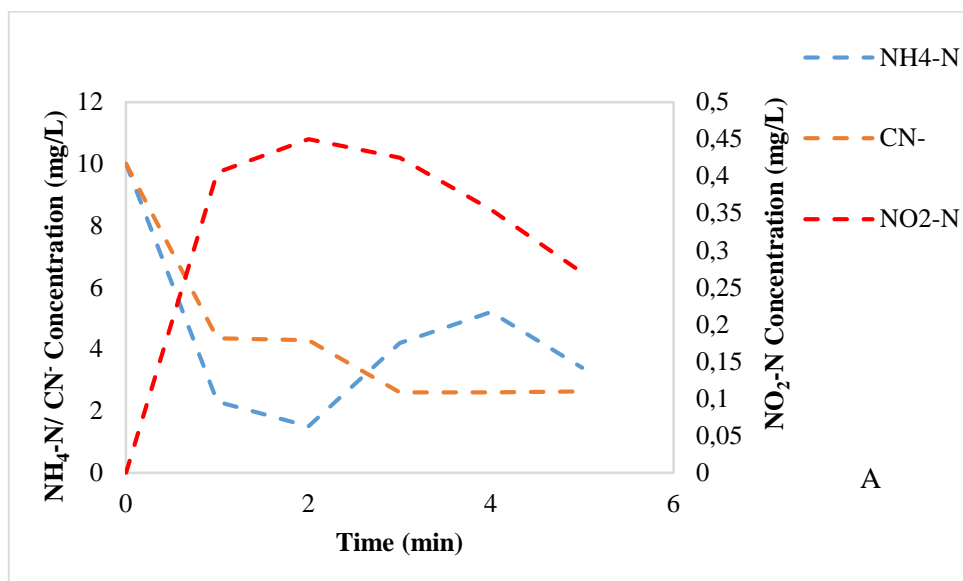
**Table 6.3.** Kinetic parameters obtained from different studies assessing nitrification and aerobic denitrification

Model	Kinetic parameters				Reference
	$V_m$	$K_s$	$K_i$	$n$	
Haldane	0.323	9.65	152.40	-	(Kim et al., 2008) SNaD under high phenol concentrations using A strain capable of phenol degradation

						(Haldane model with substrate inhibition)
	0.45	-	23.94	-	This study	SNaD in CN <sup>-</sup>
						(Haldane model without substrate inhibition)
<b>Rate law</b>	-	-	0.047	1	(Ge et al., 2015a)	Degradation of ammonia nitrogen under high phenol concentrations.
	-	-	6.29E-05	2.27	This study	SNaD in CN <sup>-</sup>
<b>Andrews</b>	0.0485	28.63	24.284		(Ge et al., 2015a)	Denitrification with nitrate inhibition
	0.36	13.22	27.54	-	This study	SNaD in CN <sup>-</sup>

\* $K_s$  is pollutant inhibition constant,  $K_i$  is the saturation constant,  $C_a$  is the concentration of the pollutant,  $n$  is the model fitting constant and  $V_m$ , is the maximum specific degradation rate of the pollutant

### 6.4.3. Effect of Cyanide on AMO, NaR, and NiR



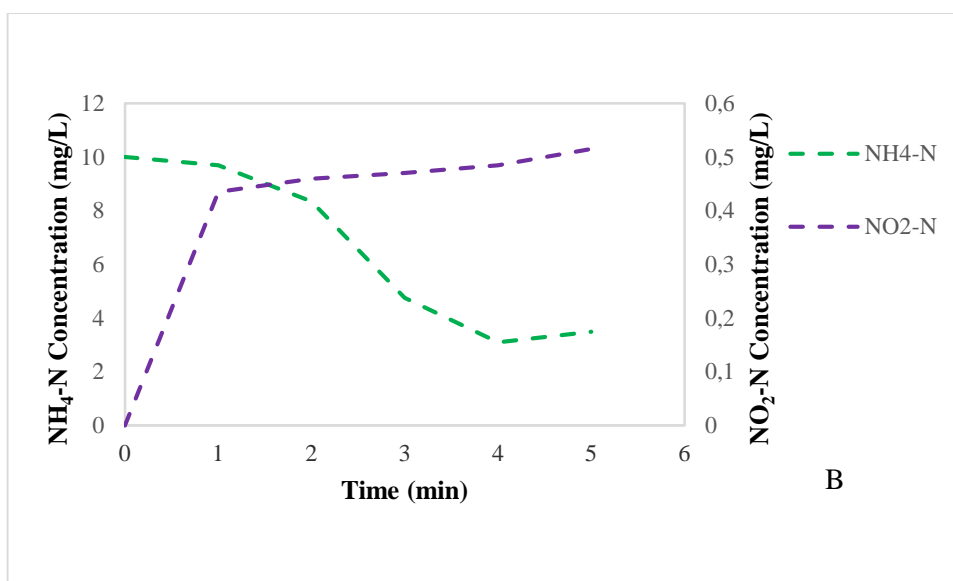


**Figure 6.4.** The activity of NH<sub>4</sub>-N, NO<sub>3</sub>-N and NO<sub>2</sub>-N oxidizing enzymes and CN<sup>-</sup> degrading enzyme. A: Effect of CN<sup>-</sup> on the induction of NH<sub>4</sub>-N, NO<sub>3</sub>-N and NO<sub>2</sub>-N oxidizing enzymes by *A. courvalinii*. B: Effect of CN<sup>-</sup> on free cell NH<sub>4</sub>-N, NO<sub>3</sub>-N and NO<sub>2</sub>-N oxidizing enzymes

Enzyme inhibition can occur in different ways such as the binding of an inhibitor onto an active site or for example a site of the AMO responsible for NH<sub>4</sub>-N oxidation. The second inhibition mechanism can involve the removal of the Cu co-factor of AMO which in turn affects the activity of AMO (Ruser, 2015). To assess the effect of CN<sup>-</sup> towards SNaD, enzyme extracts from *A. courvalinii* cultivated in batch cultures were used. The effect of CN<sup>-</sup> towards the expression of NH<sub>4</sub>-N (AMO), NO<sub>3</sub>-N (NaR) and NO<sub>2</sub>-N (NiR) oxidizing enzymes (Fig. 6.4A) was evaluated.

The activity and presence of AMO, NaR, and NiR was conducted using cell-free extracts by the addition of the enzyme solution into solutions of NH<sub>4</sub>-N. The results revealed that *A. courvalinii* was able to express AMO, and not NaR and NiR; this was shown by the decrease of NH<sub>4</sub>-N and the accumulation of NO<sub>2</sub>-N; however, there was minimal NO<sub>2</sub>-N oxidation observed thus minimal NO<sub>3</sub>-N formation and accumulation detected (see Fig. 6.4B). This observation led to a hypothesis that CN<sup>-</sup> inhibited the expression of NO<sub>3</sub>-N and NO<sub>2</sub>-N oxidizing enzymes or results in the excretion of non-active NO<sub>3</sub>-N and NO<sub>2</sub>-N oxidizing enzymes.

In addition, the competitive inhibition by the addition of CN<sup>-</sup> to free cell extract was examined. This experiment aimed to determine the effect of CN<sup>-</sup> on the expressed NH<sub>4</sub>-N, NO<sub>3</sub>-N, and NO<sub>2</sub>-N oxidizing enzymes, of which the outcomes indicated that the presence of CN<sup>-</sup> did not have an effect on the NH<sub>4</sub>-N reducing enzyme; albeit, a slow decrease of NO<sub>2</sub>-N was observed which suggested the activation of denitrification. Additionally, no NO<sub>3</sub>-N accumulation was observed which meant that *A. courvalinii* converted NO<sub>2</sub>-N directly to N<sub>2</sub>.



The activation of NO<sub>2</sub>-N genes when CN<sup>-</sup> was added to bacterial cultures, could be a confirmation that *A. courvalinii* expresses an ANR protein in response to the presence of CN<sup>-</sup> as a protective mechanism for the cyanide-resistant bacteria used in this research in order to mitigate against the toxicity of the CN<sup>-</sup>. Furthermore, the activation of this protein can lead to the induction of NAR, NIR, NOR, and N<sub>2</sub>OR although this was not confirmed in this study (Duan et al., 2015).

## 6.5. Conclusions

The growth of *Acinetobacter courvalinii* accession number AB602910.1/NR\_148843.1 was not affected by CN<sup>-</sup>. Furthermore, this microorganism was shown to carry-out SNaD under higher CN<sup>-</sup> concentration than the threshold concentration which is known to completely inhibit SNaD. The predictive ability of the rate law, Haldane, and Andrews models was assessed with results indicating that the rate law, Haldane, and Andrew's models were better models to predict NH<sub>4</sub>-N removal as the initial step in SNaD, with high R<sup>2</sup> and adj R<sup>2</sup>; thus, the evaluation of models ability to also predict CN<sup>-</sup> degradation, with the standard deviation and variance being a criterion for selection of the better predicting model. The Haldane model was found to have the lowest standard deviation for both CN<sup>-</sup> and NH<sub>4</sub>-N removal among all models evaluated. Thus it's selection as a model that is suitable to predict the detoxification of TN in wastewater, using SNaD even under CN<sup>-</sup> laden conditions.

The influence of CN<sup>-</sup> on AMO, NaR, and NiR also showed that CN<sup>-</sup> did not affect the expression and activity of NH<sub>4</sub>-N oxidizing enzymes and the assumption was made that non-viable NO<sub>3</sub>-N and NO<sub>2</sub>-N reducing enzymes were expressed. This hypothesis comes from the observation of the slow decrease in NO<sub>2</sub>-N after the addition of CN<sup>-</sup> on crude enzyme extract assays, confirming the activity of NO<sub>3</sub>-N reducing enzyme and activation of the denitrification pathway by the CN<sup>-</sup>. Although *A. courvalinii* has been shown to be able to detoxify TN under CN<sup>-</sup> conditions Physico-chemical parameters still need to be investigated in order to optimize the degradation efficiency of isolate, *A. courvalinii*.

## **CHAPTER 7**

# **PREDICTIVE CAPABILITY OF RESPONSE SURFACE METHODOLOGY AND CYBERNETIC MODELS FOR CYANOGENIC SIMULTANEOUS NITRIFICATION AND AEROBIC DENITRIFICATION (SNAD) FACILITATED BY CYANIDE-RESISTANT BACTERIA**

*Submitted as:* Ncumisa Mpongwana, Seteno Karabo Obed Ntwampe, Lovasoa Christine Razanamahandry, Boredi Silas Chidi, Elizabeth Ife Omodanisi. Predictive capability of response surface methodology and cybernetic models for cyanogenic simultaneous nitrification and aerobic denitrification (SNaD) facilitated by cyanide-resistant bacteria. Submitted to *Microorganisms*

# **CHAPTER 7:**

## **PREDICTIVE CAPABILITY OF RESPONSE SURFACE METHODOLOGY AND CYBERNETIC MODELS FOR CYANOGENIC SIMULTANEOUS NITRIFICATION AND AEROBIC DENITRIFICATION (SNaD) FACILITATED BY CYANIDE-RESISTANT BACTERIA**

### **7.1. Introduction**

The growth of a microorganism under multiple carbon source conditions can influence its performance even in large-scale wastewater treatment processes (Van Dedem & Moo-Young, 1975; Narang & Pilyugin, 2007; Solopova et al., 2014). Similarly, wastewater can be composed of different nitrogenous compounds from several industries. Current methods to treat this type of wastewater consist of traditional two-stage biological processes known as aerobic nitrification and anoxic denitrification. These treatment processes have different operating conditions and requirements such as dissolved oxygen concentration, carbon source requirements and retention time, with throughput rates of the wastewater being treated in the processes being of utmost importance. Due to high energy consumption associated with the second reactor dedicated to anaerobic denitrification, some studies have indicated the possibility of simultaneous nitrification and aerobic denitrification (SNaD).

This process is advantageous than traditional nitrification subsequent to denitrification, providing for cost-effectiveness (Kim et al., 2008; Zhang et al., 2015; Jin et al., 2014). Moreover, SNaD is a highly effective method for total nitrogen (TN), i.e. ammonium nitrogen ( $\text{NH}_4\text{-N}$ ), nitrate-nitrogen ( $\text{NO}_3\text{-N}$ ) and nitrite-nitrogen ( $\text{NO}_2\text{-N}$ ), removal from wastewater (He et al., 2016), although, the microorganism(s) used during TN removal are highly sensitive to toxicant loading, thus, SNaD is the least effective of industrial wastewater treatment methods owing to a high concentration of contaminants that may completely inhibit SNaD (Choi & Hu, 2009; Papirio et al., 2014).

The coking industry is among the industries that produce wastewater containing high quantities of pollutants such as  $\text{NH}_4\text{-N}$  in the form of ammonium sulfate, thiocyanide (SCN), free cyanide ( $\text{CN}^-$ ), etc (Ma et al., 2015). This type of wastewater may result in serious environmental contamination and other challenges associated with the disposal of such contaminated wastewater if not treated (Feng et al., 2015; Carrera et al., 2003; Kim et al., 2011a; Kim et al., 2011b) using processes such as SNaD; albeit, some

inhibitory pollutants might render this process ineffective. Kim et al. (2008) have reported that  $\text{CN}^-$  does possess the highest inhibitory effect on SNaD.

$\text{CN}^-$  containing wastewater is produced in various other industries including mining, steel making, chemical manufacturing, and petroleum industries.  $\text{CN}^-$  has been known to be more poisonous than other cyanide compounds. However, some microorganisms have been reported to be able to use  $\text{CN}^-$  and other TN constituents as nitrogenous sources, thus their suitability to be used in SNaD operations. The mechanism of  $\text{CN}^-$  tolerance and conversion, as also observed for TN removal, occurs through four general pathways that are hydrolytic; oxidative; reductive; and substitution/transfer mechanisms (Kapoor et al., 2016; Luque-Almagro et al., 2016; Razanamahandry et al., 2016).

Moreover, some studies reported the ability of cyanide degrading bacteria to degrade  $\text{CN}^-$  and subsequently nitrify and aerobically denitrify (Mekuto et al., 2015). An example is that of Mekuto et al. (2018) who successfully demonstrated the use of cyanide degrading bacteria for nitrification and aerobic denitrification under cyanogenic conditions. Ryu et al. (2015) also reported complete SNaD and simultaneous  $\text{SCN}^-$  degradation. These findings have led to the proposition of applying cyanide degrading bacteria for SNaD to eliminate the inhibitory effect of  $\text{CN}^-$  towards SNaD, which can further reduce operational costs associated with the reactor designated for biological pretreatment of  $\text{CN}^-$  (Han et al., 2013) and for downstream denitrification.

Moreover, the application of cyanide degrading bacteria will not only resolve the inhibitory effect of  $\text{CN}^-$  towards SNaD, it will also resolve the challenge of slow-growing microorganisms responsible for SNaD since cyanide degrading bacteria have higher growth rates (Ojaghi et al., 2018; Kandasamy et al., 2015). This will likely improve process performance and compensate for biomass washout. In addition, some cyanide degrading bacteria have been reported to also possess other important genes such as the gene responsible for polyhydroxyalkanoates (PHA) synthesis which can be used as an energy source when produced extracellularly during the biodegradation of pollutants, including other aromatic compounds (Luque-Almagro et al., 2016).

This is another advantageous trait of cyanide degrading bacteria. Han et al. (2013) have recommended the application of  $\text{CN}^-$  degrading bacteria for TN removal from wastewater containing a high quantity of  $\text{CN}^-$  as an alternative to mediate the effect of  $\text{CN}^-$  on SNaD with others concurring to such a strategy (Park et al., 2008; Han et al., 2013a; Han et al., 2013b). However, there is still limited information on the application of these microorganisms on a full-scale wastewater treatment process due to the possibility of unknown risks occurring. In a previous study conducted by Mpongwana et al. (2016), it was also indicated that SNaD is feasible by using  $\text{CN}^-$  tolerant bacteria to treat  $\text{CN}^-$  containing wastewater whereby the bacteria exhibited multiphase growth pattern phenomenon when supplied with both  $\text{CN}^-$  and  $\text{NH}_4\text{-N}$ ; albeit, other physiological conditions might have played a role. Generally, SNaD and  $\text{CN}^-$  degradation is known to be

affected by physiological conditions such as pH and temperature, which must be optimal for process performance efficiency.

Response surface methodology (RSM) has been widely used to predict and optimize cyanide degradation and SNaD operations (Mekuto et al., 2013), with no study having compared and assessed the capability of RSM and cybernetic models to predict the performance of SNaD under  $\text{CN}^-$  conditions.  $\text{CN}^-$  was chosen as the inhibitor in the research reported herein since it possesses a high inhibition capability for nitrification and denitrification (Inglezakis et al., 2017). This study also determined the optimum physiological conditions of the bioreactor required to facilitate SNaD in the presence of  $\text{CN}^-$  when cyanide resistant bacteria are employed. Moreover, the cybernetic models were also developed to assess their predictive ability of SNaD under  $\text{CN}^-$  conditions in comparison to the RSM model developed.

## 7.2. Objectives

- Optimisation of Physico-chemical conditions that affect simultaneous nitrification and aerobic denitrification under high cyanide conditions.
- Development of a simple cybernetic model to predict simultaneous nitrification and aerobic denitrification under high cyanide conditions.
- Compare the predictive ability of RSM models with cybernetic models towards simultaneous nitrification and aerobic denitrification under high cyanide conditions.

## 7.3. Materials and methods

The experimental design for optimization of SNaD under  $\text{CN}^-$  conditions were designed using RSM software. a 13-run experimental plan with variation in independent variables temperature and pH was generated by RSM. A basal media mentioned in section 4.1.1 was used for this study. The isolated strain was grown for 2 days prior to the addition of 20 mg  $\text{NH}_4\text{-N/L}$  and 20 mg  $\text{CN}^-/\text{L}$ . samples were collected on a 1 h interval for analysis of  $\text{CN}^-$ ,  $\text{NH}_4\text{-N}$ ,  $\text{NO}_2\text{-N}$ , and  $\text{NO}_3\text{-N}$  using Merck SA test kits and Merck ANOVA Spectroquant, all the experiments were conducted in duplicate. Multiple regression analysis was used to analyse the data. The kinetic experiments were conducted at optimised conditions in 1L batch reactor using the basal medium previously mentioned in section 4.1.1. The media was inoculated with 100 mL of overnight culture and was incubated for 168 h prior addition of 42.05 mg  $\text{CN}^-/\text{L}$  and 246.5 mg  $\text{NH}_4\text{-N/L}$ , 2mL samples were withdrawn on a 24 h interval for analysis of  $\text{NH}_4\text{-N}$ ,  $\text{CN}^-$ ,  $\text{NO}_2\text{-N}$  and  $\text{NO}_3\text{-N}$ . 5 mL sample was also collected at the beginning of the experiment to analyse the enzyme. The enzymes were extracted according to section 4.2.3. Cybernetic models were developed in reference to Fig. 4.1 for the prediction of SNaD.

## 7.4. Results and discussion

### 7.4.1. Predictive ability of Response Surface Methodology

#### 7.4.1.1. Analysis of variance (ANOVA) for TN removal

The central composite design was used to study the interaction between the independent variables, pH and temperature, that affect SNaD for TN removal. Table 3 shows analysis of variance (ANOVA) of the quadratic model used to describe TN removal. The model F-value of 17.01 for TN removal was higher than 1.0, which indicated that the variation between the model and experimental data was higher.

The predicted values of the RSM were compared with the experimental values, with the p-value being 0.0009 for the model, which is smaller than the alpha level of 0.05. This meant that there was a consequential relationship between the predicted values and the actual values of TN removal. However, other parameters such as the deviation of the model values from the actual data points (standard deviation),  $R^2$ , adjusted  $R^2$  and predicted  $R^2$  need to be considered in order to judge the adequacy of the model – see Table 7.1.

**Table 7.1.** Analysis of variance (ANOVA) of the quadratic parameters for SNaD process used for TN removal under  $CN^-$  conditions

Source	Sum of Squares	df	Mean Square	F-value	p-value	
Model	12482.87	5	2496.57	17.01	0.0009	significant
A-Temperature	1167.65	1	1167.65	7.96	0.0257	
B-pH	631.10	1	631.10	4.30	0.0768	
AB	70.78	1	70.78	0.4824	0.5097	
A <sup>2</sup>	5558.29	1	5558.29	37.88	0.0005	
B <sup>2</sup>	6434.58	1	6434.58	43.85	0.0003	
Residual	1027.19	7	146.74			
Lack of Fit	1027.19	3	342.40			
Pure Error	0.0000	4	0.0000			
Cor Total	13510.06	12				

The quadratic model was also used to predict SNaD under  $CN^-$  conditions. The significance of the parameters was determined using values of "Prob> F" less than 0.05, thus, in this case, A, A<sup>2</sup>, and B<sup>2</sup> were found to be significant for the model. Therefore, the model was improved by reducing it from Eq. 29 to Eq. 30.

$$\text{TN removal} = 78.57 - 12.08A - 8.88B + 4.21AB - 28.27A^2 - 30.41B^2 \quad (29)$$

$$\text{TN removal} = 78.57 - 12.08 A - 28.27A^2 - 30.41B^2 \quad (30)$$

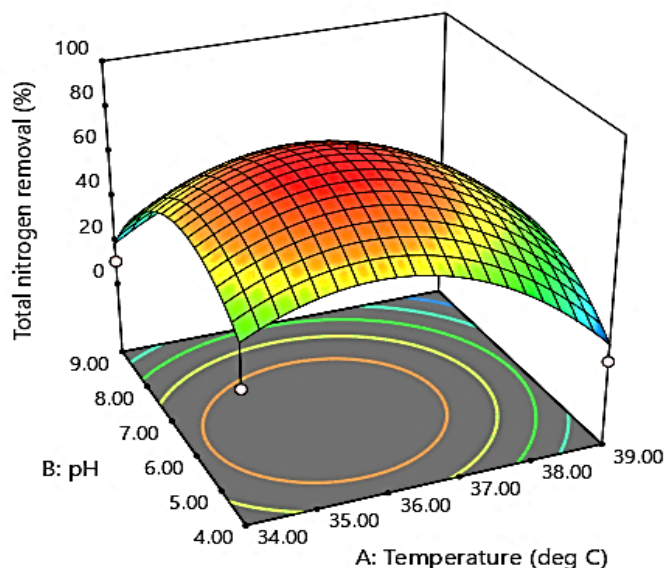


**Figure 7.1.** Surface response plot showing the interaction between pH, Temperature and TN removal.

The visualization of the predicted model was obtained using a surface response plot – see Fig 7.1. In this study, the response was set to maximize the degradation efficiency of TN in an SNaD system that contains multiple nitrogenous sources, i.e  $\text{NH}_4\text{-N}$ ,  $\text{NO}_2\text{-N}$  and  $\text{NO}_3\text{-N}$ , with  $\text{CN}^-$  as a secondary nitrogenous source or pollutant. *Acinetobacter courvalinii* was found to remove up to 78.6% of TN via SNaD from an initial concentration of 20 mg  $\text{NH}_4\text{-N/L}$  within 5 h of incubation. Li et al. (2015) reported that *Pseudomonas stutzeri* YZN-001 could remove  $\text{NH}_4\text{-N}$  at 37 °C rapidly; however, the removal of  $\text{NO}_2\text{-N}$  and  $\text{NO}_3\text{-N}$  only occurred at 30 °C. The surface plot for TN removal under cyanogenic conditions as shown in Fig 7.1, indicated that the maximum operational efficiency for the SNaD containing  $\text{CN}^-$  was located inside the experimental region. This was a confirmation of the optimum being 6.5 and 36.5 °C. Moreover, the plateau in surface response plots in Fig 7.1 indicated the suitability of operational conditions for SNaD, it also highlighted that the lowest degradation efficiency for TN removal and  $\text{CN}^-$  degradation was observed at temperature and pH of 40.04 °C and 6.5 with degradation efficiencies of approximately 5 %. When the temperature is 36.5 °C with pH being 2.96 or 10.04 the degradation efficiency for TN removal was found to be 46.1 and 5.6%, respectively. This indicated that changes in pH and temperature affect TN removal.

### 7.4.1.2. Batch reactor experiment and model simulations

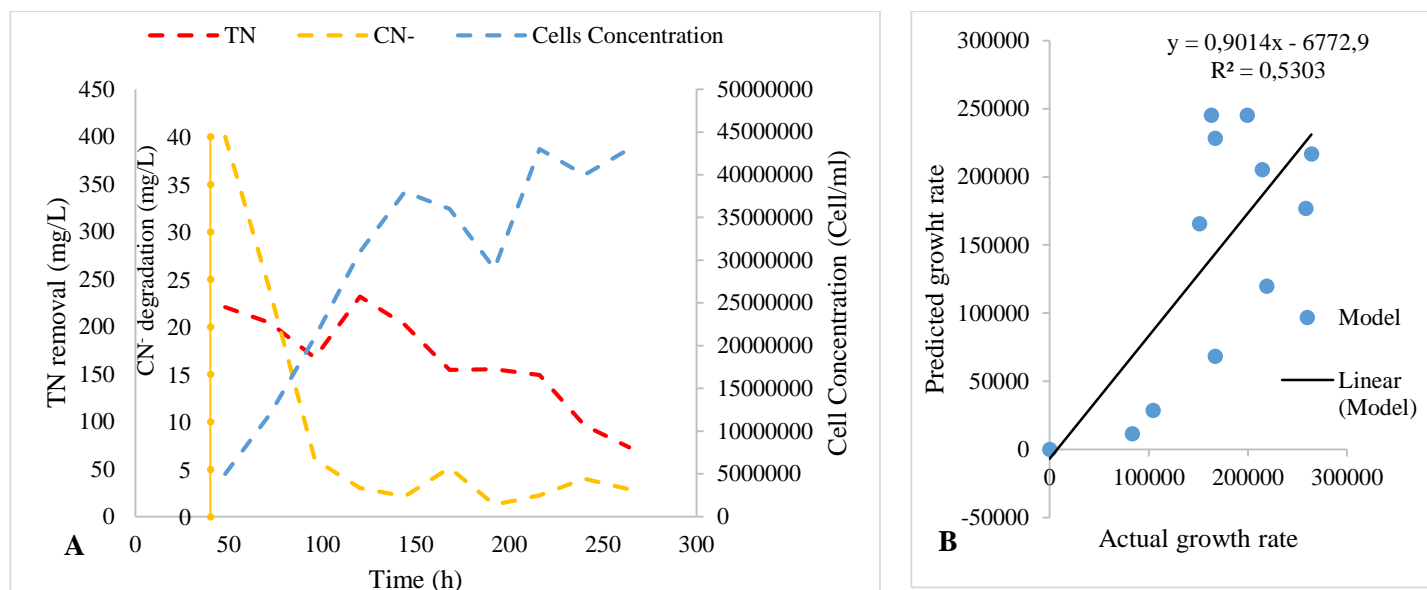


**Figure 7.2.** Degradation kinetics of TN and cyanide in a batch culture reactor. A: TN and CN<sup>-</sup> degradation and cell concentration over time. B: model fitting into biomass plot.

To generate data for the models, removal (degradation) kinetics of TN were studied at optimized conditions in 1L reactors. The initial (higher) concentration of 40 mg CN<sup>-</sup>/L and 250 mg NH<sub>4</sub>-N/L were used and the experiment was conducted for 264 h. The results indicated that up to 70.5 % of TN was removed within 264 h, see Fig. 7.2A. Duan et al. (2015) reported that a nitrification efficiency of  $91.82 \pm 1.98$  % after 42 h by *Vibrio diabolicus* SF16 was achievable in a system that does not contain CN<sup>-</sup>. Furthermore, He et al. (2015) also reported an NH<sub>4</sub>-N removal efficiency of 93.6% after 96 h of incubation with *Pseudomonas tolaasii* Y-11; albeit, the utilization of pollutants by a specific species might be sequential, with the organism utilizing the easily biodegradable pollutant with a less complex structure first, subsequent to the degradation of the second less desirable pollutants which sometimes results in multi-phased growth of the organism(s) used. The cell concentration was also studied and modeled (Fig. 7.2A). The data points of predicted growth rate versus actual growth rate were scattered, with numerous outliers from the trend line (Fig. 7.2B) which signifies that the first-order equation did not adequately represent the growth model. Moreover, the R<sup>2</sup> of 0.5303 was low, thus indicating poor prediction of the growth observed. Overall, the microorganism used in this study primarily degraded TN including CN<sup>-</sup> simultaneously, which is an interesting trait considering that CN<sup>-</sup> is a known inhibitor to nitrification, with as little as 1 mg CN<sup>-</sup>/L completely inhibiting nitrification (Kim et al., 2008).



## 7.5. Prediction ability of RSM in comparison to cybernetic models

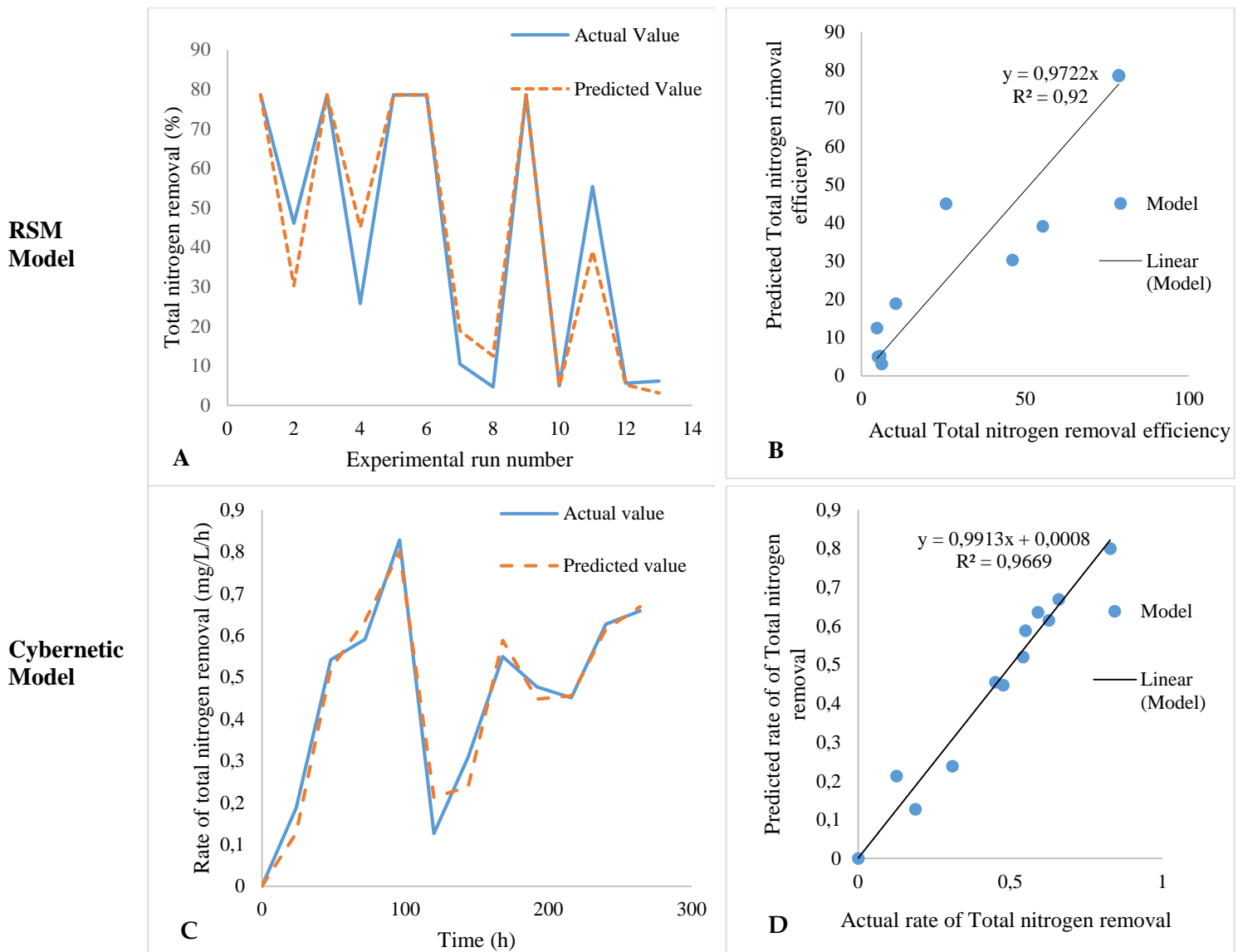


**Figure 7.3.** A comparison of the prediction ability of RSM and cybernetic models. A: prediction of TN removal efficiency by RSM model; B: parity plot comparing predicted total nitrogen removal efficiency and actual total nitrogen removal efficiency by RSM; C: Rate of TN removal predicted by cybernetic model; D: parity plot for comparing predicted rate of TN removal with actual rate of TN removal by cybernetic model.

When comparing modeled and actual SNaD performance under optimum conditions, the correlation coefficient ( $R^2$ ) of 0.92 was observed; although this high  $R^2$  was observed,  $R^2$  alone cannot verify whether the model is adequate or not, since  $R^2$  can improve with the extension of dependent variables scale regardless of whether the variable is significant or not. Thus the adjusted  $R^2$  (0.87) and predicted  $R^2$  (0.46) were considered (Table 7.3). Adjusted  $R^2$  is normally used to compare the explanatory power of a regression model, while the Adjusted  $R^2$  only account for variables that improve the model; therefore, the addition of

less significant variables decreases the Adjusted  $R^2$ . Overall, the Adjusted  $R^2$  is considered more reliable compared to the correlation coefficient. Hence, the Adjusted  $R^2$  was used to evaluate the adequacy of the model culminating in the selection of a suitable model describing SNaD for TN removal under CN conditions.

As the Adjusted  $R^2$  of 0.87 was higher; therefore, the model was deemed adequate. However, the difference between predicted  $R^2$  and adjusted  $R^2$  was above 0.2, indicating that there would be challenges with the use of the model. Hence, the model was reduced to expression as highlighted in Eq. 30. This was further confirmed by the average standard deviation (12.11) for TN removal with standard error (SE) of 5.284 (Table 7.3). The SE for TN removal indicated that the RSM model could be improved to represent the experimental data more adequately. The parity plot for TN removal was used to compare the predicted TN removal efficacy and the actual TN removal efficiency. The data points of the RSM model deviated from the trendline indicating a larger deviation of the data points from the trend line.

**Table 7.2.** Model parameter estimations

<b>Fitting constants and the values of kinetic parameters</b>	
<b>(<math>\pm 95\%</math> confidence interval)</b>	
<b>Parameters</b>	<b>Values</b>
$r_i^{max}$	0.02 mg/g.h
$K_{i1}$	2.91 mg/L
$\alpha_{e1}$	0.89 mg/g.h
$\alpha_{e2}$	1.42 mg/g.h
$\alpha_{e3}$	0.29 mg/g.h
$\alpha_{e4}$	0.03 mg/g.h
$r_{e1}$	30.42 mg/g.h
$r_{e2}$	791.97 mg/g.h
$r_{e3}$	454.71 mg/g.h
$r_{e4}$	0.11 mg/g.h
$b_1$	0.76 mg/g.h
$b_2$	20.29 mg/g.h
$b_3$	227.64 mg/g.h
$b_4$	0.01 mg/gd.h

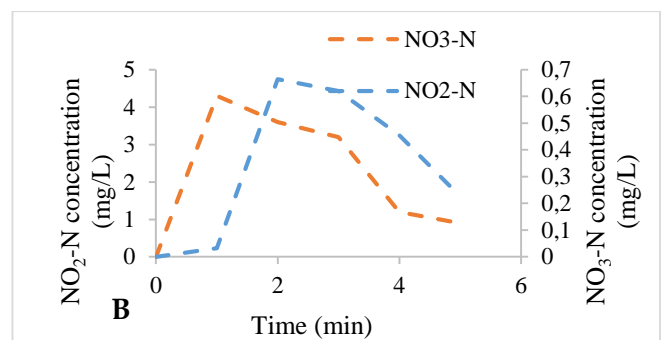
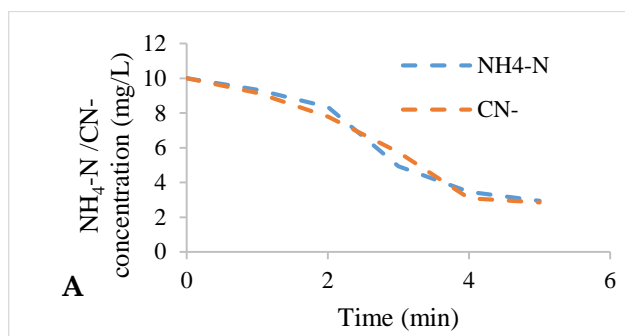
Cybernetic models were developed to predict maximum pollutant utilization rates which are presented as  $S_1$  and  $S_2$  for TN and  $CN^-$  respectively via catalysis by numerous enzymes. A cybernetic model was simulated by estimating unknown parameters using experimental data as listed in Table 7.2. The model successfully described the rate of TN removal with ( $R^2$  of 0.97, indicating a 97% suitability. Moreover, the Adjusted determination coefficient ( $Adj R^2 = 0.96$ ) was very high with the difference between  $R^2$  and the  $Adj R^2$  being 0.006. This difference is minute; therefore, it advocated for the high significance of the model. Furthermore, the variance (0.002), standard error (0.0035) and standard deviation (0.012) for TN removal were low, demonstrating that there's an insignificant difference between the predicted values from the model and the actual experimental values. Although the RSM model was shown to adequately represent TN removal, the adjusted  $R^2$  of the cybernetic model was higher than that of the RSM model. Thus, cybernetic models were selected as the best model to predict TN removal using SNaD. Furthermore, the parity plot for RSM and the cybernetic model were compared. The parity plot of cybernetic model had data points scattered closer to the trend line as opposed to RSM model which numerous outliers showing a significant deviation from the trend line (Fig. 7.3B, and D), supporting the statement that cybernetic model better predicted TN removal better in  $CN^-$  using SNaD.

**Table 7.3.** Statistical analysis of RSM and cybernetic models for SNaD under  $CN^-$  conditions

Model	Std Dev	SE Mean	R-squared	Adjusted R-squared	Predicted $R^2$
RSM	12.11	5.284	0.9240	0.8697	0.46
Cybernetic	0.012391	0.0035	0.966119	0.962731	-

Two-sided Confidence = 95% Population = 99%

## 7.6. TN/ $CN^-$ biocatalysis



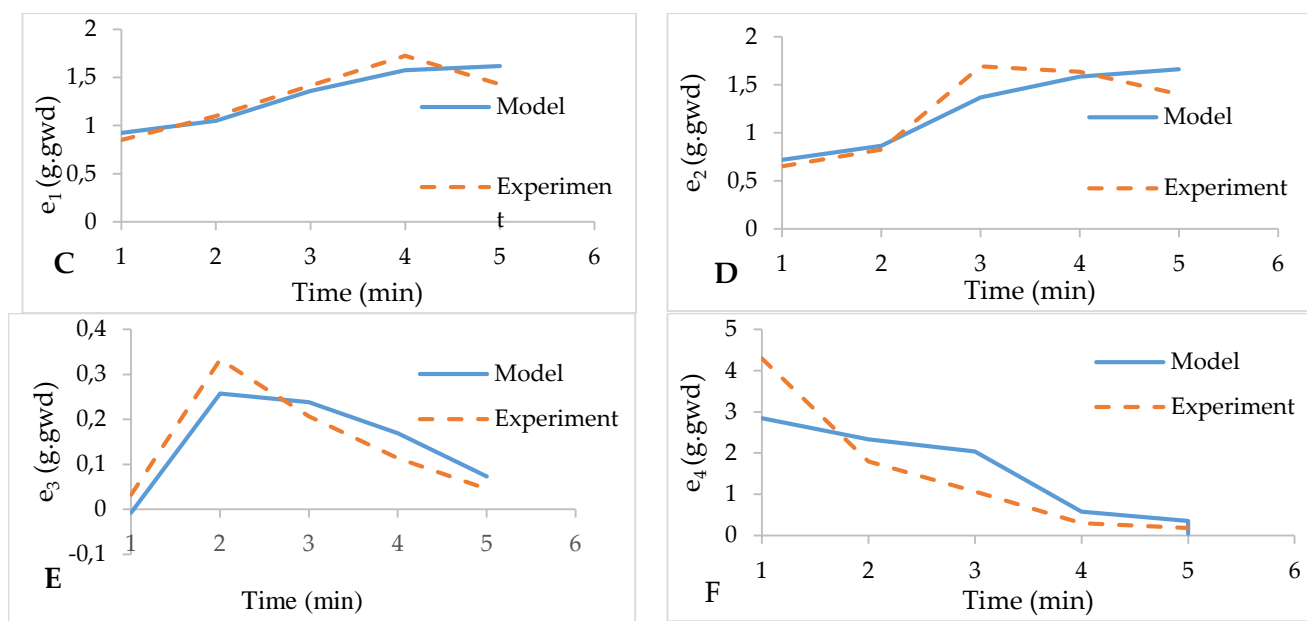


**Figure 7.4.** (a)  $\text{NH}_4\text{-N}$  and  $\text{CN}^-$  removal/ degradation. (b)  $\text{NO}_2\text{-N}$ , and  $\text{NO}_3\text{-N}$  removal. simulation of the cybernetic model into (c) level of key enzyme  $e_1$  over time. (d) level of key enzyme  $e_2$  over time. (e) level of key enzyme  $e_3$  over time. (f) level of key enzyme  $e_4$ .

SNaD involves a process whereby  $\text{NH}_4\text{-N}$  is converted into  $\text{NO}_2\text{-N}$  and further to  $\text{NO}_3\text{-N}$  which activates the production of denitrification enzymes that convert  $\text{NO}_3\text{-N}$  into  $\text{N}_2$ . Enzyme activity was determined by extracting free-cell enzymes supplemented into solutions consisting of pollutants,  $\text{NH}_4\text{-N}$  and  $\text{CN}^-$ . The decrease in the pollutants and the accumulation of the intermediates  $\text{NO}_3\text{-N}$  and  $\text{NO}_2\text{-N}$  were observed. The decrease in  $\text{NH}_4\text{-N}$  and  $\text{CN}^-$  was slow in the first two minutes of the reaction with a degradation rate of 0.83 and 1.1 mg/L/min, respectively. The degradation rates increased after the fourth minute, with the rate increased up to 1.64 and 1.73 mg/L/min were observed, respectively; albeit, the rate of degradation decreased after 5 min. Since the degradation was conducted at ambient temperature to simulate real-life WWTP conditions, the decrease in the pollutants indicated the presence of TN and  $\text{CN}^-$  degrading enzymes; moreover, the increase and decrease of intermediates  $\text{NO}_2\text{-N}$  and  $\text{NO}_3\text{-N}$  indicated the presence of denitrification enzymes; hence, the isolated microorganisms was deemed to be capable to carry-out SNaD even in the presence of  $\text{CN}^-$ . The enzyme synthesis model successfully described individual enzyme activity with  $R^2$  above 0.7 indicating a good fit of the activity models.

## 7.7. Conclusion

Response surface methodology was used to determine the optimum conditions for TN removal under  $\text{CN}^-$  conditions using *A. courvalinii*, a  $\text{CN}^-$  tolerant bacterium with TN removal capabilities in SNaD. The optimum pH and temperature were found to be 6.5 and 36.5 °C, with degradation efficiency of 78.6 % for TN and a significant (80.2 %) for  $\text{CN}^-$  degradation, respectively. Degradation kinetics of TN were also

studied in a batch reactor under the optimum conditions with the results obtained indicating that TN was degraded simultaneously with  $\text{CN}^-$  at an efficiency of 70.5 % and 97.3 %, respectively. Moreover, cybernetic modeling was found to be better at predicting SNaD under cyanogenic conditions with a higher adjusted  $R^2$  (0.96) as opposed to the RSM models with an adjusted  $R^2$  of 0.87. The cybernetic models used in this study were simplified models; thus they do not provide illuminating insights into cellular responses. Hence, additional experiments are needed to elucidate metabolic flux distributions better and to further develop models for SNaD process prediction as well as optimisation.

# **CHAPTER 8**

## **SUMMARY AND CONCLUSIONS**

# CHAPTER 8:

## SUMMARY AND CONCLUSION

### 8.1 Summary and Conclusions

Treatment of TN has become the core of WWTP(s) since wastewater containing high quantities of TN results in eutrophication. Treatment approaches for TN removal involve chemical, physical and biological treatment technologies, with biological treatment being an ideal method due to its cost-effectiveness. Traditional biological treatment of TN involves a two-stage process known as aerobic nitrification subsequent to anoxic denitrification. However, due to high energy consumption resulting from the operation of multiple reactors, various studies have proven the probability of some microorganisms to perform denitrification under aerobic conditions. This has led to the proposition to conduct nitrification and denitrification in a single reactor, giving birth to a process currently known as SNaD. This process is crucial in the WWTP since it is cost-effective and more sustainable compared to the two-stage aerobic nitrification subsequent to anoxic denitrification. Due to the significance of this process in WWTP, SNaD has drawn attention to the scientific world over the past few years.

Thus, a number of studies have been conducted, aiming to improve this process and make it more sustainable, despite all the improvements which have been done on SNaD, this process still encounters some challenges that make it difficult to implement under certain conditions such as the presence of high quantities of other toxic pollutants. Inhibition of SNaD by other pollutants present in the WWTP is one of the major challenges that hinder the application of the SNaD especially in industrial WWTP which contains highly toxic chemicals such as ammonium sulfate, SCN<sup>-</sup>, CN<sup>-</sup>. These pollutants can be lethal to the microbial population responsible for SNaD. CN<sup>-</sup> is counted among the most toxic compounds towards SNaD, with as little as 1 mg/L of CN<sup>-</sup> known to completely inhibit SNaD. This has led to the application of chemical and physical pre-treatment methods to treat wastewater containing CN<sup>-</sup> prior to SNaD; however, these methods are costly and complicated to operate.

Biological CN<sup>-</sup> removal has been used as an ideal pre-treatment alternative to detoxify treat CN<sup>-</sup> prior wastewater enters SNaD reactor. Although the biological CN<sup>-</sup> removal has been deemed the best technique for the treatment of CN<sup>-</sup>, the operation of the pretreatment reactor may result in accumulation of operational cost. Hence, some studies have suggested the application of CN<sup>-</sup> degrading microorganism for SNaD, although the application of CN<sup>-</sup> degrading bacteria have been proven to be possible, the cyanide resistant/tolerant microorganisms have not yet been applied for SNaD in large-scale wastewater operations due to limited information that is crucial in controlling of the SNaD performed by CN<sup>-</sup> degrading/ tolerant microorganisms. Thus, the aim of this study was to investigate a modeling approach suitable to describe SNaD under CN<sup>-</sup> conditions since modeling plays an important role in accurate facilitation of SNaD

process. Thermodynamic kinetics of SNaD under high  $\text{CN}^-$  loadings were initially investigated to assess the feasibility of SNaD process performed by cyanide resistant/ degrading mix consortium that was isolated from cyanogenic environments.

The results obtained indicated that  $\text{CN}^-$  did not affect the performance of a mix consortiums' nitrification abilities. The consortia were shown to degrade  $\text{CN}^-$  and sufficiently remove  $\text{NH}_4\text{-N}$  and  $\text{CN}^-$  respectively. A linear relationship was found to exist between nitrification rates and their respective Gibbs free energy with negative Gibbs free energy observed. This confirmed the feasibility of TN removal under high  $\text{CN}^-$  conditions. For a proof of concept, from the mix consortia, a single strain was also isolated and was identified as *Acinetobacter courvalinii* (accession number AB602910.1). The strain was capable of degrading  $\text{CN}^-$  and subsequent removal of TN under cyanogenic environments. Furthermore, five mathematical models (Monod, Moser, rate law, Haldane, and Andrew's model) were assessed for their ability to predict SNaD under  $\text{CN}^-$  conditions; albeit, only the Rate law, Haldane, and Andrew models successfully predicted SNaD under  $\text{CN}^-$  conditions.

Moreover, the rate law and Haldane models were also shown to predict  $\text{CN}^-$  degradation. Overall, the Haldane model was selected as a better predictor of systems with multiple nitrogenous sources due to low variance and standard deviation, which indicated an insignificant deviation of the predicted data from the experimental data for both  $\text{NH}_2\text{-N}$  and  $\text{CN}^-$  degradation. Initially, the degradation rates of  $\text{NH}_4\text{-N}$  and  $\text{CN}^-$  by *A. courvalinii* were low; hence, physiological parameters optimization using RSM. Under optimum conditions for TN removal and  $\text{CN}^-$  degradation the predictive ability of the RSM model generated was compared with the cybernetic models, with a cybernetic model being selected as the better predictor for TN removal in SNaD- $\text{CN}^-$  systems; although both RSM and cybernetic models were found to adequately represented TN removal. These results exhibited a promising clarification of the SNaD process under  $\text{CN}^-$  conditions and provide a solution in the control, management SNaD even under  $\text{CN}^-$  conditions.

## **8.2 Recommendations for future work**

From a consortium able to perform SNaD, a cyanide degrading microorganism capable of degrading  $\text{CN}^-$  and perform SNaD simultaneously was successfully isolated. This demonstrated that even at an individual species level, SNaD could be performed even under  $\text{CN}^-$ . The physio-chemical conditions were studied to optimize  $\text{CN}^-$  degradation and SNaD; moreover, the predictive ability of RSM and cybernetic models was also studied. Although cybernetic models developed were successfully used to describe SNaD under high cyanogenic conditions; the metabolic network used to develop the cybernetic models was a simplified network. It is recommended that a more detailed metabolic network for SNaD under  $\text{CN}^-$  conditions be constructed for the development of a more robust model which will describe the SNaD even when a consortium is used for such a system. This model can provide an illuminating insight into cellular response



for SNaD. Additional experiments are also needed to be conducted to better understand the metabolic flux distribution in SNaD-CN<sup>-</sup> and SNaD-toxicant systems.

## **CHAPTER 9**

## **REFERENCES**

## CHAPTER 9:

# REFERENCES

- Akinpelu, E. A., Ntwampe, S. K. O., Mpongwana, N., Nchu, F., and Ojumu, T. V. 2016. Biodegradation kinetics of free cyanide in *Fusarium oxysporum*-*Beta vulgaris* waste-metal (As, Cu, Fe, Pb, Zn) cultures under alkaline conditions. *BioResources*, 11: 2470-2482
- Ali, M. & Okabe, S. 2015. Anammox-based technologies for nitrogen removal: Advances in process start-up and remaining issues. *Chemosphere*, 141: 144–153.
- Alzate Marin, J., Caravelli, A. & Zaritzky, N. 2016. Nitrification and aerobic denitrification in anoxic–aerobic sequencing batch reactor. *Bioresour Technol*, 200: 380-387.
- Andersson, S., Dalhammar, G. & Rajarao, G.K. 2011. Influence of microbial interactions and EPS/polysaccharide composition on nutrient removal activity in biofilms formed by strains found in wastewater treatment systems. *Microbiol. Res*, 166: 449-457
- Angenent, L.T., Karim, K., Al-Dahhan, M.H., Wrenn, B.A. & Domínguez-Espinosa, R. 2004. Production of bioenergy and biochemicals from industrial and agricultural wastewater. *Trends Biotechnol*, 22: 477-485.
- Annur, M.S.M., Tan, I.K.P., Ibrahim, S. & Ramachandran, K.B. 2008. A kinetic model for growth and biosynthesis of medium-chain-length poly-(3-hydroxyalkanoates) in *Pseudomonas putida*. *Braz J Chem Eng*, 25: 217-228
- Ao, P. 2005. Metabolic network modelling: Including stochastic effects. *Comput chem eng*, 29: 2297-2303.
- Arai, H., Kodama, T. & Igarashi, Y. 1997. Cascade regulation of the two CRP/FNR-related transcriptional regulators (ANR and DNR) and the denitrification enzymes in *Pseudomonas aeruginosa*. *Mol. Microbiol*, 25: 1141-1148.
- Aslan, S. & Sozudogru, O. 2017. Individual and combined effects of nickel and copper on nitrification organisms. *Ecol. Eng*, 99: 126–133.
- Aybar, M., Pizarro, G., Boltz, J.P., Downing, L. & Nerenberg, R. 2014. Energy-efficient wastewater treatment via the air-based, hybrid membrane biofilm reactor (hybrid MfBR). *Water Sci. Technol.*, 69: 1735–1741.

Banning, N.C., Maccarone, L.D., Fisk, L.M. & Murphy, D.V. 2015. Ammonia-oxidising bacteria not archaea dominate nitrification activity in semi-arid agricultural soil. *Sci. Rep*, 5: 11146.

Basheer, S., Kut, Ö., Prenosil, J. & Bourne, J. 1992. Kinetics of enzymatic degradation of cyanide. *Biotechnol. Bioeng*, 39: 629–634.

Biggs, M.B., Medlock, G.L., Kolling, G.L. & Papin, J.A. 2015. Metabolic network modelling of microbial communities. *WIREs Syst Biol Med*, 7: 317-334

Blackall, L.L., Crocetti, G.R., Saunders, A.M. & Bond, P.L. 2002. A review and update of the microbiology of enhanced biological phosphorus removal in wastewater treatment plants. *Anton Leeuw Int J G*, 81: 681-691.

Boyle, N.R. & Morgan, J.A. 2009. Flux balance analysis of primary metabolism in *Chlamydomonas reinhardtii*. *BMC Syst. Biol*, 3: 4.

Carrera, J., Baeza, J., Vicent, T. & Lafuente, J. 2003. Biological nitrogen removal of high-strength ammonium industrial wastewater with two-sludge system. *Water Res*, 37: 4211-4221.

Chen, C., Kao, C. & Chen, S. 2008. Application of *Klebsiella oxytoca* immobilized cells on the treatment of cyanide wastewater. *Chemosphere*, 71: 133–139.

Chen, H., Liu, S., Yang, F., Xue, Y. & Wang, T. 2009. The development of simultaneous partial nitrification, ANAMMOX and denitrification (SNAD) process in a single reactor for nitrogen removal. *Bioresour. Technol*, 100: 1548–1554.

Chen, P., Li, J., Li, Q. X., Wang, Y., Li, S., Ren, T. & Wang, L. 2012. Simultaneous heterotrophic nitrification and aerobic denitrification by bacterium *Rhodococcus sp.* CPZ24. *Bioresour Technol*, 116: 266-270.

Chen, Z., Wang, X., Chen, X., Chen, J., Feng, X. & Peng, X. 2018. Nitrogen removal via nitritation pathway for low-strength ammonium wastewater by adsorption, biological desorption and denitrification. *Bioresour. Technol*, 267: 541-549.

Choi, O.K. & Hu, Z.Q. 2009. Nitrification inhibition by silver nanoparticles. *Water Sci Technol*, 59: 1699-1702.

Chowdhury, Z., Zain, S & Rashid, A. 2011. Equilibrium Isotherm Modeling, Kinetics and Thermodynamics Study for Removal of Lead from Waste Water. *E- J. Chem*, 8: 333-339

Clough, T.J., Lanigan, G.J., de Klein, C.A., Samad, M.S., Morales, S.E., Rex, D., Bakken, L.R., Johns, C., Condrón, L.M. & Grant, J. 2017. Influence of soil moisture on codenitrification fluxes from a urea-affected pasture soil. *Sci. Rep.*, 7: 2185.

Conway, T. 1992. The Entner-Doudoroff pathway: history, physiology and molecular biology. *FEMS Microbiol Rev.*, 9: 1-27.

Cui, J., Wang, X., Yuan, Y., Guo, X., Gu, X. & Jian, L. 2014. Combined ozone oxidation and biological aerated filter processes for treatment of cyanide containing electroplating wastewater. *Chem. Eng.*, 241: 184–189.

Daims, H., Lebedeva, E., Pjevac, P., Han, P., Herbold, C., Albertsen, M., Jehmlich, N., Palatinszky, M., Vierheilig, J., Bulaev, A., Kirkegaard, R., von Bergen, M., Rattei, T., Bendinger, B., Nielsen, P. & Wagner, M. 2015. Complete nitrification by *Nitrospira* bacteria. *Nature*, 528: 504-509.

Daverey, A., Chen, Y.C., Dutta, K., Huang, Y.T. & Lin, J.G. 2015. Start-up of simultaneous partial nitrification, anammox and denitrification (SNAD) process in sequencing batch biofilm reactor using novel biomass carriers. *Bioresour. Technol.*, 190: 480–486.

De Sanctis, D., Ascenzi, P., Bocedi, A., Dewilde, S., Burmester, T., Hankeln, T., Moens, L. & Bolognesi, M. 2006. Cyanide binding and heme cavity conformational transitions in *Drosophila melanogaster* hexacoordinate hemoglobin. *Biochemistry*, 45: 10054–10061.

Duan, J., Fang, H., Su, B., Chen, J. & Lin, J. 2015. Characterization of halophilic heterotrophic nitrification–aerobic denitrification bacterium and its application on the treatment of saline wastewater. *Bioresour. Technol.*, 179: 421–428.

Dwivedi, N., Balomajumder, C. & Mondal, P. 2016. Comparative evaluation of cyanide removal by adsorption, biodegradation, and simultaneous adsorption and biodegradation (SAB) process using *Bacillus cereus* and almond shell. *J. Environ. Biol.*, 37: 551.

Ebeling, J.M., Timmons, M.B. & Bisogni, J.J. 2006. Engineering analysis of the stoichiometry of photoautotrophic, autotrophic, and heterotrophic removal of ammonia–nitrogen in aquaculture systems. *Aquaculture*, 257: 346-358.

Edwards, J.S., Covert, M. & Palsson, B. 2002. Metabolic modelling of microbes: The flux-balance approach. *Environ. Microbiol.*, 4: 133–140.

Eliasson, J. 2015. The rising pressure of global water shortages. *Nature News*, 517: 6.

Feng, C., Huang, L., Yu, H., Yi, X. & Wei, C. 2015. Simultaneous phenol removal, nitrification and denitrification using microbial fuel cell technology. *Water Res*, 76: 160-170.

Gao, D., Peng, Y. & Wu, W.M. 2010. Kinetic model for biological nitrogen removal using shortcut nitrification-denitrification process in sequencing batch reactor. *Environ. Sci. Technol*, 44: 5015-5021.

Ge, Q., Yue, X. & Wang, G. 2015a. Simultaneous heterotrophic nitrification and aerobic denitrification at high initial phenol concentration by isolated bacterium *Diaphorobacter* sp. PD-7. *Chin. J. Chem. Eng*, 23: 835-841.

Ge, S., Wang, S., Yang, X., Qiu, S., Li, B. & Peng, Y. 2015b. Detection of nitrifiers and evaluation of partial nitrification for wastewater treatment: A review. *Chemosphere*, 140: 85–98.

Geissen, V., Mol, H., Klumpp, E., Umlauf, G., Nadal, M., van der Ploeg, M., van de Zee, S.E. & Ritsema, C.J. 2015. Emerging pollutants in the environment: a challenge for water resource management. *ISWCR*, 3: 57-65.

Gernaey, K.V., van Loosdrecht, M.C., Henze, M., Lind, M. & Jørgensen, S.B. 2004. Activated sludge wastewater treatment plant modelling and simulation: state of the art. *Environ Modell Softw*, 19: 763-783.

Gunatilake, S.K. 2015. Methods of removing heavy metals from industrial wastewater. *Methods*, 1: 14.

Gupta, N., Balomajumder, C. & Agarwal, V. 2010. Enzymatic mechanism and biochemistry for cyanide degradation: A review. *J. Hazard. Mater*, 176: 1–13.

Hamed, M.M., Khalafallah, M.G. & Hassanien, 2004. E.A. Prediction of wastewater treatment plant performance using artificial neural networks. *Environ Modell Softw*, 19: 919-928.

Han, Y., Jin, X., Wang, F., Liu, Y. & Chen, X. 2013a. Successful startup of a full-scale acrylonitrile wastewater biological treatment plant (ACN-WWTP) by eliminating the inhibitory effects of toxic compounds on nitrification. *Water Sci. Technol*, 69: 553–559.

Han, Y., Jin, X., Wang, Y., Liu, Y & Chen, X. 2013b. Inhibitory effect of cyanide on nitrification process and its eliminating method in a suspended activated sludge process. *Environ sci pollut r*, 21: 2706-2713

- Han, Y., Jin, X., Wang, Y., Liu, Y. & Chen, X. 2014. Inhibitory effect of cyanide on nitrification process and its eliminating method in a suspended activated sludge process. *Environ. Sci. Pollut. Res*, 21: 2706–2713.
- He, Q., Zhang, W., Zhang, S. & Wang, H. 2017. Enhanced nitrogen removal in an aerobic granular sequencing batch reactor performing simultaneous nitrification, endogenous denitrification and phosphorus removal with low superficial gas velocity. *Chem. Eng. J*, 326: 1223–1231.
- He, T., Li, Z., Sun, Q., Xu, Y. & Ye, Q. 2016. Heterotrophic nitrification and aerobic denitrification by *Pseudomonas tolaasii* Y-11 without nitrite accumulation during nitrogen conversion. *Bioresour Technol*, 200: 493-499.
- Hu, M. Wang, X., Wen, X. & Xia, Y. 2012. Microbial community structures in different wastewater treatment plants as revealed by 454-pyrosequencing analysis. *Bioresour. Technol*, 117: 72-79.
- Huang, X., Urata, K., Wei, Q., Yamashita, Y., Hama, T. & Kawagoshi, Y. 2016. Fast start-up of partial nitritation as pre-treatment for anammox in membrane bioreactor. *Biochem. Eng. J*, 105: 371–378.
- Inglezakis, V., Malamis, S., Omirkhan, A., Nauruzbayeva, J., Makhtayeva, Z., Seidakhmetov, T. & Kudarova, A. 2017. Investigating the inhibitory effect of cyanide, phenol and 4-nitrophenol on the activated sludge process employed for the treatment of petroleum wastewater. *J Environ Manage*, 203: 825-830.
- Inglezakis, V., Malamis, S., Omirkhan, A., Nauruzbayeva, J., Makhtayeva, Z., Seidakhmetov, T. & Kudarova, A. 2017. Investigating the inhibitory effect of cyanide, phenol and 4-nitrophenol on the activated sludge process employed for the treatment of petroleum wastewater. *J Environ Manage*, 203: 825-830.
- Itoba-Tombo, E.F. 2019. Spatial and temporal distribution of pollutants from different land use/land-cover types of the bottelary river catchment. In *New Horizon in wastewater Management Emerging Monitoring and Remediation Strategies*, Fosso-Kankeu, E., Ed., Nova Science Publishers: New York, NY, USA, Volume 3: 65–86.
- Ji, B., Yang, K., Zhu, L., Jiang, Y., Wang, H., Zhou, J. & Zhang, H. 2015. Aerobic denitrification: A review of important advances of the last 30 years. *Biotechnol. Bioproc. Eng*, 20: 643–651.
- Jin, R., Liu, T., Liu, G., Zhou, J., Huang, J & Wang, A. 2014. Simultaneous Heterotrophic Nitrification and Aerobic Denitrification by the Marine Origin Bacterium *Pseudomonas* sp. ADN-42. *Applied Biochemistry and Biotechnology*, 175: 2000-2011

Kandasamy, S., Dananjeyan, B., Krishnamurthy, K. & Benckiser, G. 2015. Aerobic cyanide degradation by bacterial isolates from cassava factory wastewater. *Braz. J. Microbiol*, 46: 659-666.

Kanyenda, G., Ntwampe, S.K.O., Mpongwana, N., Godongwana, B. 2018. Mathematical Exposition of Simultaneous Nitrification and Aerobic Denitrification. In Proceedings of the 10th Int’I Conference on Advances in Science, Engineering, Technology & Healthcare {ASETH-18}, Cape Town, South Africa, 19–20 November, pp. 242–245, ISBN 978-81-938365-2-1. Available online: <https://doi.org/10.17758/EARES4.EAP1118258> (28 October 2019).

Kao, C.M., Liu, J.K., Lou, H.R., Lin, C.S. & Chen, S.C. 2003. Biotransformation of cyanide to methane and ammonia by *Klebsiella oxytoca*. *Chemosphere*, 50: 1055–1061.

Kapoor, V., Elk, M., Li, X. & Santo Domingo, J.W. 2016. Inhibitory effect of cyanide on wastewater nitrification determined using SOUR and RNA-based gene-specific assays. *Lett Appl Microbiol*, 63: 155-161.

Kapoor, V., Elk, M.;Li, X & Santo Domingo, J. 2016. Inhibitory effect of cyanide on wastewater nitrification determined using SOUR and RNA-based gene-specific assays. *Lett Appl Microbiol*, 63: 155-161

Kapoor, V., Li, X., Elk, M., Chandran, K., Impellitteri, C. & Santo Domingo, J. 2015. Impact of Heavy Metals on Transcriptional and Physiological Activity of Nitrifying Bacteria. *Environ Sci Technol*, 49: 13454-13462.

Kauffman, K.J., Prakash, P. & Edwards, J.S. 2003. Advances in flux balance analysis. *Curr Opin Biotechnol*, 14: 491-496.

Khamar, Z., Makhdoumi-Kakhki, A. & Mahmudy Gharai, M. 2015. Remediation of cyanide from the gold mine tailing pond by a novel bacterial co-culture. *Int. Biodeterior. Biodegrad*, 99: 123–128.

Khardenavis, A., Kapley, A. & Purohit, H. 2007. Simultaneous nitrification and denitrification by diverse *Diaphorobacter* sp. *Appl. Microbiol. Biotechnol*, 77: 403–409.

Khataee, A., Vafaei, F & Jannatkah, M. 2013. Biosorption of three textile dyes from contaminated water by filamentous green algal *Spirogyra* sp.: Kinetic, isotherm and thermodynamic studies. *Int Biodeterior Biodegradation*, 83: 33-40

Kim, D., Ryu, H., Kim, M., Kim, J. & Lee, S. 2007. Enhancing struvite precipitation potential for ammonia nitrogen removal in municipal landfill leachate. *J. Hazard. Mater*, 146: 81–85.



- Kim, Y., Cho, H., Lee, D., Park, D. & Park, J. 2011a. Comparative study of free cyanide inhibition on nitrification and denitrification in batch and continuous flow systems. *Desalination*, 279: 439-444.
- Kim, Y., Lee, D., Park, C., Park, D. & Park, J. 2011b. Effects of free cyanide on microbial communities and biological carbon and nitrogen removal performance in the industrial activated sludge process. *Water Res*, 45: 1267-1279.
- Kim, Y., Park, D., Lee, D & Park, J. 2008. Inhibitory effects of toxic compounds on nitrification process for cokes wastewater treatment. *J Hazard Mater*, 152: 915-921
- Kim, Y., Park, D., Lee, D. & Park, J. 2007. Instability of biological nitrogen removal in a cokes wastewater treatment facility during summer. *J Hazard Mater*, 141: 27-32.
- Kim, Y., Park, H., Cho, K. & Park, J. 2013. Long term assessment of factors affecting nitrifying bacteria communities and N-removal in a full-scale biological process treating high strength hazardous wastewater. *Bioresour. Technol*, 134: 180–189.
- Koch, G., Egli, K., Van der Meer, J.R. & Siegrist, H. 2000. Mathematical modeling of autotrophic denitrification in a nitrifying biofilm of a rotating biological contactor. *Water Sci. Technol*, 41: 191–198.
- Kompala, D.S., Ramkrishna, D. & Tsao, G.T. 1984. Cybernetic modeling of microbial growth on multiple substrates. *Biotechnol Bioeng*, 26: 1272-1281.
- Kushwaha, J., Srivastava, V. & Mall, I. 2010. Treatment of dairy wastewater by commercial activated carbon and bagasse fly ash: Parametric, kinetic and equilibrium modelling, disposal studies. *Bioresour. Technol*, 101: 3474-3483.
- Lambert, J. L., Ramasamy, J. & Paukstelis, J. V. 1975. Stable reagents for the colorimetric determination of cyanide by modified Koenig reactions. *Anal Chem*, 47: 916-918.
- Le, P.P., Bahl, A. & Ungar, L.H. 2004. Using prior knowledge to improve genetic network reconstruction from microarray data. *In silico biology*, 4: 335-353.
- Levy-Booth, D., Prescott, C. & Grayston, S. 2014. Microbial functional genes involved in nitrogen fixation, nitrification and denitrification in forest ecosystems. *Soil Biol. Biochem*, 75: 11–25.
- Li, C., Yang, J., Wang, X., Wang, E., Li, B., He, R. & Yuan, H. 2015a. Removal of nitrogen by heterotrophic nitrification–aerobic denitrification of a phosphate accumulating bacterium *Pseudomonas stutzeri* YG-24. *Bioresour Technol*, 182: 18-25.

- Li, G., Puyol, D., Carvajal-Arroyo, J., Sierra-Alvarez, R. & Field, J. 2014. Inhibition of anaerobic ammonium oxidation by heavy metals. *J Chem Technol Biotechnol*, 90: 830-837.
- Li, G., Puyol, D., Carvajal-Arroyo, J.M., Sierra-Alvarez, R. & Field, J.A. 2015b. Inhibition of anaerobic ammonium oxidation by heavy metals. *J. Chem. Technol. Biotechnol*, 90: 830–837.
- Li, Q., Lu, H., Yin, Y., Qin, Y., Tang, A., Liu, H. & Liu, Y. 2019. Synergic effect of adsorption and biodegradation enhance cyanide removal by immobilized *Alcaligenes sp.* strain DN25. *J. Hazard. Mater*, 364: 367-375.
- Lin, J., Meng, Y., Shi, Y. & Lin, X. 2019. Complete Genome Sequences of *Colwellia sp.* Arc7-635, a Denitrifying Bacterium Isolated from Arctic Seawater. *Curr. Microbiol*,76: 1–5.
- Liu, G. & Wang, J. 2012. Probing the stoichiometry of the nitrification process using the respirometric approach. *Water Res*, 46: 5954-5962
- Liu, Y., Ai, G.M., Miao, L.L. & Liu, Z.P. 2016. Marinobacter strain NNA5, a newly isolated and highly efficient aerobic denitrifier with zero N<sub>2</sub>O emission. *Bioresour. Technol*, 206: 9–15.
- Lochmatter, S. & Holliger, C. 2014. Optimization of operation conditions for the startup of aerobic granular sludge reactors biologically removing carbon, nitrogen, and phosphorous. *Water Res*, 59: 58–70.
- Low, E.W. & Chase, H.A. 1999. Reducing production of excess biomass during wastewater treatment. *Water Res*, 33: 1119-1132.
- Luque-Almagro, V.M., Blasco, R., Martínez-Luque, M., Moreno-Vivián, C., Castillo, F. & Roldán, M.D. 2011. Bacterial cyanide degradation is under review: *Pseudomonas pseudoalcaligenes* CECT5344, a case of an alkaliphilic cyanotroph. *Biochem. Soc. Trans*, 39: 269–274.
- Luque-Almagro, V.M., Cabello, P., Sáez, L.P., Olaya-Abril, A., Moreno-Vivián, C. & Roldán, M.D. 2018. Exploring anaerobic environments for cyanide and cyano-derivatives microbial degradation. *Appl. Microbiol. Biotechnol*, 102: 1067–1074.
- Luque-Almagro, V.M., Moreno-Vivián, C. & Roldán, M.D. 2016. Biodegradation of cyanide wastes from mining and jewellery industries. *Curr. Opin. Biotechnol*, 38: 9–13.
- Lüttge, A. 2006. Crystal dissolution kinetics and Gibbs free energy. *J Electron Spectros Relat Phenomena* , 150: 248-259
- Lyu, S., Chen, W., Zhang, W., Fan, Y. & Jiao, W. 2016. Wastewater reclamation and reuse in China: opportunities and challenges. *J Environ Sci*, 39: 86-96.

- Ma, Q., Qu, Y., Shen, W., Zhang, Z., Wang, J., Liu, Z., Li, D., Li, H. & Zhou, J. 2015. Bacterial community compositions of coking wastewater treatment plants in steel industry revealed by Illumina high-throughput sequencing. *Bioresour Technol*, 179: 436-443
- Ma, W., Han, Y., Ma, W., Han, H., Zhu, H., Xu, C., Li, K. & Wang, D. 2017. Enhanced nitrogen removal from coal gasification wastewater by simultaneous nitrification and denitrification (SND) in an oxygen-limited aeration sequencing batch biofilm reactor. *Bioresour. Technol*, 244: 84–91.
- Mahadevan, R., Edwards, J.S. & Doyle III, F.J. 2002. Dynamic flux balance analysis of diauxic growth in *Escherichia coli*. *Biophys. J*, 83: 1331-1340.
- Mahvi, A.H. 2008. Sequencing batch reactor: A promising technology in wastewater treatment. *J. Environ. Health Sci*, 5: 79–90.
- Mandli, A.R., Venkatesh, K.V. & Modak, J.M. 2015. Constraints based analysis of extended cybernetic models. *Biosystems*, 137: 45-54.
- McLellan, S.L., Huse, S.M., Mueller-Spitz, S.R., Andreishcheva, E.N. & Sogin, M.L. 2010. Diversity and population structure of sewage-derived microorganisms in wastewater treatment plant influent. *Environ. Microbiol*, 12: 378-392.
- Medhi, K., Singhal, A., Chauhan, D. and Thakur, I. 2017. Investigating the nitrification and denitrification kinetics under aerobic and anaerobic conditions by *Paracoccus denitrificans* ISTOD1. *Bioresour Technol*, 242: 334-343.
- Mekuto, L., Jackson, V.A. & Ntwampe, S.K. 2013. Biodegradation of free cyanide using *Bacillus* sp. consortium dominated by *Bacillus safensis*, *Lichenformis* and *Tequilensis* strains: A bioprocess supported solely with whey. *J. Bioremediat. Biodegrad*, 2–7, doi:10.4172/2155-6199.S18-004.
- Mekuto, L., Kim, Y.M., Ntwampe, S.K., Mewa-Ngongang, M., Mudumbi, N., Baptist, J., Dlangamandla, N., Itoba-Tombo, E.F. & Akinpelu, E.A. 2018. Heterotrophic nitrification-aerobic denitrification potential of cyanide and thiocyanate degrading microbial communities under cyanogenic conditions. *Environ. Eng. Sci*, 24: 254–262.
- Mekuto, L., Ntwampe, S.K.O. & Jackson, V.A. 2015. Biodegradation of free cyanide and subsequent utilisation of biodegradation by-products by *Bacillus* consortia: Optimisation using response surface methodology. *Environ. Sci. Pollut. Res. Int*, 22: 10434–10443.
- Mirbagheri, S., Poshtegal, M & Parisai, M. 2010. Removing of urea and ammonia from petrochemical industries with the objective of reuse, in a pilot scale: Surveying of the methods of waste water treatment. *Desalination*, 256: 70-76

- Monod J. 1942. The growth of bacterial cultures. *Annu Rev Microbiol*, 3: 371–394
- Mpongwana, N., Ntwampe, S., Mekuto, L., Akinpelu, E., Dyantyi, S & Mpentshu, Y. 2016. Isolation of high-salinity-tolerant bacterial strains, *Enterobacter sp.*, *Serratia sp.*, *Yersinia sp.*, for nitrification and aerobic denitrification under cyanogenic conditions. *Water Sci Technol*, 73: 2168-75
- Mpongwana, N., Ntwampe, S.K.O., Omodanisi, E.I., Chidi, B.S. & Razanamahandry. L.C. 2019. Sustainable Approach to Eradicate the Inhibitory Effect of Free-Cyanide on Simultaneous Nitrification and Aerobic Denitrification during Wastewater Treatment. *Sustainability*, 11: 6180
- Murugesan, T., Durairaj, N., Ramasamy, M., Jayaraman, K., Palaniswamy, M. & Jayaraman, A. 2018. Analeptic agent from microbes upon cyanide degradation. *Appl. Microbiol. Biotechnol*, 102: 1557–1565.
- Narang, A. & Pilyugin, S. 2007. Bacterial gene regulation in diauxic and non-diauxic growth. *J. Theor. Biol*, 244: 326-348.
- Narang, A., Konopka, A. & Ramkrishna, D. 1997. Dynamic analysis of the cybernetic model for diauxic growth. *Chem. Eng. Sci*, 52: 2567-2578.
- Norton-Brandão, D., Scherrenberg, S. & van Lier, J. 2013. Reclamation of used urban waters for irrigation purposes—A review of treatment technologies. *J. Environ. Manag*, 122: 85–98.
- Ntwampe, S.K. & Santos, B.A. 2013. Potential of agro-waste extracts as supplements for the continuous bioremediation of free cyanide contaminated wastewater. *J. Environ. Chem. Eng*, 7: 493–497.
- Ofițeru, I.D., Lunn, M., Curtis, T.P., Wells, G.F., Criddle, C.S., Francis, C.A. & Sloan, W.T., 2010. Combined niche and neutral effects in a microbial wastewater treatment community. *PNAS*, 107: 15345-15350.
- Ojaghi, A., Tonkaboni, S.Z.S., Shariati, P. & Ardejani, F.D. 2018. Novel cyanide electro-biodegradation using *Bacillus pumilus* ATCC 7061 in aqueous solution. *J. environ. health sci. eng*, 16: 99-108.
- Oller, I., Malato, S. & Sánchez-Pérez, J. 2011. Combination of advanced oxidation processes and biological treatments for wastewater decontamination—A review. *Sci. Total Environ*, 409: 4141–4166.
- Özel, Y.K., Gedikli, S., Aytar, P., Ünal, A., Yamaç, M., Çabuk, A. & Kolankaya, N. 2010. New fungal biomasses for cyanide biodegradation. *J. Biosci. Bioeng*, 110: 431–435.

- Pal, R.R., Khardenavis, A.A. & Purohit, H.J. 2015. Identification and monitoring of nitrification and denitrification genes in *Klebsiella pneumoniae* EGD-HP19-C for its ability to perform heterotrophic nitrification and aerobic denitrification. *Funct. Integr. Genom*, 15: 63–76.
- Papirio, S., Zou, G., Ylinen, A., Di Capua, F., Pirozzi, F. & Puhakka, J.A. 2014. Effect of arsenic on nitrification of simulated mining water. *Bioresour. Technol*, 164: 149–154.
- Park, D., Lee, D., Kim, Y. & Park, J. 2008. Bioaugmentation of cyanide-degrading microorganisms in a full-scale cokes wastewater treatment facility. *Bioresour Technol*, 99: 2092-2096.
- Patnaik, P.R. 2000. Are microbes intelligent beings?: An assessment of cybernetic modeling. *Biotechnol. Adv*, 18: 267-288
- Patton, C. J. & Crouch, S. R. 1977. Spectrophotometric and kinetics investigation of the Berthelot reaction for the determination of ammonia. *Anal Chem*, 49: 464-469.
- Peng, Y. & Zhu, G. 2006. Biological nitrogen removal with nitrification and denitrification via nitrite pathway. *Appl. Microbiol. Biotechnol*, 73: 15-26.
- Perez-Garcia, O., Lear, G. & Singhal, N. 2016. Metabolic network modeling of microbial interactions in natural and engineered environmental systems. *Front Microbiol*, 7: 673.
- Perez-Garcia, O., Villas-Boas, S.G., Swift, S., Chandran, K. & Singhal, N. 2014. Clarifying the regulation of NO/N<sub>2</sub>O production in *Nitrosomonas europaea* during anoxic–oxic transition via flux balance analysis of a metabolic network model. *Water Res*, 60: 267-277.
- Pradhan, N., Thi, S.S. & Wuertz, S. 2019. Inhibition factors and kinetic model for anaerobic ammonia oxidation in a granular sludge bioreactor with *Candidatus Brocadia*. *Chem. Eng. J*, 123618.
- Ramavandi, B. 2016. Adsorption potential of NH<sub>4</sub>Br-soaked activated carbon for cyanide removal from wastewater. *Indian J. Chem. Technol*, 22: 183–193.
- Ramkrishna, D. & Song, H.S. 2012. Dynamic models of metabolism: Review of the cybernetic approach. *AIChE Journal*, 58: 986-997.
- Ramkrishna, D.O.R.A.I.S.W.A.M.I. 1982. A cybernetic perspective of microbial growth. In *Foundations of biochemical engineering Kinetics and Thermodynamics in Biological Systems*, Harvey. W. B., Terry Papoutsakis, E., Stephanopoulos., ACS publications, University of California, Berkeley G, 161-178.

- Razanamahandry, L.C., Andrianisa, H.A., Karoui, H., Kouakou, K.M. & Yacouba, H., 2016. Biodegradation of free cyanide by bacterial species isolated from cyanide-contaminated artisanal gold mining catchment area in Burkina Faso. *Chemosphere*, 157: 71-78.
- Richards, D. & Shieh, W. 1989. Anoxic-oxic activated-sludge of cyanides and phenols. *Biotechnol. Bioeng*, 33, 32-38.
- Rider, B. & Mellon, M. 1946. Colorimetric determination of nitrites. *Industrial & Engineering Chem Anal*, 18: 96-99
- Rinágelová, A., Kaplan, O., Veselá, A.B., Chmátal, M., Křenková, A., Plíhal, O., Pasquarelli, F., Cantarella, M. & Martínková, L. 2014. Cyanide hydratase from *Aspergillus niger* K10: Overproduction in *Escherichia coli*, purification, characterization and use in continuous cyanide degradation. *Process. Biochem*, 49: 445–450.
- Rodríguez, J., Lema, J & Kleerebezem, R. 2008. Energy-based models for environmental biotechnology. *Trends Biochem Sci*, 26: 366-374
- Rottenberg, H & Gutman, M. 1977. Control of the rate of reverse electron transport in submitochondrial particles by the free energy. *Biochem J*, 16: 3220-3227
- Ruser, R. & Schulz, R. 2015. The effect of nitrification inhibitors on the nitrous oxide (N<sub>2</sub>O) release from agricultural soils—A review. *Plant Nutr. Soil Sci*, 178: 171–188.
- Ryu, B.G., Kim, W., Nam, K., Kim, S., Lee, B., Park, M.S. & Yang, J.W. 2015. A comprehensive study on algal–bacterial communities shift during thiocyanate degradation in a microalga-mediated process. *Bioresour. Technol*, 191: 496–504.
- Safa, Z.J., Aminzadeh, S., Zamani, M. & Motallebi, M. 2017. Significant increase in cyanide degradation by *Bacillus* sp. M01 PTCC 1908 with response surface methodology optimization. *AMB Express*, 7: 200.
- Salazar-Benites, G., Dyer, C., Bott, C., Kennedy, A., Williamson, A. & DeVries, A. 2016. Some Serious BNR Intensification: Combining cost-effective cyanide treatment, chemically-enhanced primary treatment, and advanced aeration controls to achieve nitrogen removal in a high-rate activated sludge plant. *Proc. Water Environ. Fed*, 2016: 4651–4680.
- Samer, M. 2015. Biological and chemical wastewater treatment processes. *Wastewater Treatment Engineering*, 1-50.

- Santos, B.A.Q., Ntwampe, S.K.O., Doughari, J.H. & Muchatibaya, G. 2013. Application of Citrus sinensis solid waste as a pseudo-catalyst for free cyanide conversion under alkaline conditions. *BioResources*, 8: 3461–3467.
- Sauer, M., Porro, D., Mattanovich, D. & Branduardi, P. 2008. Microbial production of organic acids: Expanding the markets. *Trends Biotechnol*, 26: 100–108.
- Seifi, M. & Fazaelpoor, M. 2012. Modeling simultaneous nitrification and denitrification (SND) in a fluidized bed biofilm reactor. *Appl. Math. Model*, 36: 5603-5613
- Sharma, M., Akhter, Y. & Chatterjee, S. 2019. A review on remediation of cyanide containing industrial wastes using biological systems with special reference to enzymatic degradation. *World J. Microbiol. Biotechnol*, 35: 70.
- Sheng, G.P., Yu, H.Q. & Li, X.Y. 2010. Extracellular polymeric substances (EPS) of microbial aggregates in biological wastewater treatment systems: a review. *Biotechnol. Adv*, 28: 882-894.
- Shoda, M. & Ishikawa, Y. 2014. Heterotrophic nitrification and aerobic denitrification of high-strength ammonium in anaerobically digested sludge by *Alcaligenes faecalis* strain No. 4. *J. Biosci. Bioeng*, 117: 737–741.
- Shoda, M. & Ishikawa, Y. 2015. Heterotrophic nitrification and aerobic denitrification of a wastewater from a chemical company by *Alcaligenes faecalis* no. 4. *Int. J. Water Wastewater Treat*, 1: 1–5.
- Show, K.Y., Lee, D.J. & Pan, X. 2013. Simultaneous biological removal of nitrogen–sulfur–carbon: Recent advances and challenges. *Biotechnol. Adv*, 31: 409–420.
- Sin, G., Kaelin, D., Kampschreur, M.J., Takacs, I., Wett, B., Gernaey, K.V., Rieger, L., Siegrist, H. & van Loosdrecht, M. 2008. Modelling nitrite in wastewater treatment systems: A discussion of different modelling concepts. *Water Sci. Technol*, 58: 1155–1171.
- Singh, M. & Srivastava, R.K. 2011. Sequencing batch reactor technology for biological wastewater treatment: A review. *Asia-Pac. J. Chem. Eng*, 6: 3–13.
- Singh, N. & Balomajumder, C. 2016. Simultaneous removal of phenol and cyanide from aqueous solution by adsorption onto surface modified activated carbon prepared from coconut shell. *J. Water Process. Eng*, 9: 233–245.
- Sokic-Lazic, D. & Minteer, S.D. 2008. Citric acid cycle biomimic on a carbon electrode. *Biosens Bioelectron*, 24: 939-944.

- Solopova, A., van Gestel, J., Weissing, F., Bachmann, H., Teusink, B., Kok, J. & Kuipers, O. 2014. Bet-hedging during bacterial diauxic shift. *Proc Natl Acad Sci U S A*, 111: 7427-7432.
- Stephen F. A., Thomas L. M., Alejandro A. S., Jinghui Z., Zheng Z., Webb M., David J. L. 1997. Gapped BLAST and PSI-BLAST: a new generation of protein database search programs. *Nucleic Acids Res*, 25: 3389-3402.
- Suga, K., Van Dedem, G. & Moo-Young, M. 1975. Degradation of polysaccharides by endo and exo enzymes: A theoretical analysis. *Biotechnol Bioeng*, 17: 433-439.
- Szabó, E., Hermansson, M., Modin, O., Persson, F. & Wilén, B.M. 2016. Effects of wash-out dynamics on nitrifying bacteria in aerobic granular sludge during start-up at gradually decreased settling time. *Water*, 8: 172.
- Tiong, B.E.L.I.N.D.A., Bahari, Z.M., Lee, N.S.I.S., Jaafar, J., Ibrahim, Z. & Shahir, S. 2015. Cyanide degradation by *Pseudomonas pseudoalcaligenes* strain W2 isolated from mining effluent. *Sains Malays*, 44: 233–238.
- Toyoda, S., Yoshida, N. & Koba, K. 2015. Isotopocule analysis of biologically produced nitrous oxide in various environments. *Mass Spectrom. Rev*, 36: 135–160.
- Van Dedem, G. & Moo-Young, 1975. M. A model for *diauxic* growth. *Biotechnol Bioeng*, 17: 1301-1312.
- Vasiliadou, I.A., Pavlou, S. & Vayenas, D.V. 2006. A kinetic study of hydrogenotrophic denitrification. *Process Biochem*, 41: 1401-1408.
- Wagner, M. 2015. Complete nitrification by *Nitrospira* bacteria. *Nature*, 528: 504-509.
- Wagner, M., Loy, A., Nogueira, R., Purkhold, U., Lee, N. & Daims, H. 2002. Microbial community composition and function in wastewater treatment plants. *Anton Leeuw Int J G*, 81: 665-680.
- Wang, X., Wang, S., Xue, T., Li, B., Dai, X. & Peng, Y. 2015. Treating low carbon/nitrogen (C/N) wastewater in simultaneous nitrification-endogenous denitrification and phosphorous removal (SNDPR) systems by strengthening anaerobic intracellular carbon storage. *Water Res*, 77: 191-200.
- Wang, X., Wang, S., Zhao, J., Dai, X., Li, B. & Peng, Y. 2016. A novel stoichiometries methodology to quantify functional microorganisms in simultaneous (partial) nitrification-endogenous denitrification and phosphorus removal (SNEDPR). *Water Res*, 95: 319-329.



- Wang, X., Wang, W., Zhang, Y., Zhang, J., Li, J., Wang, S. & Chen, G. 2019. Isolation and characterization of *Acinetobacter* sp. JQ1004 and evaluation of its inhibitory kinetics by free ammonia. *Desalin Water Treat*, 147: 316-325.
- Watts, M.P. & Moreau, J.W. 2016. New insights into the genetic and metabolic diversity of thiocyanate-degrading microbial consortia. *Appl. Microbiol. Biotechnol*, 100: 1101–1108.
- Wiechert, W. 2001. <sup>13</sup>C metabolic flux analysis. *Metab Eng*, 3: 195-206.
- Wild, S.R., Rudd, T. & Neller, A., 1994. Fate and effects of cyanide during wastewater treatment processes. *Sci. total environ*, 156: 93-107.
- Wu, D., Senbayram, M., Well, R., Brüggemann, N., Pfeiffer, B., Loick, N., Stempfhuber, B., Dittert, K. & Bol, R. 2017. Nitrification inhibitors mitigate N<sub>2</sub>O emissions more effectively under straw-induced conditions favoring denitrification. *Soil Biol. Biochem*, 104: 197–207.
- Ye, L., Zhang, T., Wang, T. & Fang, Z. 2012. Microbial structures, functions, and metabolic pathways in wastewater treatment bioreactors revealed using high-throughput sequencing. *Environ. Technol*, 46: 13244-13252.
- Yunjie, R., Mohammad, J. T., Dedong, K., Huifeng, L., Heping, Z., Xiangyang, X., Yu, L. & Lei, C. 2020. Nitrogen Removal Performance and Metabolic Pathways Analysis of a Novel Aerobic Denitrifying Halotolerant *Pseudomonas balearica* strain RAD-17. *Microorganism*, 8: 72.
- Zhang, J., Wu, P., Hao, B. & Yu, Z. 2011. Heterotrophic nitrification and aerobic denitrification by the bacterium *Pseudomonas stutzeri* YZN-001. *Bioresour. Technol*, 102: 9866-9869.
- Zhang, J., Zhou, J., Han, Y. & Zhang, X. 2014. Start-up and bacterial communities of single-stage nitrogen removal using anammox and partial nitritation (SNAP) for treatment of high strength ammonia wastewater. *Bioresour. Technol*, 169: 652–657.
- Zhang, Q., Liu, Y., Ai, G., Miao, L., Zheng, H. & Liu, Z. 2012. The characteristics of a novel heterotrophic nitrification–aerobic denitrification bacterium, *Bacillus methylotrophicus* strain L7. *Bioresour. Technol*, 108: 35–44.
- Zhang, T., Ding, L., Ren, H., Guo, Z & Tan, J. 2010. Thermodynamic modeling of ferric phosphate precipitation for phosphorus removal and recovery from wastewater. *J Hazard Mater*, 176: 444-450
- Zhang, Y., Shi, Z., Chen, M., Dong, X. & Zhou, J. 2015. Evaluation of simultaneous nitrification and denitrification under controlled conditions by an aerobic denitrifier culture. *Bioresour. Technol*, 175: 602–605.

Zheng, M., He, D., Ma, T., Chen, Q., Liu, S., Ahmad, M., Gui, M. & Ni, J. 2014. Reducing NO and N<sub>2</sub>O emission during aerobic denitrification by newly isolated *Pseudomonas stutzeri* PCN-1. *Bioresour. Technol*, 162: 80–88.

Zhou, X.J., Kao, M.C.J., Huang, H., Wong, A., Nunez-Iglesias, J., Primig, M., Aparicio, O.M., Finch, C.E., Morgan, T.E. & Wong, W.H. 2005. Functional annotation and network reconstruction through cross-platform integration of microarray data. *Nat. Biotechnol*, 23, 238.

## **CHAPTER 10**

## **APPENDICES**

# CHAPTER 10:

## APPENDIX A

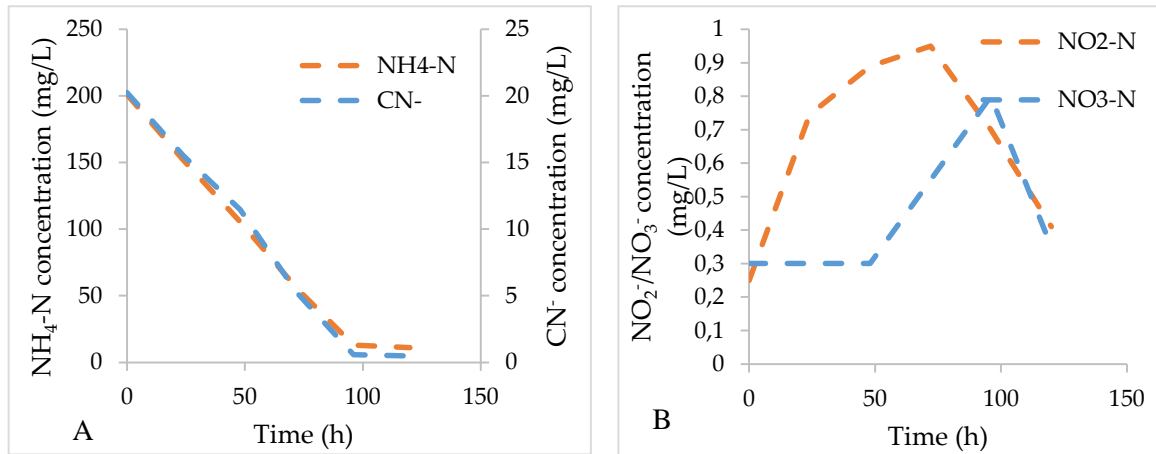
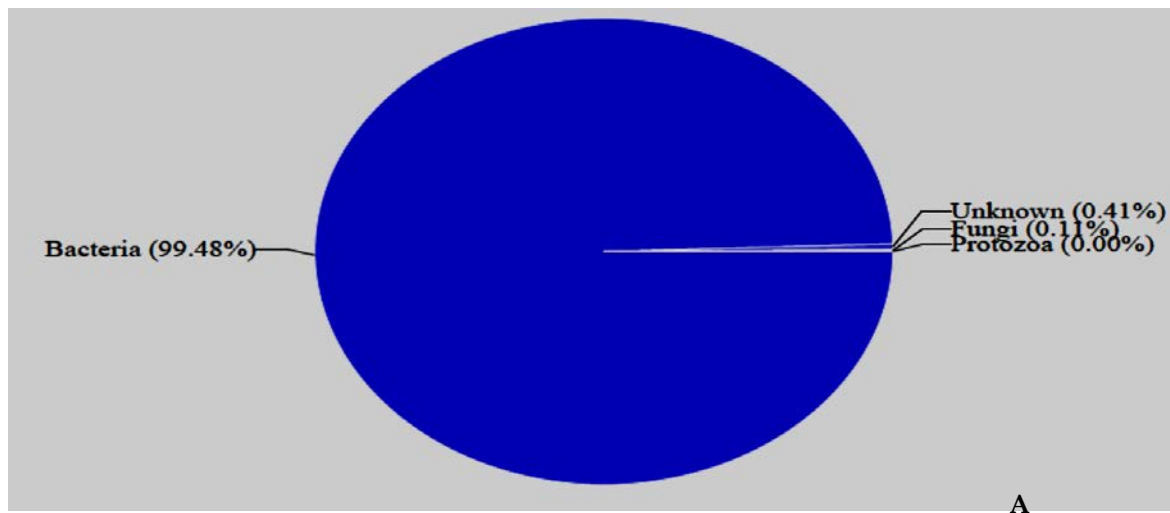
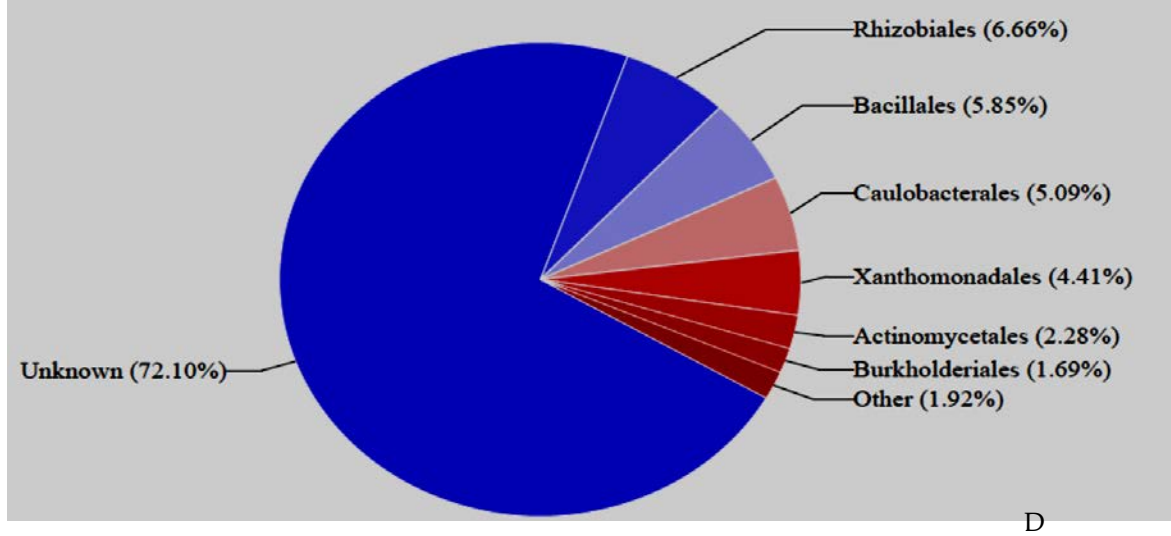
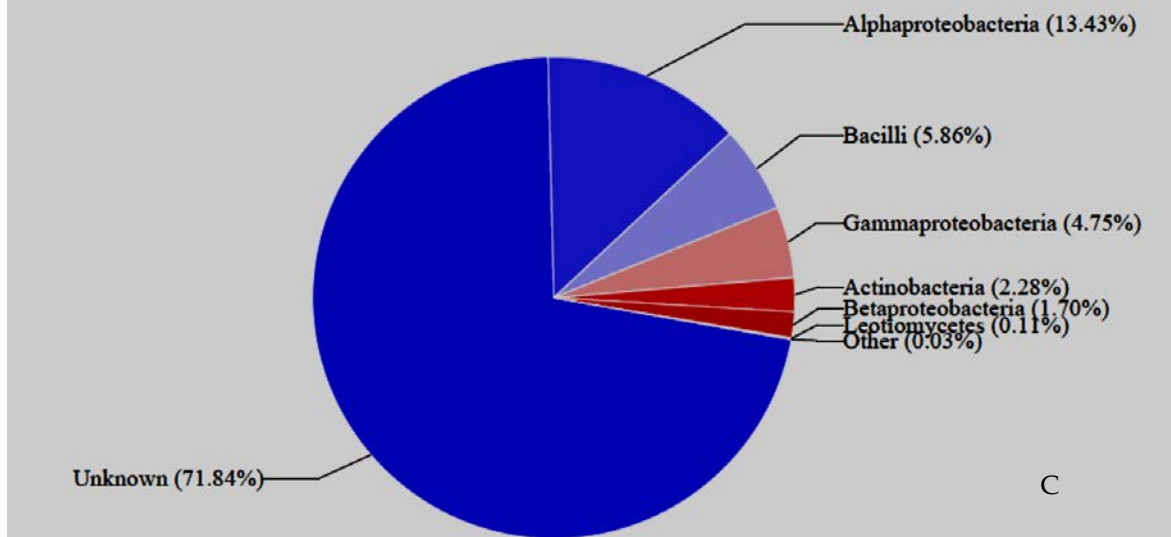
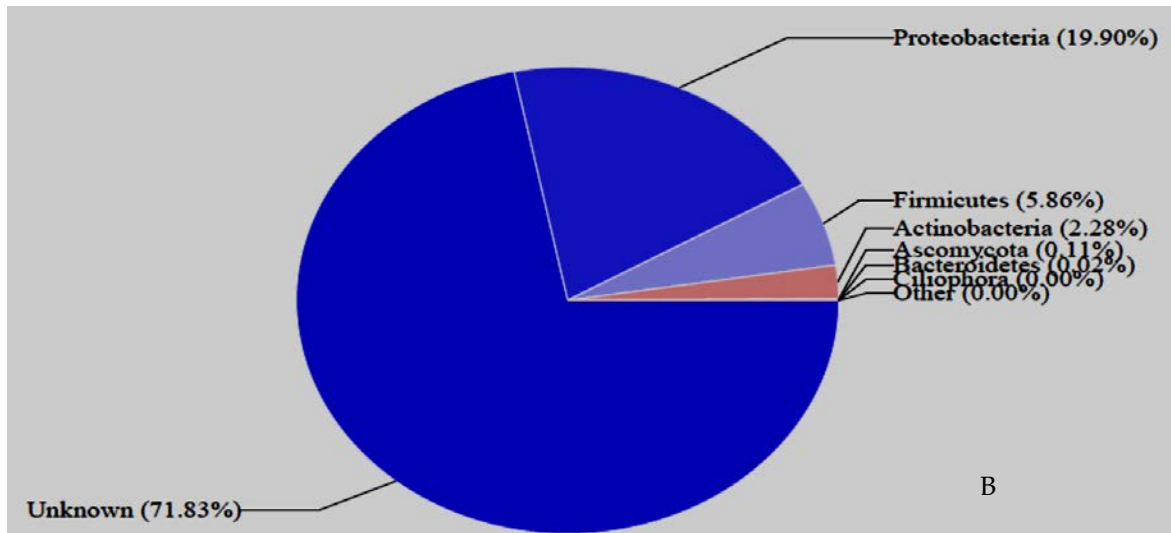
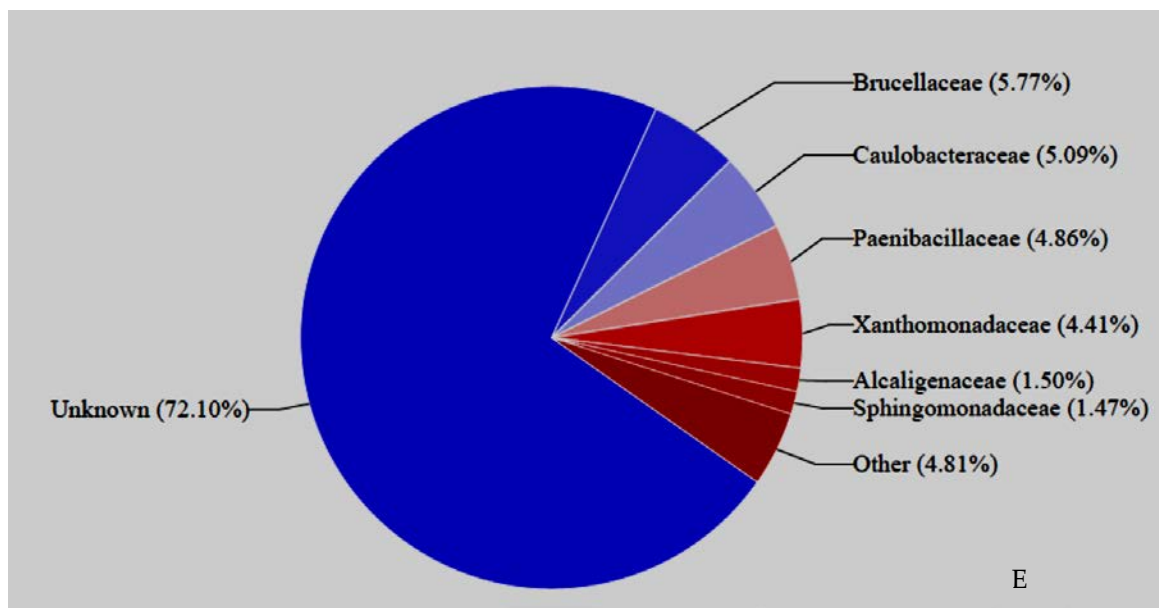


Figure 10.1. Simultaneous nitrification and aerobic denitrification performed by cyanide degrading mix consortia under high cyanide conditions. (a) NH<sub>4</sub>-N and CN<sup>-</sup> degradation profile. (b) NO<sub>2</sub>-N and NO<sub>3</sub>-N degradation and accumulation profile.







**Figure 10.2.** metagenomics report for the consortium. (a): Kingdom classification. (b): Phylum classification. (c): Class classification. (d); Order classification. E: Family classification.

**Table 10.1.** Estimated values of kinetic parameters for the models for  $\text{NH}_4\text{-N}$  degradation, a limiting step in nitrification

Model	Fitting constants and the values of kinetic Parameter ( $\pm 95\%$ confidence interval)					
	$V_m$ ( $h^{-1}$ )	$K_i$ ( $mgL^{-1}$ )	$K_s$ ( $mgL^{-1}$ )	$N$ (-)	$R^2$	variance
Monod	-1.19	92.91	-	-	0.48	0.09
$\frac{dC_a}{dt} = \frac{V_m * C_a}{K_i + C_a}$						
Moser	0.26	1.55	-	-0.24	0.09	0.23
$\frac{dC_a}{dt} = V_m \left[ \frac{C_a^n}{K_i + C_a^n} \right]$						

**Table 10.2.** Estimated values of kinetic parameters for the models for  $\text{CN}^-$  degradation, a limiting step in nitrification

Model	Fitting constants and the values of kinetic parameter ( $\pm 95\%$ confidence interval)					
	$V_m$ ( $h^{-1}$ )	$K_i$ ( $mgL^{-1}$ )	$K_s$ ( $mgL^{-1}$ )	$n$ (-)	$R^2$	variance
Monod	-0.32	-9.50	-	-	0.28	0.48
$\frac{dC_a}{dt} = \frac{V_m * C_a}{K_i + C_a}$						
Moser	0.026	44.43	-	0.98	0.75	0.22
$\frac{dC_a}{dt} = V_m \left[ \frac{C_a^n}{K_i + C_a^n} \right]$						
<b>Model with substrate inhibition</b>						

<b>Andrews</b>	-0.29	-1.39	43.42	-	-0.99	1.75
$-\frac{dC_a}{dt} = V_m \left[ 1 - \frac{K_i}{C_a} \right] \left[ 1 + \frac{C_a}{K_s} \right]$						

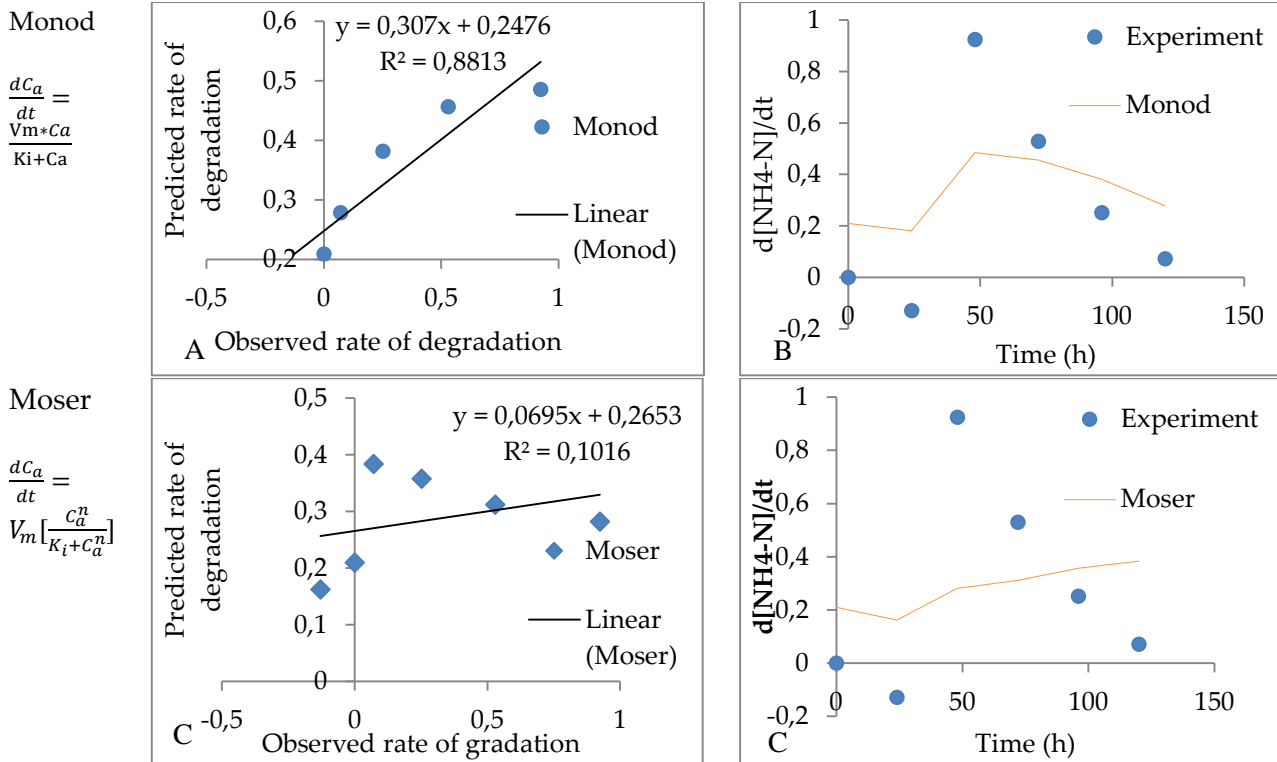


**Figure 10.3.** Parity plots of predicted values versus experimental values. Assimilations of the model data into  $\text{NH}_4\text{-N}$  degradation experimental data (Monod and Moser). (a) parity plot for the Monod equation. (b) simulation of predicted rate of reaction by Monod into experimental data. (c) parity plot for Moser equation. (d) simulation of predicted rate of reaction by Moser into experimental data.

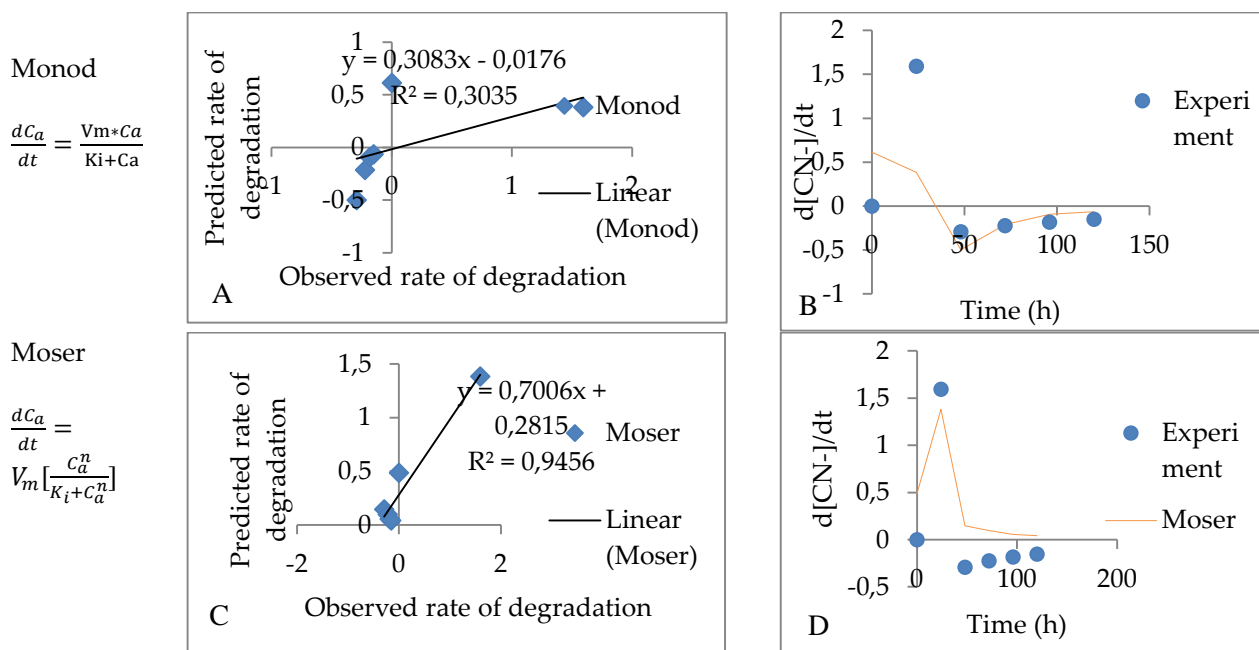




**Figure 10.4.** Parity plots of predicted values versus experimental values. Assimilations of the model data into CN- degradation experimental data (Monod, Moser, and Andrews). (a) parity plot for the Monod equation. (b) simulation of predicted rate of reaction by Monod into experimental data. (c) parity plot for Moser equation. (d) simulation of predicted rate of reaction by Moser into experimental data.